



Search for physics beyond the standard model in events with jets and two same-sign or at least three charged leptons in proton-proton collisions at $\sqrt{s} = 13$ TeV

The CMS Collaboration*

Abstract

A data sample of events from proton-proton collisions with at least two jets, and two isolated same-sign or three or more charged leptons, is studied in a search for signatures of new physics phenomena. The data correspond to an integrated luminosity of 137 fb^{-1} at a center-of-mass energy of 13 TeV, collected in 2016–2018 by the CMS experiment at the LHC. The search is performed using a total of 168 signal regions defined using several kinematic variables. The properties of the events are found to be consistent with the expectations from standard model processes. Exclusion limits at 95% confidence level are set on cross sections for the pair production of gluinos or squarks for various decay scenarios in the context of supersymmetric models conserving or violating R parity. The observed lower mass limits are as large as 2.1 TeV for gluinos and 0.9 TeV for top and bottom squarks. To facilitate reinterpretations, model-independent limits are provided in a set of simplified signal regions.

"Published in the European Physical Journal C as doi:10.1140/epjc/s10052-020-8168-3."

1 Introduction

In the standard model (SM), the production of multiple jets in conjunction with two same-sign (SS) or three or more charged leptons is a very rare process in proton-proton (pp) collisions. These final states provide a promising starting point in the search for physics beyond the SM (BSM). Many models attempting to address the shortcomings of the SM lead to such signatures. Examples include the production of supersymmetric (SUSY) particles [1, 2], SS top quark pairs [3, 4], scalar gluons (sgluons) [5, 6], heavy scalar bosons of extended Higgs sectors [7, 8], Majorana neutrinos [9], and vector-like quarks [10].

In SUSY models [11–19], the decay chain of pair-produced gluinos or squarks can contain multiple W or Z bosons, with the potential to have at least one pair of SS W bosons. Such a decay chain is realized, for example in gluino pair production, when a gluino decays into a top quark-antiquark pair and a neutralino, or into a pair of quarks and a chargino that subsequently decays into a W boson and a neutralino. In R parity [20] conserving (RPC) scenarios, the lightest SUSY particle is neutral and stable and escapes detection, leading to an imbalance in the measured transverse momentum. The magnitude of the missing transverse momentum strongly depends on the details of the model, and in particular on the mass spectrum of the particles involved. Scenarios with R parity violation (RPV) [21, 22] additionally allow decays of SUSY particles into SM particles only, leading in many cases to signatures with little or no missing transverse momentum. For many SUSY models, the SS and multilepton signatures provide complementarity with searches in the zero- or one-lepton final states, and they are particularly suitable for probing compressed mass spectra and other scenarios involving low-momentum leptons or low missing transverse momentum. Both the ATLAS [23] and CMS [24, 25] Collaborations have carried out searches in these channels using LHC data collected up to and including 2016. The ATLAS Collaboration has also recently released a search with the full data set recorded between 2015 and 2018 [26].

In this paper, we extend and refine the searches described in Refs. [24, 25] using a larger data set of pp collisions at $\sqrt{s} = 13$ TeV recorded by the CMS detector at the CERN LHC in 2016–2018, corresponding to an integrated luminosity of 137 fb^{-1} . We base our search on an initial selection of events with at least two hadronic jets and two SS or three or more light leptons (electrons and muons), including those from leptonic decays of τ leptons. Several signal regions (SRs) are then constructed with requirements on variables such as the number of leptons, the number of jets (possibly identified as originating from b quarks), and the magnitude of missing transverse momentum. A simultaneous comparison of the observed and SM plus BSM expected event yields in all SRs is performed to constrain the BSM models described in Section 2. After a brief description of the CMS experiment in Section 3, we present the details of the search strategy and event selection in Section 4 and discuss the various relevant backgrounds from SM processes in Section 5. The systematic uncertainties considered in the analysis are presented in Section 6. In Section 7, the observed yields are compared to the background expectation and the results are interpreted to constrain the various BSM models introduced earlier. Model independent limits are also derived. Finally, the main results are summarized in Section 8.

2 Background and signal simulation

Monte Carlo (MC) simulations are used to study the SM backgrounds and to estimate the event selection efficiency of the BSM signals under consideration. Three sets of simulated events for each process are used in order to match the different data taking conditions in 2016, 2017, and 2018.

The hard scattering process of the dominant backgrounds estimated from simulation (including the $t\bar{t}W$, $t\bar{t}Z$ and WZ contributions) is simulated with the MADGRAPH5_aMC@NLO 2.2.2 (2.4.2) [27–29] generator for 2016 (2017 and 2018) conditions. An exception is the WZ process for the 2016 conditions that, as with a few subdominant backgrounds, is simulated using the POWHEG v2 [30–34] next-to-leading order (NLO) generator. Samples of signal events, as well as of SS W boson pairs and other very rare SM processes, are generated at leading order (LO) accuracy with MADGRAPH5_aMC@NLO, with up to two additional partons in the matrix element calculations. The set of parton distribution functions (PDFs) used was NNPDF3.0 [35] for the 2016 simulation and NNPDF3.1 [36] for the 2017 and 2018 simulations.

Parton showering and hadronization, as well as the double parton scattering production of $W^\pm W^\pm$, are described using the PYTHIA 8.230 generator [37] with the CUETP8M1 (CP5) underlying event tune for 2016 (2017 and 2018) simulation [38–40]. The response of the CMS detector is modeled using the GEANT4 program [41] for SM background samples, while the CMS fast simulation package [42, 43] is used for signal samples.

To improve the MADGRAPH5_aMC@NLO modeling of the multiplicity of additional jets from initial-state radiation (ISR), 2016 MC events are reweighted according to the number of ISR jets (N_j^{ISR}). The reweighting factors are extracted from a study of the light-flavor jet multiplicity in dilepton $t\bar{t}$ events. They vary between 0.92 and 0.77 for N_j^{ISR} between 1 and 4, with one half of the deviation from unity taken as the systematic uncertainty. This reweighting is not necessary for the 2017 and 2018 MC samples that are generated using an updated PYTHIA tune.

The phenomenology of a given SUSY model strongly depends on its underlying details such as the masses of the SUSY particles and their couplings with the SM particles and each other, many of which can be free parameters. The signal models used by this search are simplified SUSY models [44, 45] of either gluino or squark pair production, followed by a variety of RPC (Figs. 1 and 2) or RPV (Fig. 3) decays and where several leptons can arise in the final state. Production cross sections are calculated at approximate next-to-next-to-leading order plus next-to-next-to-leading logarithmic (NNLO+NNLL) accuracy [46–58]. The branching fractions for the decays shown are assumed to be 100%, unless otherwise specified, and all decays are assumed to be prompt.

Gluino pair production models giving rise to signatures with up to four b quarks and up to four W bosons are shown in Fig. 1. In these models, the gluino decays to the lightest squark ($\tilde{g} \rightarrow \tilde{q}q$), which in turn decays to same-flavor ($\tilde{q} \rightarrow q\tilde{\chi}_1^0$) or different-flavor ($\tilde{q} \rightarrow q'\tilde{\chi}_1^\pm$) quarks. The chargino ($\tilde{\chi}_1^\pm$) decays to a W boson and a neutralino ($\tilde{\chi}_1^0$) via $\tilde{\chi}_1^\pm \rightarrow W^\pm \tilde{\chi}_1^0$, where the $\tilde{\chi}_1^0$ is taken to be the lightest stable SUSY particle and escapes detection.

The first scenario, denoted by T1tttt and displayed in Fig. 1a, includes an off-shell top squark (\tilde{t}) leading to the three-body decay of the gluino, $\tilde{g} \rightarrow t\bar{t}\tilde{\chi}_1^0$, resulting in events with four W bosons and four b quarks. Figure 1b presents a similar model (T5ttbbWW) where the gluino decay results in a chargino that further decays into a neutralino and a W boson. The model shown in Fig. 1c (T5tttt) is the same as T1tttt except that the intermediate top squark is on-shell. The mass splitting between the \tilde{t} and the $\tilde{\chi}_1^0$ is taken to be $m_{\tilde{t}} - m_{\tilde{\chi}_1^0} = m_t$, where m_t is the top quark mass. This choice maximizes the kinematic differences between this model and T1tttt, and also corresponds to one of the most challenging regions of parameter space for the observation of the $\tilde{t} \rightarrow t\tilde{\chi}_1^0$ decay since the neutralino is produced at rest in the top squark rest frame. The decay chain of Fig. 1d (T5ttcc) is identical to that of T5tttt except that the \tilde{t} decay involves a c quark. In Fig. 1e, the decay process includes a virtual light-flavor squark, leading to three-body decays of $\tilde{g} \rightarrow qq'\tilde{\chi}_1^\pm$ or $\tilde{g} \rightarrow qq'\tilde{\chi}_2^0$, with a resulting signature

of two W bosons, two Z bosons, or one of each (the case shown in Fig. 2e), and four light-flavor jets. This model, T5qqqqWZ, with a resulting signature of one W boson and one Z boson, is studied with two different assumptions for the chargino mass: $m_{\tilde{\chi}_1^\pm} = 0.5(m_{\tilde{g}} + m_{\tilde{\chi}_1^0})$, and $m_{\tilde{\chi}_1^\pm} = m_{\tilde{\chi}_1^0} + 20 \text{ GeV}$, producing on- and off-shell bosons, respectively. The model is also considered with the assumption of decays to two W bosons exclusively (T5qqqqWW).

Figure 2a shows a model of bottom squark production with subsequent decay of $\tilde{b}_1 \rightarrow t\tilde{\chi}_1^\pm$, yielding two b quarks and four W bosons. This model, T6ttWW, is considered as a function of the the lightest bottom squark, \tilde{b}_1 , and $\tilde{\chi}_1^\pm$ masses. The $\tilde{\chi}_1^0$ mass is fixed to be 50 GeV, causing two of the W bosons to be produced off-shell when the $\tilde{\chi}_1^\pm$ mass is less than approximately 130 GeV. Figure 2b displays a model similar to T6ttWW, but with top squark pair production and a subsequent decay of $\tilde{t}_2 \rightarrow \tilde{t}_1 H/Z$, with $\tilde{t}_1 \rightarrow t\tilde{\chi}_1^0$, producing signatures with two H bosons, two Z bosons, or one of each. In this model, T6ttHZ, the $\tilde{\chi}_1^0$ mass is fixed such that $m(\tilde{t}_1) - m(\tilde{\chi}_1^0) = m_t$.

The R parity violating decays considered in this analysis are T1qqqqL (Fig. 3a) and T1tbs (Fig. 3b). In T1qqqqL, the gluino decays to the lightest squark ($\tilde{g} \rightarrow \tilde{q}q$), which in turn decays to a quark ($\tilde{q} \rightarrow q\tilde{\chi}_1^0$), but decays with the $\tilde{\chi}_1^0$ off shell (violating R parity) into two quarks and a charged lepton, giving rise to a prompt 5-body decay of the gluino. In T1tbs, each gluino decays into three different SM quarks (a top, a bottom, and a strange quark).

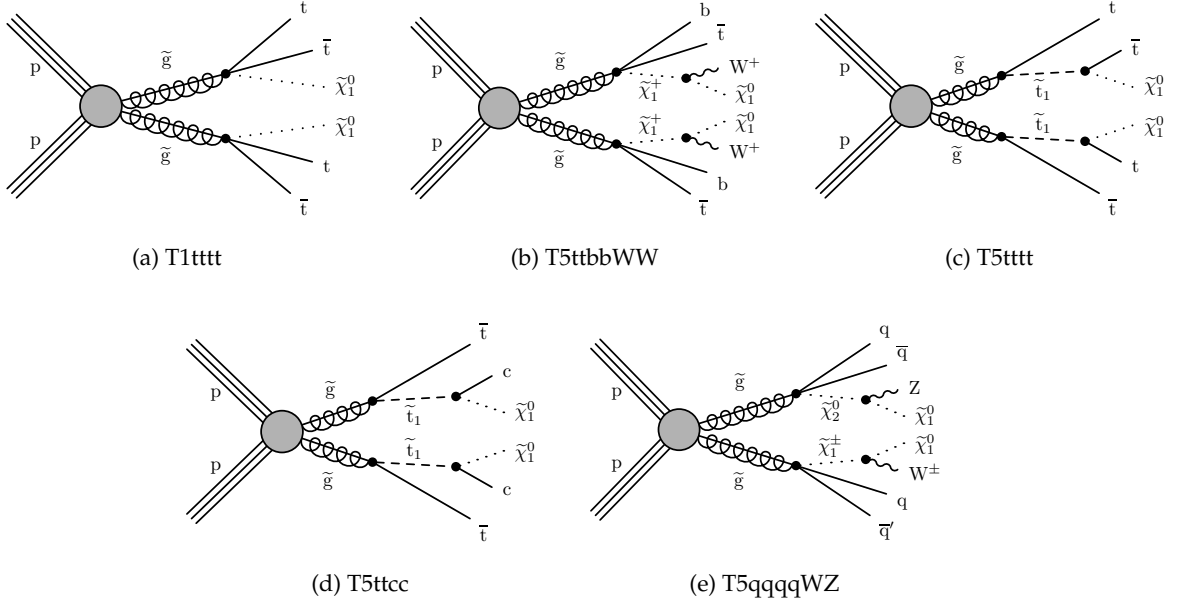


Figure 1: Diagrams illustrating the simplified RPC SUSY models with gluino production considered in this analysis.

3 The CMS detector and event reconstruction

The central feature of the CMS detector is a superconducting solenoid of 6 m internal diameter, providing a magnetic field of 3.8 T. Within the solenoid volume are a silicon pixel and strip tracker, a lead tungstate crystal electromagnetic calorimeter (ECAL), and a brass and scintillator hadron calorimeter (HCAL), each composed of a barrel and two endcap sections. Forward calorimeters extend the pseudorapidity (η) coverage provided by the barrel and endcap detectors. Muons are detected in gas-ionization chambers embedded in the steel flux-return yoke

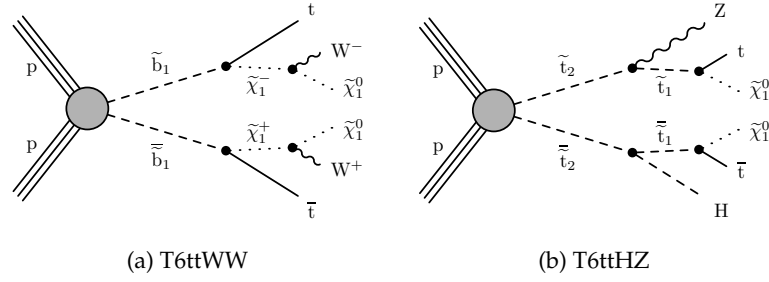


Figure 2: Diagrams illustrating the simplified RPC SUSY models with squark production considered in this analysis.

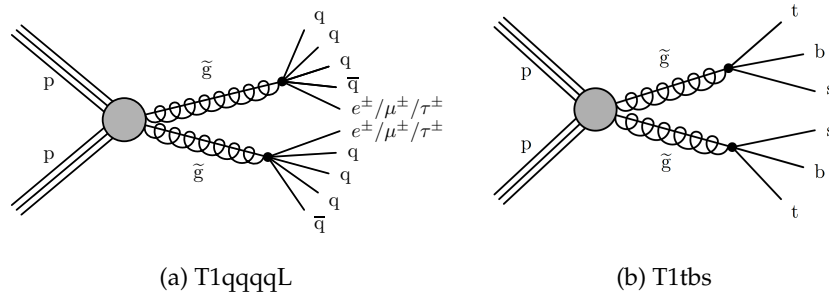


Figure 3: Diagrams illustrating the two simplified RPV SUSY models considered in this analysis.

outside the solenoid. A more detailed description of the CMS detector, together with a definition of the coordinate system used and the relevant kinematic variables, can be found in Ref. [59].

Events of interest are selected using a two-tiered trigger system [60]. The first level, composed of custom hardware processors, uses information from the calorimeters and muon detectors to select events at a rate of around 100 kHz within a fixed time interval of less than $4 \mu\text{s}$. The second level, known as the high-level trigger, consists of a farm of processors running a version of the full event reconstruction software optimized for fast processing, and reduces the event rate to around 1 kHz before data storage.

The reconstructed vertex with the largest value of summed physics-object squared-transverse-momentum is taken to be the primary pp interaction vertex. The physics objects are the jets, clustered using the jet finding algorithm of Refs. [61, 62] with the tracks assigned to the vertex as inputs, and the associated missing transverse momentum, taken as the negative vector sum of the transverse momentum (p_T) of those jets.

The particle-flow (PF) algorithm [63] aims to reconstruct and identify each individual particle in an event, with an optimized combination of information from the various elements of the CMS detector. The energy of photons is directly obtained from the ECAL measurement. The energy of electrons is determined from a combination of the electron momentum at the primary interaction vertex as determined by the tracker, the energy of the corresponding ECAL cluster, and the energy sum of all bremsstrahlung photons spatially compatible with the electron track [64]. The momentum of muons is obtained from the curvature of the corresponding track, combining information from the silicon tracker and the muon system [65]. The energy of charged hadrons is determined from a combination of their momentum measured in the tracker and the matching ECAL and HCAL energy deposits, corrected for the response function of the calorimeters to hadronic showers. The energy of neutral hadrons is obtained from

the corresponding corrected ECAL and HCAL energies.

Hadronic jets are clustered from charged PF candidates associated with the primary vertex and from all neutral PF candidates using the anti- k_T algorithm [61, 62] with a distance parameter of 0.4. The jet momentum is determined as the vectorial sum of all PF candidate momenta in the jet. An offset correction is applied to jet energies to take into account the contribution from pileup [66]. Additional jet energy corrections are derived from simulation to bring the detector response to unity, and are improved with in situ measurements of the energy balance in dijet, multijet, photon+jets, and leptonically decaying Z+jets events [67, 68]. Additional selection criteria are applied to each jet to remove jets potentially dominated by instrumental effects or reconstruction failures. Jets originating from b quarks are identified as b-tagged jets using a deep neural network algorithm, DeepCSV [69], with a working point chosen such that the efficiency to identify a b jet is 55–70% for a jet p_T between 20 and 400 GeV. The misidentification rate for a light-flavor jet is 1–2% in the same jet p_T range.

The vector \vec{p}_T^{miss} is defined as the projection onto the plane perpendicular to the beams of the negative vector sum of the momenta of all reconstructed PF candidates in an event [70]. Its magnitude, called missing transverse momentum, is referred to as p_T^{miss} . The scalar p_T sum of all jets in an event is referred to as H_T .

4 Search strategy and event selection

The search strategy is similar to the one adopted in Refs. [24, 25]. The event selection requires the presence of at least two hadronic jets and at least two leptons, among which is an SS pair, as described below. Each selected event is assigned to an SR, based on its content. Maximum likelihood fits of the background (or signal plus background) predictions to the data in all SRs are then performed. Such a strategy ensures sensitivity to a broad range of possible signatures of new physics, even beyond the signal benchmarks considered in this analysis.

The kinematic requirements applied to leptons and jets are presented in Table 1. The analysis requires at least two jets with $p_T > 40$ GeV and two light SS leptons with $p_T > 15$ GeV (10 GeV) for electrons (muons). Electrons are identified based on a discriminant using shower shape and track quality variables, while the muon identification relies on the quality of the geometrical matching between the tracker and muon system measurements. In order to reject leptons from the decay of heavy flavor hadrons, the tracks are required to have an impact parameter compatible with the position of the primary vertex. Several isolation criteria are also applied, based on the scalar sum of hadron and photon p_T within a cone centered on the lepton direction and whose radius decreases with its p_T , the ratio of the p_T of the lepton to that of the closest jet, and the relative p_T of the lepton to that of the closest jet after lepton momentum subtraction. These criteria are designed to mitigate the loss of lepton efficiency caused by lepton-jet overlaps that occurs frequently in events with significant hadronic activity. A more detailed description of the set of identification and isolation variables used in the lepton selection can be found in Ref. [71].

The lepton reconstruction and identification efficiency is in the range of 45–70% (70–90%) for electrons (muons), with $p_T > 25$ GeV, increasing as a function of p_T and reaching the maximum value for $p_T > 60$ GeV. In the low-momentum regime, $15 < p_T < 25$ GeV for electrons and $10 < p_T < 25$ GeV for muons, the efficiencies are approximately 40% for electrons and 55% for muons. The lepton trigger efficiency for electrons is in the range of 90–98%, converging to the maximum value for $p_T > 30$ GeV, and it is around 92% for muons.

Table 1: Transverse momentum and pseudorapidity requirements for leptons and jets. Note that the p_T thresholds to count jets and b-tagged jets are different; the jet multiplicity N_{jets} includes b-tagged jets if their p_T exceeds 40 GeV.

| Object | p_T (GeV) | $ \eta $ |
|---------------|-------------|----------|
| Electrons | >15 | <2.5 |
| Muons | >10 | <2.4 |
| Jets | >40 | <2.4 |
| b-tagged jets | >25 | <2.4 |

In order to reduce backgrounds from the decays of c- and b-hadrons or from the Drell–Yan process, we reject events with same-flavor lepton pairs with invariant mass ($m_{\ell\ell}$) less than 12 GeV, where leptons are reconstructed with a looser set of requirements compared to the nominal selection. Furthermore, events containing a lepton pair with $m_{\ell\ell} < 8$ GeV, regardless of charge or flavor, are rejected in order to emulate a similar condition applied at the trigger level. Events are then separated according to the p_T of the leptons forming the SS pair: high-high if both have $p_T > 25$ GeV, low-low if both have $p_T < 25$ GeV, and high-low otherwise.

Two sets of trigger algorithms are used to select the events: pure dilepton triggers, which require the presence of two isolated leptons with p_T thresholds on the leading (subleading) lepton in the 17–23 (8–12) GeV range, and dilepton triggers with no isolation requirements, a lower p_T threshold of 8 GeV, an invariant mass condition $m_{\ell\ell} > 8$ GeV to reject low mass resonances, and with a minimum H_T in the range of 300–350 GeV. The ranges listed here reflect the varying trigger conditions during the data taking periods. The pure dilepton triggers are used to select high-high and high-low pairs, while low-low pairs are selected using the triggers with H_T requirements.

Six exclusive categories are then defined as follows:

- High-High SS pair, significant p_T^{miss} (HH): exactly 2 leptons, both with $p_T > 25$ GeV, and $p_T^{\text{miss}} > 50$ GeV;
- High-Low SS pair, significant p_T^{miss} (HL): exactly 2 leptons, one with $p_T > 25$ GeV, one with $p_T < 25$ GeV, and $p_T^{\text{miss}} > 50$ GeV;
- Low-Low SS pair, significant p_T^{miss} (LL): exactly 2 leptons, both with $p_T < 25$ GeV and $p_T^{\text{miss}} > 50$ GeV;
- Low p_T^{miss} (LM): exactly 2 leptons, both with $p_T > 25$ GeV, and $p_T^{\text{miss}} < 50$ GeV; and
- Multilepton with an on-shell Z boson (on-Z ML): ≥ 3 leptons, at least one with $p_T > 25$ GeV, $p_T^{\text{miss}} > 50$ GeV, \geq Z boson candidate formed by a pair of opposite-sign (OS), same-flavor leptons with $76 < m_{\ell\ell} < 106$ GeV.
- Multilepton without an on-shell Z boson (off-Z ML): same as on-Z ML but without a Z boson candidate.

The categories are typically sensitive to different new physics scenarios and enriched in different SM backgrounds. For example the HH category drives the sensitivity for most of the RPC scenarios (T1tttt, T5ttbbWW, T5tttt, T1tttt, T5qqqqWW) with a large mass splitting between the gluino and the lightest neutralino. The HL and LL categories become relevant for a lower mass splitting when one or both leptons tend to be soft. Scenarios resulting in the presence of one or multiple Z bosons in the final state such as T5qqqqWZ and T6ttHZ will typically be primarily constrained by the on-Z or off-Z category, also depending on the considered SUSY mass spectrum. Finally the LM category enhances the analysis sensitivity for RPV scenarios, in particular for T1qqqqL where no genuine p_T^{miss} is expected.

Various SRs are constructed based on the jet multiplicity N_{jets} , the b-tagged jet multiplicity N_b , H_T , p_T^{miss} , the charge of the SS pair, and m_T^{min} , which is defined below. The m_T^{min} variable, introduced in Ref. [71], is defined as the minimum of the transverse masses calculated from each of the leptons forming the SS pair and \bar{p}_T^{miss} , except for the on-Z ML category where we only consider the transverse mass computed using the leptons not forming the Z candidate. It is characterized by a kinematic cutoff for events where p_T^{miss} only arises from the leptonic decay of a single W boson and is effective at discriminating signal and background signatures.

A subset of SRs is split by the charge of the leptons in an SS pair which is used to take advantage of the charge asymmetry in most of the background processes, such as WZ, $t\bar{t}W$ or SS WW. The SRs corresponding to each category, HH, HL, LL, LM, on-Z ML, and off-Z ML, are summarized in Tables 2, 3, 4, 5, 6 and 7, respectively. The binning ranges are chosen to maximize the sensitivity to a variety of SUSY benchmark points and are such that the expected SM yield in any SR has relative statistical uncertainties typically smaller than unity.

Table 2: The SR definitions for the HH category. Charge-split regions are indicated with (++) and (--). The three highest H_T regions are split only by N_{jets} , resulting in 62 regions in total. Quantities are specified in units of GeV where applicable.

| N_b | m_T^{min} | p_T^{miss} | N_{jets} | $H_T < 300$ | $H_T \in [300, 1125]$ | $H_T \in [1125, 1300]$ | $H_T \in [1300, 1600]$ | $H_T > 1600$ |
|-----------|--------------------|---------------------|-----------------------|--------------------------|-----------------------|---|---|---|
| 0 | <120 | 50–200 | 2–4 | SR1 | SR2 | SR54 $N_{\text{jets}} < 5$ | SR55 $N_{\text{jets}} < 5$ | SR56 $N_{\text{jets}} < 5$ |
| | | | ≥ 5 | SR3 | SR4 | | | |
| | | 200–300 | 2–4 | | SR5 (++) / SR6 (--) | | | |
| | ≥ 5 | | SR7 | | | | | |
| | >120 | 50–200 | 2–4 | | SR8 (++) / SR9 (--) | | | |
| | | | ≥ 5 | | SR10 | | | |
| 200–300 | | 2–4 | | | | | | |
| 1 | <120 | 50–200 | 2–4 | SR11 | SR12 | SR57 $N_{\text{jets}} = 5 \text{ or } 6$ | SR58 $N_{\text{jets}} = 5 \text{ or } 6$ | SR59 $N_{\text{jets}} = 5 \text{ or } 6$ |
| | | | ≥ 5 | SR13 (++) / SR14 (--) | SR15 (++) / SR16 (--) | | | |
| | | 200–300 | 2–4 | | SR17 (++) / SR18 (--) | | | |
| | ≥ 5 | | SR19 | | | | | |
| | >120 | 50–200 | 2–4 | | SR20 (++) / SR21 (--) | | | |
| | | | ≥ 5 | | SR22 | | | |
| 200–300 | | 2–4 | | | | | | |
| 2 | <120 | 50–200 | 2–4 | SR23 | SR24 | SR60 $N_{\text{jets}} > 6$ | SR61 $N_{\text{jets}} > 6$ | SR62 $N_{\text{jets}} > 6$ |
| | | | ≥ 5 | SR25 (++) / SR26 (--) | SR27 (++) / SR28 (--) | | | |
| | | 200–300 | 2–4 | | SR29 (++) / SR30 (--) | | | |
| | ≥ 5 | | SR31 | | | | | |
| | >120 | 50–200 | 2–4 | | SR32 (++) / SR33 (--) | | | |
| | | | ≥ 5 | | SR34 | | | |
| 200–300 | | 2–4 | | | | | | |
| ≥ 3 | <120 | 50–200 | 2–4 | SR35 (++) / SR36 (--) | SR37 (++) / SR38 (--) | SR46 (++) / SR47 (--) | SR48 (++) / SR49 (--) | SR50 (++) / SR51 (--) |
| | | | ≥ 5 | SR36 (--) | SR39 (++) / SR40 (--) | | | |
| | | 200–300 | 2–4 | | SR37 (++) / SR38 (--) | | | |
| | ≥ 5 | | SR39 (++) / SR40 (--) | | | | | |
| | >120 | 50–300 | 2–4 | | SR42 (++) / SR43 (--) | | | |
| | | | ≥ 5 | | SR41 | | | |
| 200–300 | | 2–4 | | | | | | |
| Inclusive | Inclusive | 300–500 | 2–4 | — | SR46 (++) / SR47 (--) | | | |
| | | >500 | ≥ 5 | | SR48 (++) / SR49 (--) | | | |
| | | 300–500 | | | SR50 (++) / SR51 (--) | | | |
| | | >500 | | | SR52 (++) / SR53 (--) | | | |

Table 3: The SR definitions for the HL category. Charge-split regions are indicated with (++) and (--). There are 43 regions in total. Quantities are specified in units of GeV where applicable.

| N_b | m_T^{\min} | p_T^{miss} | N_{jets} | $H_T < 300$ | $H_T \in [300, 1125]$ | $H_T \in [1125, 1300]$ | $H_T > 1300$ |
|-----------|--------------|---------------------|-------------------|--------------------------|-----------------------|--------------------------|--------------------------|
| 0 | <120 | 50–200 | 2–4 | SR1 | SR2 | SR40 (++) / SR41 (--) | SR42 (++) / SR43 (--) |
| | | | ≥ 5 | | SR4 | | |
| | | 200–300 | 2–4 | SR3 | SR5 (++) / SR6 (--) | | |
| | | | ≥ 5 | | SR7 | | |
| 1 | <120 | 50–200 | 2–4 | SR8 | SR9 | | |
| | | | ≥ 5 | SR10 (++) / SR11 (--) | SR12 (++) / SR13 (--) | | |
| | | 200–300 | 2–4 | | SR14 | | |
| | | | ≥ 5 | | SR15 (++) / SR16 (--) | | |
| 2 | <120 | 50–200 | 2–4 | SR17 | SR18 | | |
| | | | ≥ 5 | SR19 (++) / SR20 (--) | SR21 (++) / SR22 (--) | | |
| | | 200–300 | 2–4 | | SR23 (++) / SR24 (--) | | |
| | | | ≥ 5 | | SR25 | | |
| ≥ 3 | <120 | 50–200 | ≥ 2 | SR26 (++) / SR27 (--) | SR28 (++) / SR29 (--) | | |
| | | 200–300 | | SR30 | | | |
| Inclusive | >120 | 50–300 | ≥ 2 | SR31 | SR32 | | |
| Inclusive | Inclusive | 300–500 | 2–4 | — | SR33 (++) / SR34 (--) | | |
| | | >500 | | | SR35 (++) / SR36 (--) | | |
| | | 300–500 | ≥ 5 | | SR37 (++) / SR38 (--) | | |
| | | >500 | | | SR39 | | |

Table 4: The SR definitions for the LL category. All SRs in this category require $N_{\text{jets}} \geq 2$. There are 8 regions in total. Quantities are specified in units of GeV where applicable.

| N_b | m_T^{\min} | H_T | $p_T^{\text{miss}} \in [50, 200]$ | $p_T^{\text{miss}} > 200$ |
|-----------|--------------|-------|-----------------------------------|---------------------------|
| 0 | <120 | >400 | SR1 | SR2 |
| 1 | | | SR3 | SR4 |
| 2 | | | SR5 | SR6 |
| ≥ 3 | | | SR7 | |
| Inclusive | >120 | | SR8 | |

Table 5: The SR definitions for the LM category. All SRs in this category require $p_T^{\text{miss}} < 50$ GeV and $H_T > 300$ GeV. The two high- H_T regions are split only by N_{jets} , resulting in 11 regions in total. Quantities are specified in units of GeV where applicable.

| N_b | N_{jets} | $H_T \in [300, 1125]$ | $H_T \in [1125, 1300]$ | $H_T > 1300$ |
|----------|-------------------|-----------------------|----------------------------------|-----------------------------------|
| 0 | 2–4 | SR1 | SR8 ($N_{\text{jets}} < 5$) | SR10 ($N_{\text{jets}} < 5$) |
| | ≥ 5 | SR2 | | |
| 1 | 2–4 | SR3 | | |
| | ≥ 5 | SR4 | | |
| 2 | 2–4 | SR5 | SR9 ($N_{\text{jets}} \geq 5$) | SR11 ($N_{\text{jets}} \geq 5$) |
| | ≥ 5 | SR6 | | |
| ≥ 3 | ≥ 2 | SR7 | | |

Table 6: The SR definitions for the on-Z ML category. All SRs in these categories require $N_{\text{jets}} \geq 2$. Regions marked with † are split by $m_T^{\text{min}} = 120 \text{ GeV}$, with the high- m_T^{min} region specified by the second SR label. There are 23 regions in total. Quantities are specified in units of GeV where applicable.

| N_b | H_T | $p_T^{\text{miss}} \in [50, 150]$ | $p_T^{\text{miss}} \in [150, 300]$ | $p_T^{\text{miss}} \geq 300$ |
|-----------|------------|-----------------------------------|------------------------------------|------------------------------|
| 0 | <400 | SR1/SR2 † | SR3/SR4 † | SR22/SR23 † |
| | 400–600 | SR5/SR6 † | SR7/SR8 † | |
| 1 | <400 | SR9 | SR10 | |
| | 400–600 | SR11 | SR12 | |
| 2 | <400 | SR13 | SR14 | |
| | 400–600 | SR15 | SR16 | |
| ≥ 3 | <600 | SR17 | | |
| Inclusive | ≥ 600 | SR18/SR19 † | SR20/SR21 † | |

Table 7: The SR definitions for the off-Z category. All SRs in these categories require $N_{\text{jets}} \geq 2$. Regions marked with † are split by $m_T^{\text{min}} = 120 \text{ GeV}$, with the high- m_T^{min} region specified by the second SR label. There are 21 regions in total. Quantities are specified in units of GeV where applicable.

| N_b | H_T | $p_T^{\text{miss}} \in [50, 150]$ | $p_T^{\text{miss}} \in [150, 300]$ | $p_T^{\text{miss}} \geq 300$ |
|-----------|------------|-----------------------------------|------------------------------------|------------------------------|
| 0 | <400 | SR1/SR2 † | SR3/SR4 † | SR20/SR21 † |
| | 400–600 | SR5 | SR6 | |
| 1 | <400 | SR7 | SR8 | |
| | 400–600 | SR9 | SR10 | |
| 2 | <400 | SR11 | SR12 | |
| | 400–600 | SR13 | SR14 | |
| ≥ 3 | <600 | SR15 | | |
| Inclusive | ≥ 600 | SR16/SR17 † | SR18/SR19 † | |

5 Backgrounds

Several SM processes can lead to the signatures studied in this analysis. There are three background categories, depending on the lepton content of the event:

- Events with two or more prompt leptons, including an SS pair;
- Events with at least one nonprompt lepton (defined below); and
- Events with a pair of OS leptons, one of which is reconstructed with the wrong charge.

The first category includes a variety of low cross section processes where multiple electroweak bosons are produced, possibly in the decay of top quarks, which then decay leptonically leading to an SS lepton pair. This category usually dominates the background yields in SRs with large p_T^{miss} or H_T and in most of the ML SRs with a Z candidate. The main contributions arise from the production of a WZ or an SS W pair, or of a $t\bar{t}$ pair in association with a W, Z or H boson. The event yields for these processes are estimated individually. In contrast, the expected event yields from other rare processes (including ZZ, triple boson production, tWZ , tZq , $t\bar{t}\bar{t}$, and double parton scattering) are summed up into a single contribution denoted as “Rare”. Processes including a genuine photon, such as $W\gamma$, $Z\gamma$, $t\bar{t}\gamma$, and $t\gamma$, are also considered and grouped together. They are referred to as “ $X\gamma$ ”. All contributions from this category are estimated using simulated samples. Correction factors are applied to take into account small differences between data and simulation, including trigger, lepton selection, and b tagging efficiencies, with associated systematic uncertainties listed in Section 6.

The second category consists of events where one of the selected leptons, generically denoted as “nonprompt lepton”, is either a decay product of a heavy flavor hadron or, more rarely, a misidentified hadron. This category is typically the dominant one in SRs with moderate or low p_T^{miss} or low m_T^{min} (except for the on-Z ML SRs). This background is estimated directly from data using the “tight-to-loose” method [24, 25]. This method is based on the probability for a nonprompt lepton passing loose selection criteria to also satisfy the tighter lepton selection used in the analysis. The number of events in an SR with N leptons, including at least one nonprompt lepton, can be estimated by applying this probability to a corresponding control region (CR) of events with N loose leptons where at least one of them fails the tight selection.

The measurement of the tight-to-loose ratio is performed in a sample enriched in dijet events with exactly one loose lepton, low p_T^{miss} , and low m_T^{min} . This sample is contaminated by prompt leptons from W boson decays. The contamination is estimated from the m_T^{min} distribution, and it is subtracted before calculating the ratio. The tight-to-loose ratio is computed separately for electrons and muons, and is parameterized as a function of the lepton η and p_T^{corr} . The p_T^{corr} variable is defined as the sum of the lepton p_T and the energy in the isolation cone exceeding the isolation threshold value applied to tight leptons. This parametrization improves the stability of the tight-to-loose ratio with respect to variations in the p_T of the partons from which the leptons originate.

The performance of the tight-to-loose ratio was assessed in a MC closure test. A tight-to-loose ratio was extracted from a MC sample of QCD events. This ratio was then used to predict the number of events with one prompt and one nonprompt SS dileptons in MC $t\bar{t}$ and W +jets events. The predicted and observed rates of SS dileptons were compared as a function of kinematic properties and found to agree within 30%. The data driven estimate was also compared to a direct prediction from simulation and a similar level of agreement was reached.

The final category is a subdominant background in all SRs and corresponds to events where

the charge of a lepton is incorrectly measured. Charge misidentification primarily occurs when an electron undergoes bremsstrahlung in the tracker material or in the beam pipe. Similarly to the tight-to-loose method, the number of SS lepton pairs where one of the leptons has its charge misidentified can be determined using the number of OS pairs and the knowledge of the charge misidentification rate. We use simulation to parameterize this rate as a function of p_T and η for electrons and find values varying between 10^{-5} (central electrons with $p_T \approx 20$ GeV) and 5×10^{-3} (forward electrons with $p_T \approx 200$ GeV). To calibrate the charge misidentification rate, we exploit the fact that charge misidentification only has a small effect on the electron energy measurement in the calorimeter. As a result, electron pairs from Z boson decays yield a sharp peak near the Z mass even when one of the electrons has a misidentified charge. The SS dielectron invariant mass distributions in data and MC can then be used to derive a correction factor to the MC charge misidentification rate. Good agreement between data and MC is found in 2016, while the charge misidentification rate in simulation corresponding to 2017 and 2018 data needs to be scaled up by a factor of 1.4. Muon charge misidentification arises from a relatively large uncertainty in the transverse momentum at high momentum or from a poor quality track. The various criteria applied in this analysis on the quality of the muon reconstruction lead to a misidentification rate at least one order of magnitude smaller than for electrons according to simulation. The muon charge misassignment has also been studied using cosmic ray muons with p_T up to several hundred GeV, confirming the predictions from simulation [72]. It is therefore neglected. Correction factors are however applied to the simulation to account for a possible difference in the selection efficiency related to these criteria.

6 Systematic uncertainties

The predicted yields of signal and background processes are affected by several sources of uncertainty, summarized in Table 8. Depending on their source, they are treated as fully correlated or uncorrelated between the three years of data taking. Signal and background contributions estimated from simulation are affected by experimental uncertainties in the efficiency of the trigger, lepton reconstruction and identification [64, 73], the efficiency of b tagging [69], the jet energy scale [67], the integrated luminosity [74–76]. An uncertainty is also assigned to the value of the inelastic cross section, which affects the pileup rate [77] and that can impact the description of the jet multiplicity or the p_T^{miss} resolution. Simulation is also affected by theoretical uncertainties, which are evaluated by varying the factorization and renormalization scales up and down by a factor of two, and by using different PDFs within the NNPDF3.0 and 3.1 PDF sets [35, 36, 78]. These uncertainties can affect both the overall yield (normalization) and the relative population (shape) across the SRs. Background normalization uncertainties are increased to 30%, either to account for the additional hadronic activity required (for WZ and $W^\pm W^\pm$) or to take into consideration recent measurements (for $t\bar{t}W$, $t\bar{t}Z$) [79, 80]. The Rare and $X\gamma$ backgrounds, which are less well understood experimentally and theoretically, are assigned a 50% uncertainty.

To account for possible mismodeling of the flavor of additional jets, an additional 70% uncertainty is applied to $t\bar{t}W$, $t\bar{t}Z$, and $t\bar{t}H$ events produced in association with a pair of b jets, reflecting the measured ratio of $t\bar{t}b\bar{b}/t\bar{t}j\bar{j}$ cross sections reported in Ref. [81].

As discussed in Section 5, the nonprompt lepton and charge misidentification backgrounds are estimated from CRs. The associated uncertainties include the statistical uncertainties in the CR yields, as well as the systematic uncertainties in the extrapolations from the CRs to the SRs, as described below. In the case of the nonprompt lepton background, we include a 30% uncertainty from studies of the closure of the method in simulation. Furthermore, the uncertainty

in the measurement of the tight-to-loose ratio, because of the prompt lepton contamination, results in a 1–30% additional uncertainty in the background yields. The charge misidentification background is assigned a 20% uncertainty based on a comparison of the kinematic properties of simulated and data events in the $Z \rightarrow e^+e^-$ CR with one electron or positron having a misidentified charge.

In general, the systematic uncertainties with the largest impact on the expected limits defined below are related to the lepton identification and isolation scale factors, the cross section of the rare processes, and the WZ background normalization.

Table 8: Summary of the sources of systematic uncertainty and their effect on the yields of different processes in the SRs. The first two groups list experimental and theoretical uncertainties assigned to processes estimated using simulation, while the last group lists uncertainties assigned to processes whose yield is estimated from the data. The uncertainties in the first group also apply to signal samples. Reported values are representative for the most relevant signal regions.

| Source | Typical uncertainty (%) | Correlation across years |
|---------------------------------------|-------------------------|--------------------------|
| Integrated luminosity | 2.3–2.5 | Uncorrelated |
| Lepton selection | 2–10 | Uncorrelated |
| Trigger efficiency | 2–7 | Uncorrelated |
| Pileup | 0–6 | Uncorrelated |
| Jet energy scale | 1–15 | Uncorrelated |
| b tagging | 1–10 | Uncorrelated |
| Simulated sample size | 1–20 | Uncorrelated |
| Scale and PDF variations | 10–20 | Correlated |
| Theoretical background cross sections | 30–50 | Correlated |
| Nonprompt leptons | 30 | Correlated |
| Charge misidentification | 20 | Uncorrelated |
| N_J^{ISR} | 1–30 | Uncorrelated |

7 Results and interpretation

The distributions of the variables used to define the SRs after the event selection are shown in Fig. 4. Background yields shown as stacked histograms in Figs. 4, 5, and 6 are those determined following the prescriptions detailed in Section 5. The overall data yields exceed expectation by an amount close to the systematic uncertainty. However, no particular trend that is not covered by the uncertainties discussed in the previous sections, is seen in the distributions. The significance of the excess is of similar magnitude in all categories, with a maximum of around 2 standard deviations (s.d.) in the off-Z ML category.

The results of the search, broken down by SR, are presented in Figs. 5 and 6, and are summarized in Table 9. No significant deviation with respect to the SM background prediction is observed. The largest excess of events found by fitting the data with the background-only hypothesis is in HH SR54, corresponding to a local significance of 2.6 s.d. Its neighboring bin, HH SR55, which is adjacent along the H_T dimension, has a deficit of events in the data corresponding to a significance of 1.8 s.d.

These results are then interpreted as experimental constraints on the cross sections for the signal models discussed in Section 2. For each model, event yields in all SRs are used to obtain

exclusion limits on the production cross section at 95% confidence level (CL) with an asymptotic formulation of the modified frequentist CL_s criterion [82–85], where uncertainties are incorporated as nuisance parameters and profiled [84]. This procedure takes advantage of the differences in the distribution of events amongst the SR between the various SM backgrounds and the signal considered. The normalizations of the various backgrounds are in particular allowed to float within their uncertainties in the global fit, resulting in several backgrounds (nonprompt lepton, $t\bar{t}W/Z/H$ and rare processes) being pulled up by around 1 s.d. for most of the signal points considered, which are often characterized by a distinctive distribution of events across the SRs. This observation is consistent with the current measurements of $t\bar{t}W$ and $t\bar{t}Z$ processes performed by the ATLAS and CMS Collaborations [79, 80]. The limits obtained are then used together with the theoretical cross section calculations to exclude regions of SUSY parameter space.

Figure 7 shows observed and expected exclusion limits for simplified models of gluino pair production with each gluino decaying to off- or on-shell third-generation squarks. These models were introduced in Section 2 and denoted as T1tttt, T5ttbbWW, T5tttt, and T5ttcc. Similarly, Figs. 8 and 9 show the corresponding limits for T5qqqqWZ and T5qqqqWW, with two different assumptions on the chargino mass. Note that the T5qqqqWZ model assumes equal probabilities for the decay of the gluino into $\tilde{\chi}_1^+$, $\tilde{\chi}_1^-$, and $\tilde{\chi}_2^0$. The exclusion limits for T6ttWW and T6ttHZ are displayed in Figs. 10 and 11, respectively. In the T6ttHZ model, the heavier top squark decays into a lighter top squark and a Z or H boson. The three sets of exclusion limits shown in Fig. 11 correspond to the branching fraction $\mathcal{B}(\tilde{t}_2 \rightarrow \tilde{t}_1 Z)$ having values of 0, 50, and 100%.

Finally, Fig. 12 shows observed and expected limits on the cross section of gluino pair production as a function of the gluino masses in the two RPV models described in Section 2. The observed and expected exclusions on the gluino mass are similar and reach 2.1 and 1.7 TeV for the T1qqqqL and T1tbs models, respectively.

The analysis sensitivity for the various models studied in Figs. 7–11 is often driven by the event yields in a few SRs (off-Z ML21, HH53 and HH52), where a slight excess of data is observed. This in particular applies to the uncompressed mass regime, resulting in an observed limit weaker than the expected one by one or two s.d. In the compressed mass regime, however, other SRs can become dominant, for example when the hadronic activity becomes limited. This happens in the T5qqqqWZ and T5qqqqWW models where the gluino and the lightest neutralino present a limited mass splitting (the region close to the diagonal in the left plots of Figs. 8 and 9). In those scenarios the on-Z ML4 and HH3 SRs provide the best sensitivity, respectively. Additionally, if the intermediate chargino is nearly degenerate in mass with the lightest neutralino, both leptons become soft and LL SRs such as LL2 become relevant. Such a situation is encountered in the phase space region close to the diagonal in the right plots of Figs. 8 and 9. On-Z SRs (especially on-Z ML23) become important for models where an on-shell Z boson is produced (bottom plot in Fig. 11). The limits on the RPV models presented in Fig. 12 are mostly driven by another set of SRs (HH62 and LM11, the latter becoming more relevant for lower masses).

Compared to the previous versions of the analysis [24, 25], the limits for the RPC models extend the gluino and squark mass observed and expected exclusions by up to 200 GeV because of the increase in the integrated luminosity and the corresponding re-optimization of SR definitions. These results also complement searches for gluino pair production conducted by CMS in final states with 0 or 1 lepton [86–88]. For the T1tttt scenario, the expected sensitivity of this analysis suffers from a lower branching fraction that makes it uncompetitive in the uncompressed mass

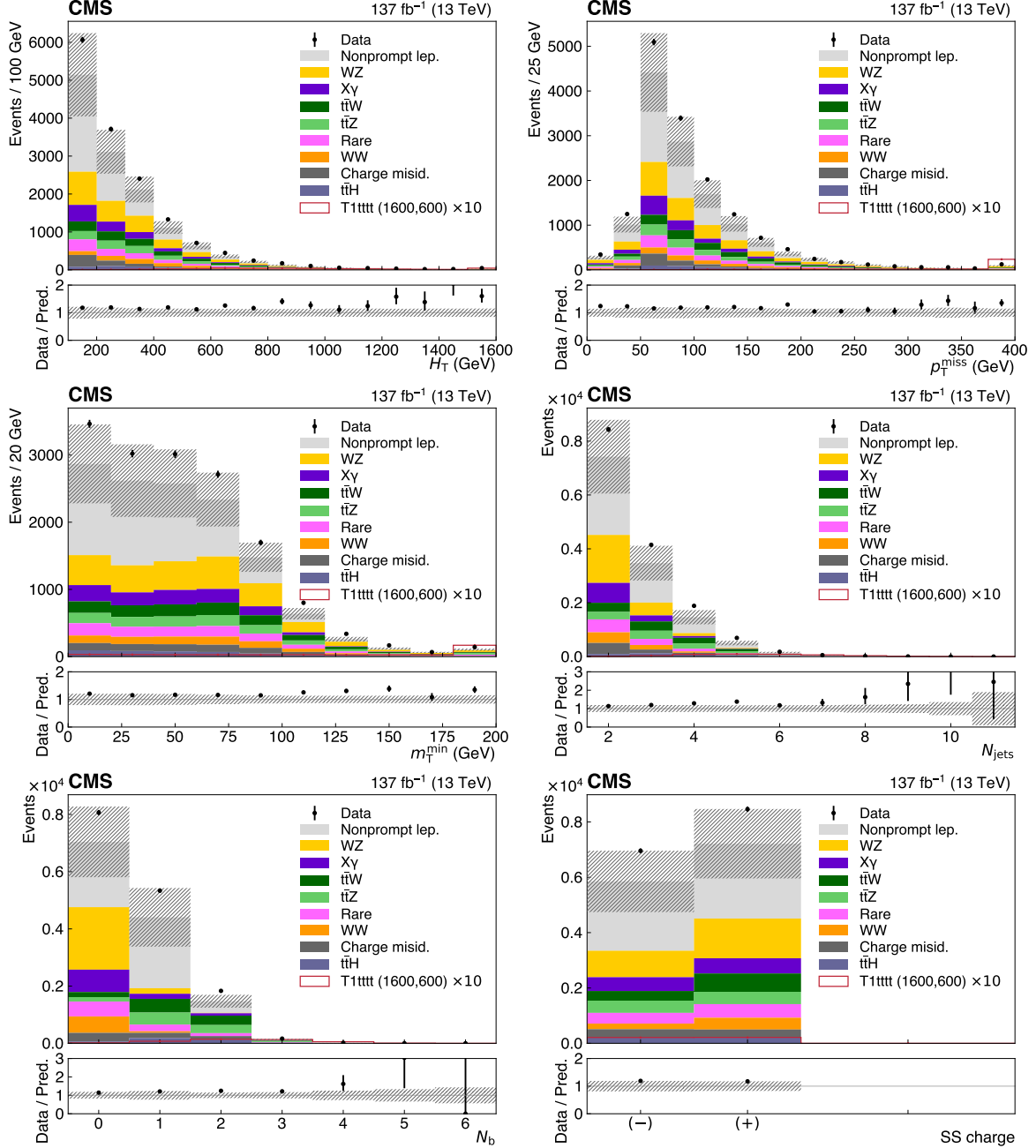


Figure 4: Distributions of the main analysis variables after the event selection: H_T , p_T^{miss} , m_T^{min} , N_{jets} , N_b , and the charge of the SS pair, where the last bin includes the overflow (where applicable). The hatched area represents the total statistical and systematic uncertainty in the background prediction. The lower panels show the ratio of the observed event yield to the background prediction. The prediction for the SUSY model T1tttt with $m_{\tilde{g}} = 1600$ GeV and $m_{\tilde{\lambda}_1} = 600$ GeV is overlaid.

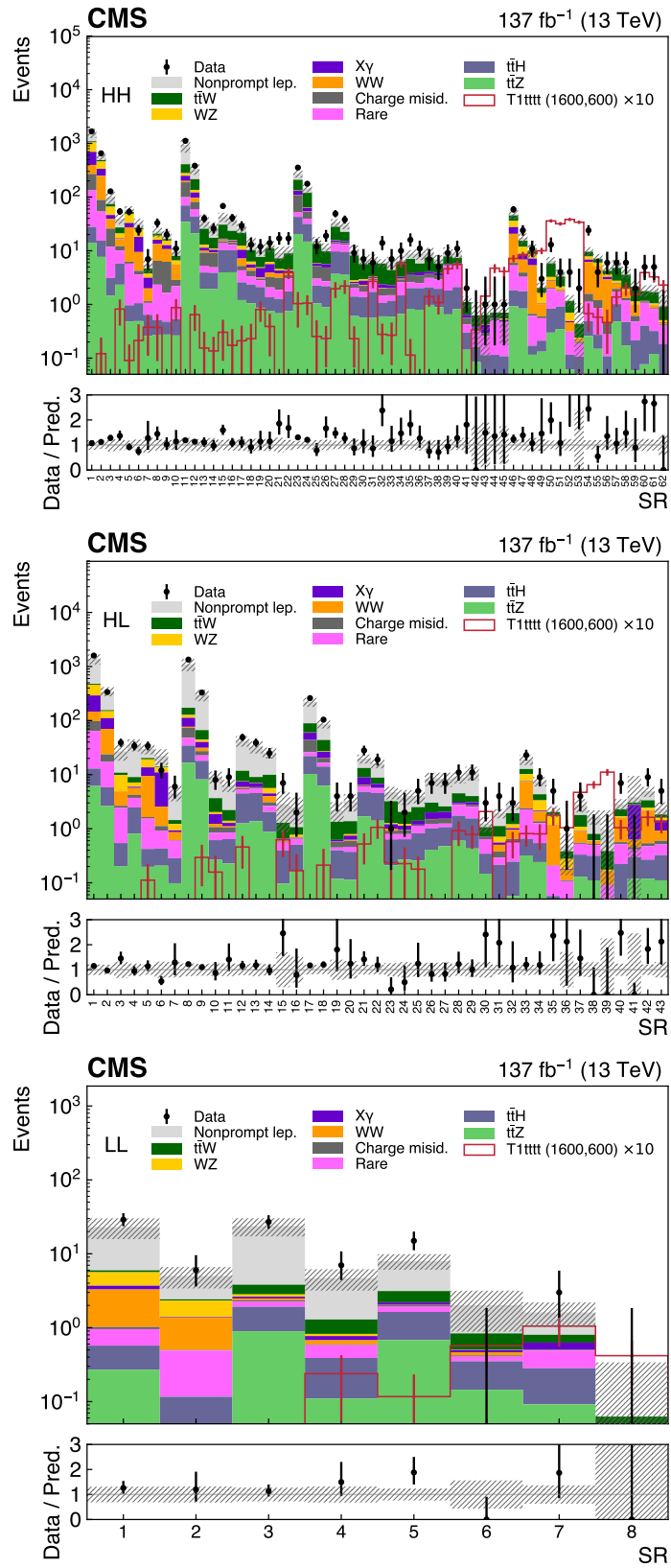


Figure 5: Expected and observed SR yields for the HH, HL, LL signal categories. The hatched area represents the total statistical and systematic uncertainty in the background prediction.

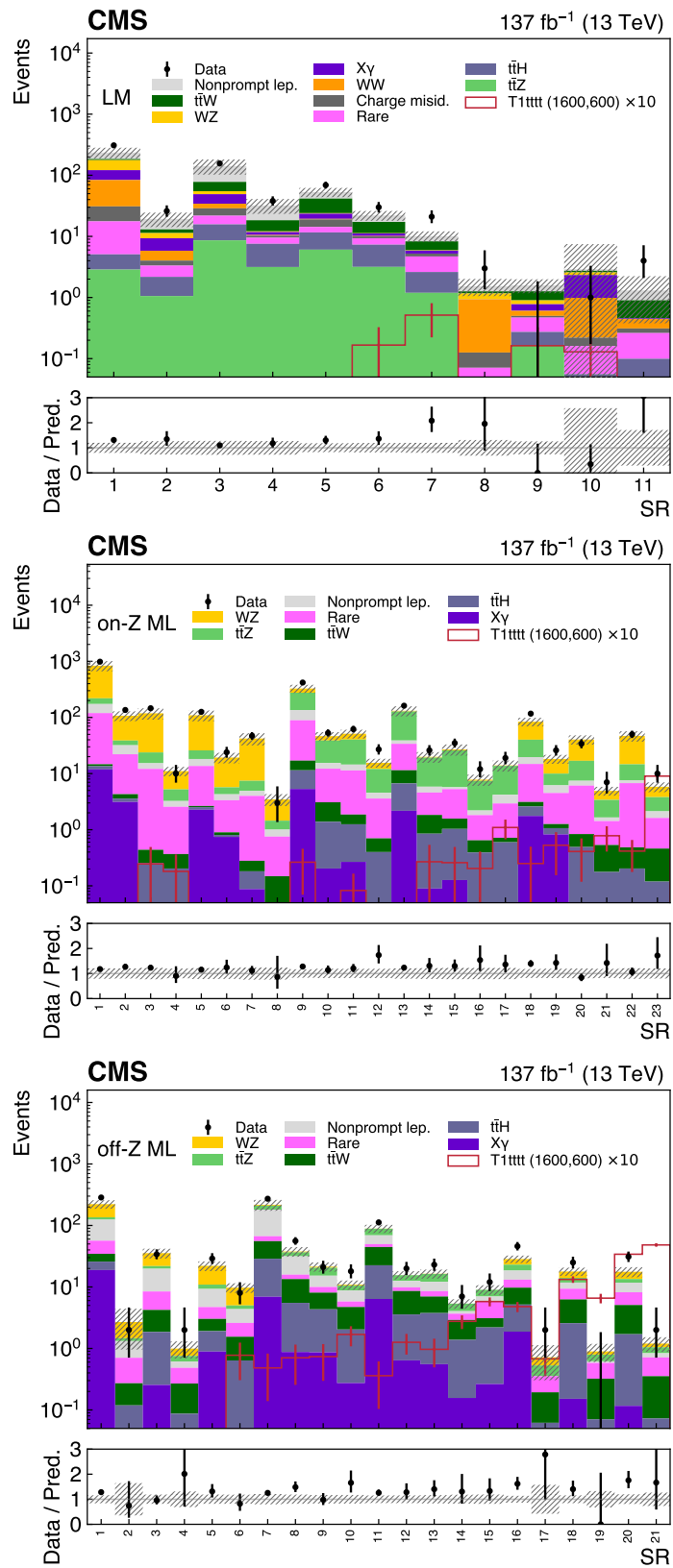


Figure 6: Expected and observed SR yields for the LM, on-Z ML, off-Z ML signal categories. The hatched area represents the total statistical and systematic uncertainty in the background prediction.

Table 9: Expected background event yields, total uncertainties, and observed event yields in the SRs used in this search.

| HH regions | | | HL regions | | | LM regions | | |
|------------|-------------|------|------------|-------------|------|------------------|-------------|------|
| SR | Expected SM | Obs. | SR | Expected SM | Obs. | SR | Expected SM | Obs. |
| 1 | 1560 ± 300 | 1673 | 1 | 1390 ± 300 | 1593 | 1 | 235 ± 47 | 309 |
| 2 | 582 ± 93 | 653 | 2 | 348 ± 67 | 337 | 2 | 19.3 ± 5.2 | 26 |
| 3 | 100 ± 25 | 128 | 3 | 26.9 ± 8.8 | 39 | 3 | 142 ± 39 | 156 |
| 4 | 39.5 ± 8.5 | 54 | 4 | 35.9 ± 9.1 | 34 | 4 | 32.2 ± 8.8 | 38 |
| 5 | 57.7 ± 9.9 | 53 | 5 | 29.8 ± 6.0 | 34 | 5 | 53.0 ± 9.1 | 69 |
| 6 | 32.5 ± 7.1 | 24 | 6 | 22.2 ± 7.2 | 12 | 6 | 22.0 ± 4.0 | 30 |
| 7 | 5.5 ± 1.8 | 7 | 7 | 4.7 ± 1.4 | 6 | 7 | 10.1 ± 2.0 | 21 |
| 8 | 22.9 ± 5.1 | 33 | 8 | 1100 ± 280 | 1342 | 8 | 1.53 ± 0.48 | 3 |
| 9 | 19.5 ± 3.9 | 20 | 9 | 299 ± 71 | 330 | 9 | 1.58 ± 0.41 | 0 |
| 10 | 9.6 ± 1.9 | 11 | 10 | 9.1 ± 2.3 | 8 | 10 | 2.9 ± 2.9 | 1 |
| 11 | 940 ± 270 | 1115 | 11 | 6.4 ± 1.6 | 9 | 11 | 1.31 ± 0.93 | 4 |
| 12 | 340 ± 81 | 384 | 12 | 42.1 ± 9.2 | 49 | on-Z ML regions | | |
| 13 | 36.3 ± 9.5 | 40 | 13 | 33.0 ± 8.4 | 39 | SR | Expected SM | Obs. |
| 14 | 26.8 ± 7.4 | 26 | 14 | 25.8 ± 5.9 | 25 | 1 | 840 ± 170 | 985 |
| 15 | 42.7 ± 8.6 | 68 | 15 | 2.8 ± 2.0 | 7 | 2 | 107 ± 21 | 136 |
| 16 | 37.9 ± 8.6 | 41 | 16 | 2.5 ± 1.3 | 2 | 3 | 119 ± 27 | 146 |
| 17 | 26.5 ± 6.2 | 29 | 17 | 222 ± 42 | 260 | 4 | 11.1 ± 2.1 | 10 |
| 18 | 14.3 ± 3.6 | 13 | 18 | 86 ± 15 | 104 | 5 | 109 ± 24 | 126 |
| 19 | 10.6 ± 2.5 | 12 | 19 | 2.22 ± 0.90 | 4 | 6 | 19.3 ± 4.1 | 24 |
| 20 | 12.3 ± 2.9 | 14 | 20 | 3.2 ± 1.1 | 4 | 7 | 42 ± 10 | 47 |
| 21 | 9.2 ± 2.7 | 17 | 21 | 19.8 ± 3.8 | 28 | 8 | 3.47 ± 0.84 | 3 |
| 22 | 10.1 ± 2.1 | 17 | 22 | 16.1 ± 3.0 | 19 | 9 | 327 ± 54 | 419 |
| 23 | 272 ± 43 | 354 | 23 | 4.7 ± 1.3 | 1 | 10 | 46.5 ± 8.4 | 53 |
| 24 | 147 ± 25 | 177 | 24 | 4.0 ± 1.2 | 2 | 11 | 51.3 ± 9.1 | 62 |
| 25 | 15.3 ± 2.9 | 12 | 25 | 4.0 ± 1.1 | 5 | 12 | 15.6 ± 2.8 | 27 |
| 26 | 11.4 ± 2.4 | 19 | 26 | 8.5 ± 2.4 | 7 | 13 | 131 ± 27 | 162 |
| 27 | 33.4 ± 5.4 | 49 | 27 | 8.4 ± 2.5 | 7 | 14 | 19.9 ± 4.3 | 26 |
| 28 | 30.1 ± 4.9 | 38 | 28 | 8.9 ± 2.2 | 11 | 15 | 26.9 ± 6.1 | 35 |
| 29 | 10.4 ± 2.2 | 9 | 29 | 10.9 ± 3.1 | 11 | 16 | 7.8 ± 1.8 | 12 |
| 30 | 6.6 ± 1.3 | 7 | 30 | 1.25 ± 0.39 | 3 | 17 | 14.0 ± 3.1 | 19 |
| 31 | 6.9 ± 1.5 | 6 | 31 | 1.92 ± 0.37 | 4 | 18 | 84 ± 15 | 117 |
| 32 | 5.9 ± 1.1 | 14 | 32 | 2.77 ± 0.56 | 3 | 19 | 18.2 ± 3.3 | 26 |
| 33 | 6.1 ± 1.6 | 7 | 33 | 19.1 ± 4.1 | 23 | 20 | 40.4 ± 7.6 | 34 |
| 34 | 6.8 ± 1.3 | 10 | 34 | 7.5 ± 1.5 | 9 | 21 | 4.92 ± 0.88 | 7 |
| 35 | 8.8 ± 1.5 | 16 | 35 | 2.12 ± 0.49 | 5 | 22 | 46.9 ± 9.9 | 50 |
| 36 | 8.7 ± 2.0 | 11 | 36 | 0.47 ± 0.33 | 1 | 23 | 5.8 ± 1.2 | 10 |
| 37 | 9.4 ± 1.9 | 7 | 37 | 2.75 ± 0.77 | 4 | off-Z ML regions | | |
| 38 | 7.0 ± 1.3 | 5 | 38 | 1.68 ± 0.50 | 0 | SR | Expected SM | Obs. |
| 39 | 9.6 ± 2.1 | 9 | 39 | 0.97 ± 0.97 | 0 | 1 | 222 ± 36 | 285 |
| 40 | 8.6 ± 1.7 | 11 | 40 | 2.83 ± 0.70 | 7 | 2 | 2.7 ± 1.7 | 2 |
| 41 | 1.10 ± 0.32 | 2 | 41 | 3.8 ± 3.8 | 0 | 3 | 35.5 ± 6.4 | 34 |
| 42 | 0.63 ± 0.49 | 0 | 42 | 4.9 ± 1.0 | 9 | 4 | 0.99 ± 0.31 | 2 |
| 43 | 0.67 ± 0.60 | 1 | 43 | 2.36 ± 0.72 | 5 | 5 | 22.1 ± 4.0 | 29 |
| 44 | 0.74 ± 0.27 | 1 | LL regions | | | 6 | 9.7 ± 1.7 | 8 |
| 45 | 0.71 ± 0.53 | 1 | SR | Expected SM | Obs. | 7 | 217 ± 44 | 272 |
| 46 | 47.8 ± 9.7 | 59 | 1 | 23.0 ± 7.2 | 29 | 8 | 37.7 ± 6.8 | 56 |
| 47 | 17.3 ± 3.8 | 24 | 2 | 5.0 ± 1.6 | 6 | 9 | 21.4 ± 3.7 | 21 |
| 48 | 10.3 ± 2.9 | 11 | 3 | 23.8 ± 6.6 | 27 | 10 | 10.9 ± 1.9 | 18 |
| 49 | 2.06 ± 0.49 | 3 | 4 | 4.7 ± 1.5 | 7 | 11 | 89 ± 14 | 112 |
| 50 | 6.5 ± 1.1 | 13 | 5 | 8.0 ± 1.9 | 15 | 12 | 15.6 ± 2.4 | 20 |
| 51 | 3.72 ± 0.79 | 4 | 6 | 2.0 ± 1.1 | 0 | 13 | 16.4 ± 2.7 | 23 |
| 52 | 1.21 ± 0.29 | 4 | 7 | 1.61 ± 0.59 | 3 | 14 | 5.36 ± 0.95 | 7 |
| 53 | 0.44 ± 0.44 | 2 | 8 | 0.06 ± 0.06 | 0 | 15 | 9.0 ± 1.6 | 12 |
| 54 | 9.8 ± 1.8 | 24 | | | | 16 | 28.4 ± 3.9 | 46 |
| 55 | 7.3 ± 1.4 | 4 | | | | 17 | 0.72 ± 0.41 | 2 |
| 56 | 4.44 ± 0.98 | 6 | | | | 18 | 17.8 ± 2.8 | 25 |
| 57 | 5.7 ± 1.1 | 6 | | | | 19 | 0.89 ± 0.29 | 0 |
| 58 | 4.0 ± 1.0 | 6 | | | | 20 | 17.7 ± 3.3 | 31 |
| 59 | 2.24 ± 0.53 | 2 | | | | 21 | 1.20 ± 0.32 | 2 |
| 60 | 1.83 ± 0.44 | 5 | | | | | | |
| 61 | 1.88 ± 0.40 | 5 | | | | | | |
| 62 | 1.35 ± 0.56 | 0 | | | | | | |

regime. However, for a nearly degenerate mass spectrum, the SM background becomes of higher importance and the presence of an SS lepton pair significantly reduces it, leading to a similar sensitivity. The constraints on the two RPV models that were not previously included demonstrate the sensitivity of the analysis to RPV scenarios. The final state is particularly well suited to study the T1qqqqL model since no leptonic branching fraction penalty applies, resulting in exclusion limits on the gluino mass beyond 2.1 TeV, comparable to other results in fully hadronic final states [87, 88]. The limits obtained on the T1tbs model are stronger than those previously obtained in the one-lepton channel based on the analysis of the 2016 dataset [89]. They are expected to remain competitive after an update with the full Run 2 dataset.

Model-independent limits are also set on the product of cross section, branching fraction, detector acceptance, and reconstruction efficiency, for the production of an SS lepton pair with at least two extra jets and $H_T > 300$ GeV. For this purpose, we select events from the HH and LM categories and calculate limits as a function of minimum p_T^{miss} or H_T requirements starting at 300 and 1400 GeV, respectively. In order to remove the overlap between the two conditions, events selected for the H_T scan must also satisfy $p_T^{\text{miss}} < 300$ GeV. The corresponding limits are presented in Fig. 13.

Finally, in order to facilitate reinterpretations of our results, we present in Table 10 the expected and observed yields for a number of inclusive SRs. This procedure focuses on events with large H_T , p_T^{miss} , N_b , and/or N_{jets} , and the SRs are defined such that they typically lead to 5 to 10 expected background events. The last column in the table indicates the upper limit at 95% CL on the number of BSM events in each SR.

Table 10: Inclusive SR definitions, expected background yields and uncertainties, and observed yields, as well as the observed 95% CL upper limits on the number of BSM events contributing to each region. No uncertainty in the signal acceptance is assumed in calculating these limits. A dash (—) indicates that a particular selection is not required.

| SR | Category | N_{jets} | N_b | H_T (GeV) | p_T^{miss} (GeV) | m_T^{min} (GeV) | SM expected | Obs. | $N_{\text{BSM}}^{\text{max}}$ (95% CL) |
|-------|----------|-------------------|----------|-------------|---------------------------|--------------------------|-----------------|------|--|
| ISR1 | | ≥ 2 | 0 | ≥ 1000 | ≥ 250 | — | 12.7 ± 7.4 | 16 | 12.32 |
| ISR2 | | ≥ 2 | ≥ 2 | ≥ 1100 | — | — | 11.0 ± 3.8 | 14 | 11.33 |
| ISR3 | | ≥ 2 | 0 | — | ≥ 500 | — | 10.4 ± 9.7 | 13 | 11.26 |
| ISR4 | | ≥ 2 | ≥ 2 | — | ≥ 300 | — | 11.4 ± 3.8 | 17 | 14.22 |
| ISR5 | | ≥ 2 | 0 | — | ≥ 250 | ≥ 120 | 6.6 ± 5.7 | 10 | 10.77 |
| ISR6 | HH | ≥ 2 | ≥ 2 | — | ≥ 200 | ≥ 120 | 6.3 ± 1.3 | 8 | 8.22 |
| ISR7 | | ≥ 8 | — | — | — | — | 7.0 ± 2.8 | 12 | 12.17 |
| ISR8 | | ≥ 6 | — | — | — | ≥ 120 | 6.2 ± 1.4 | 10 | 10.45 |
| ISR9 | | ≥ 2 | ≥ 3 | ≥ 800 | — | — | 7.8 ± 3.5 | 8 | 7.53 |
| ISR10 | | ≥ 2 | — | ≥ 700 | — | — | 10.4 ± 9.0 | 12 | 10.37 |
| ISR11 | | ≥ 2 | — | — | ≥ 200 | — | 12.1 ± 5.6 | 13 | 9.94 |
| ISR12 | LL | ≥ 6 | — | — | — | — | 7.1 ± 4.3 | 7 | 7.10 |
| ISR13 | | ≥ 2 | ≥ 3 | — | — | — | 1.61 ± 0.39 | 3 | 5.70 |
| ISR14 | | ≥ 2 | 0 | ≥ 1200 | < 50 | — | 3.6 ± 3.6 | 3 | 5.10 |
| ISR15 | LM | ≥ 2 | ≥ 2 | ≥ 1000 | < 50 | — | 2.34 ± 0.51 | 4 | 6.41 |
| ISR16 | | ≥ 2 | 0 | ≥ 1000 | ≥ 300 | — | 5.6 ± 1.6 | 7 | 7.78 |
| ISR17 | ML | ≥ 2 | ≥ 2 | ≥ 1000 | — | — | 5.7 ± 1.9 | 7 | 7.62 |

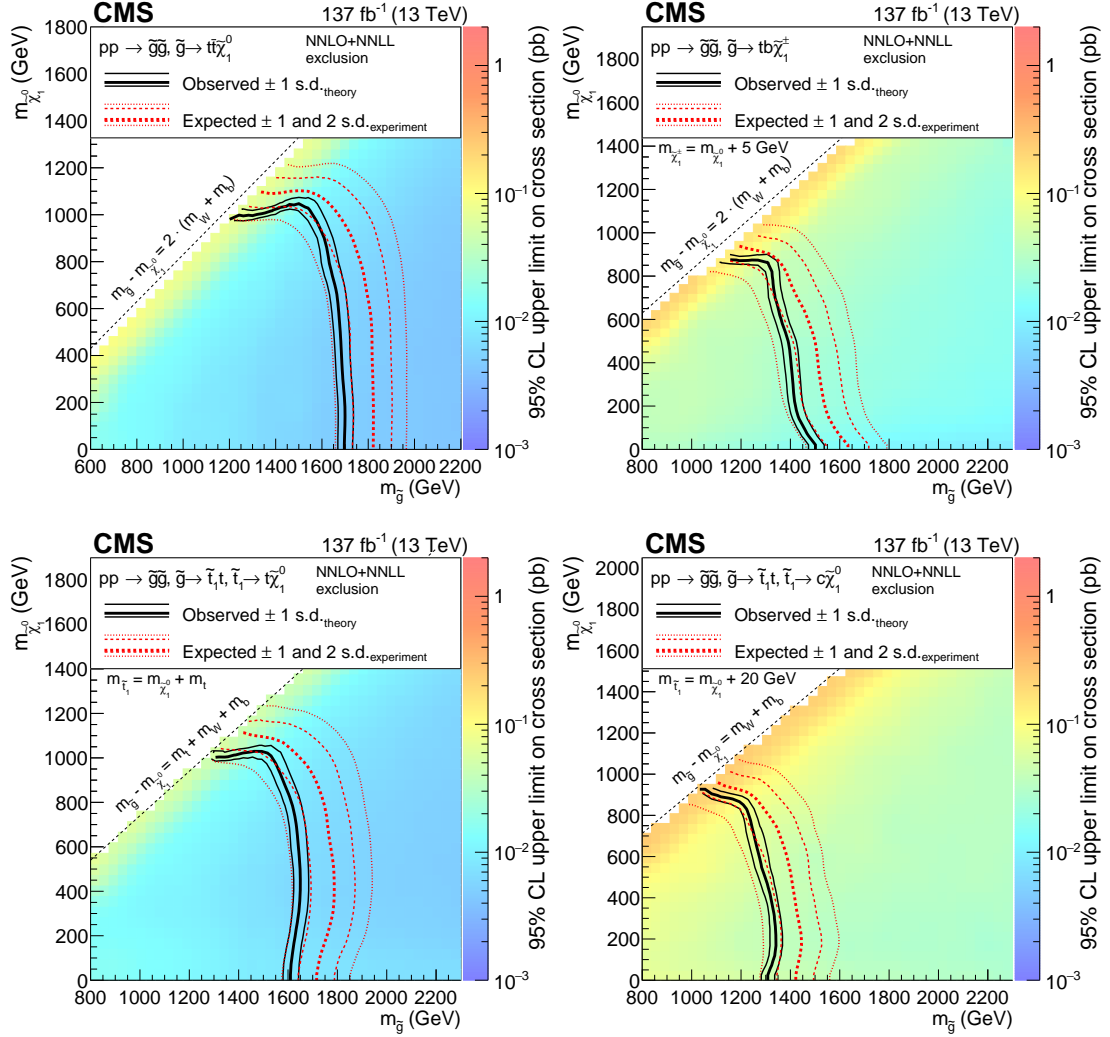


Figure 7: Exclusion regions at 95% CL in the $m_{\tilde{\chi}_1^0}$ versus $m_{\tilde{g}}$ plane for the T1tttt (upper left) and T5ttbbWW (upper right) models, with off-shell third-generation squarks, and the T5tttt (lower left) and T5ttcc (lower right) models, with on-shell third-generation squarks. For the T5ttbbWW model, $m_{\tilde{\chi}_1^\pm} = m_{\tilde{\chi}_1^0} + 5 \text{ GeV}$, for the T5tttt model, $m_{\tilde{t}} - m_{\tilde{\chi}_1^0} = m_t$, and for the T5ttcc model, $m_{\tilde{t}} - m_{\tilde{\chi}_1^0} = 20 \text{ GeV}$ and the decay proceeds through $\tilde{t} \rightarrow c\tilde{\chi}_1^0$. The right-hand side color scale indicates the excluded cross section values for a given point in the SUSY particle mass plane. The solid black curves represent the observed exclusion limits assuming the approximate-NNLO+NNLL cross sections [46–51, 58] (thick line), or their variations of ± 1 standard deviations (s.d.) (thin lines). The dashed red curves show the expected limits with the corresponding ± 1 s.d. and ± 2 s.d. uncertainties. Excluded regions are to the left and below the limit curves.

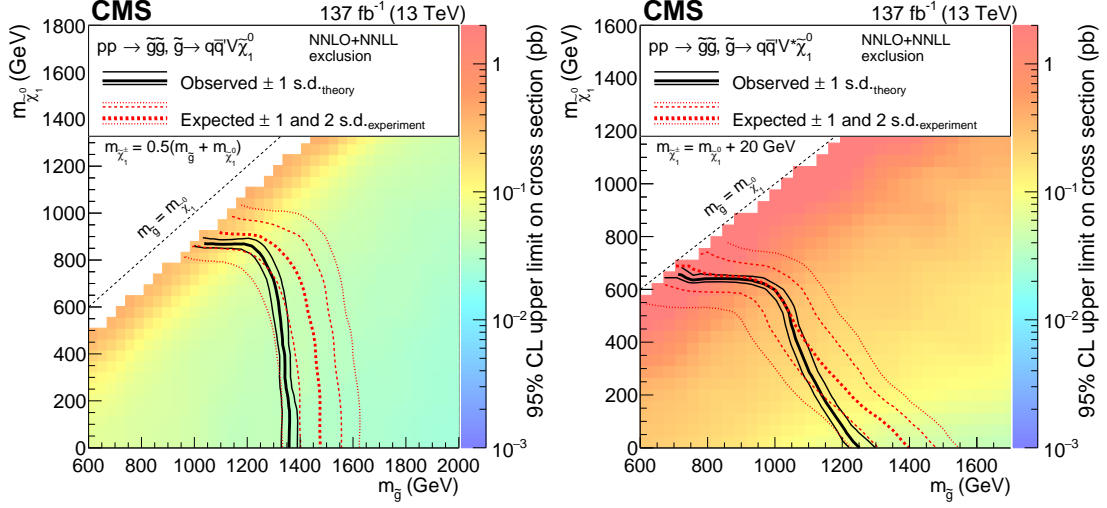


Figure 8: Exclusion regions at 95% CL in the plane of $m_{\tilde{\chi}_1^0}$ versus $m_{\tilde{g}}$ for the T5qqqqWZ model with $m_{\tilde{\chi}_1^\pm} = 0.5(m_{\tilde{g}} + m_{\tilde{\chi}_1^0})$ (left) and with $m_{\tilde{\chi}_1^\pm} = m_{\tilde{\chi}_1^0} + 20$ GeV (right). The notations are as in Fig. 7.

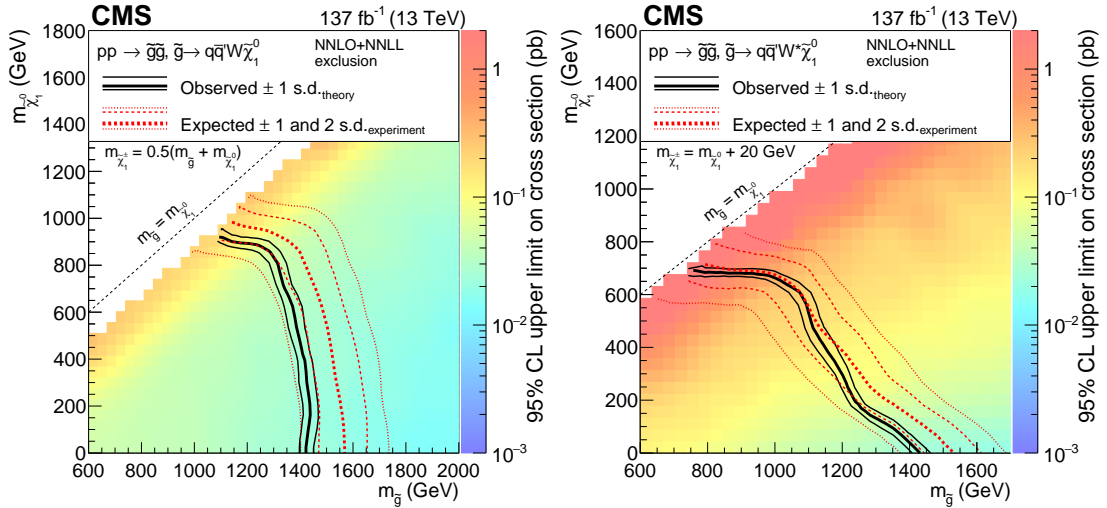


Figure 9: Exclusion regions at 95% CL in the plane of $m_{\tilde{\chi}_1^0}$ versus $m_{\tilde{g}}$ for the T5qqqqWW model with $m_{\tilde{\chi}_1^\pm} = 0.5(m_{\tilde{g}} + m_{\tilde{\chi}_1^0})$ (left) and with $m_{\tilde{\chi}_1^\pm} = m_{\tilde{\chi}_1^0} + 20$ GeV (right). The notations are as in Fig. 7.

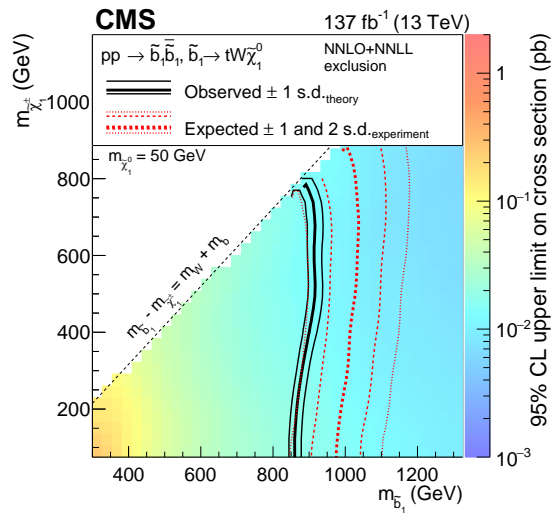


Figure 10: Exclusion regions at 95% CL in the plane of $m_{\tilde{\chi}_1^\pm}$ versus $m_{\tilde{b}_1}$ for the T6ttWW model with $m_{\tilde{\chi}_1^0} = 50$ GeV. The notations are as in Fig. 7.

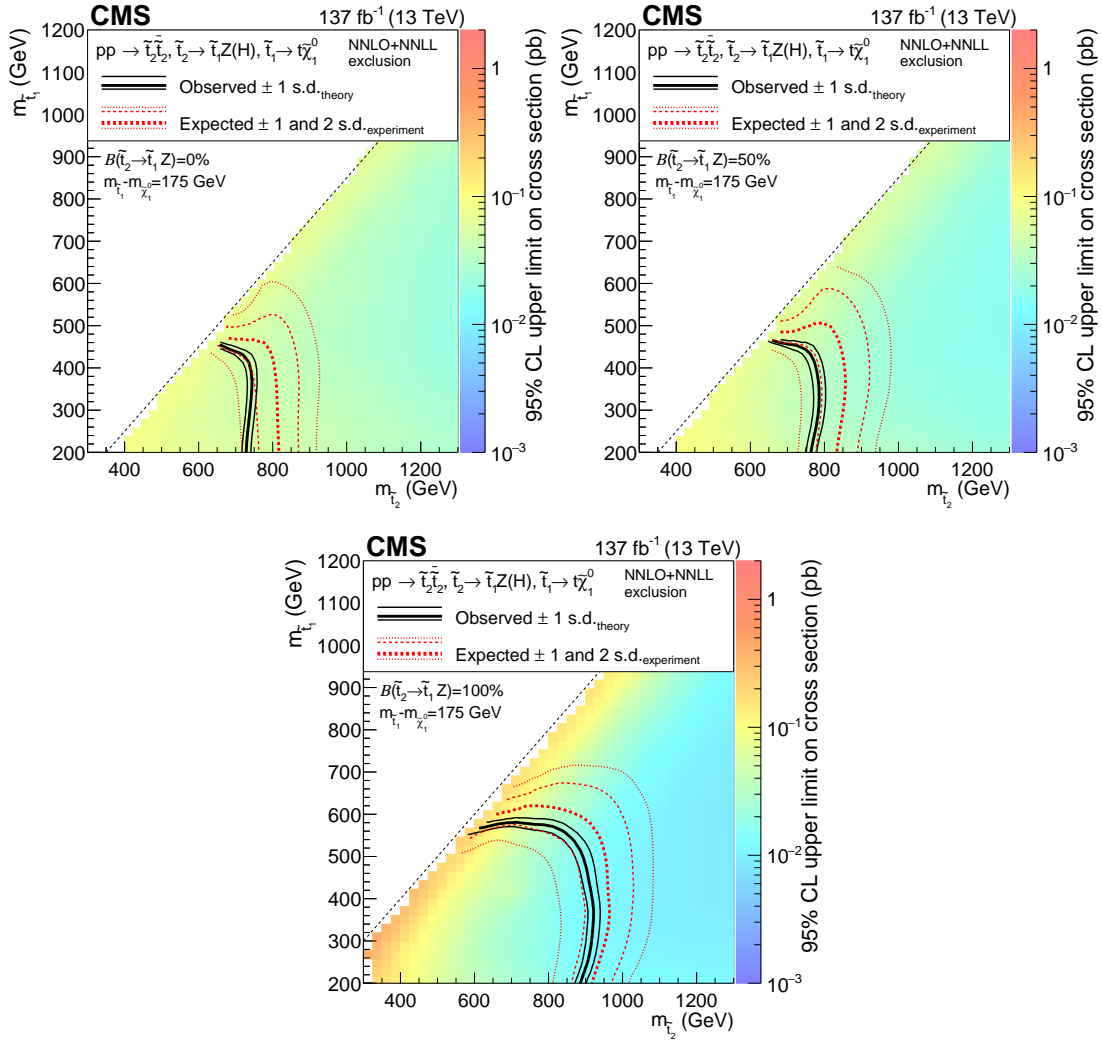


Figure 11: Exclusion regions at 95% CL in the plane of $m(\tilde{t}_1)$ versus $m(\tilde{t}_2)$ for the T6ttHZ model with $m(\tilde{t}_1) - m(\tilde{\chi}_1^0) = 175$ GeV. The three exclusions represent $\mathcal{B}(\tilde{t}_2 \rightarrow \tilde{t}_1 Z)$ of 0, 50, and 100%, respectively. The notations are as in Fig. 7.

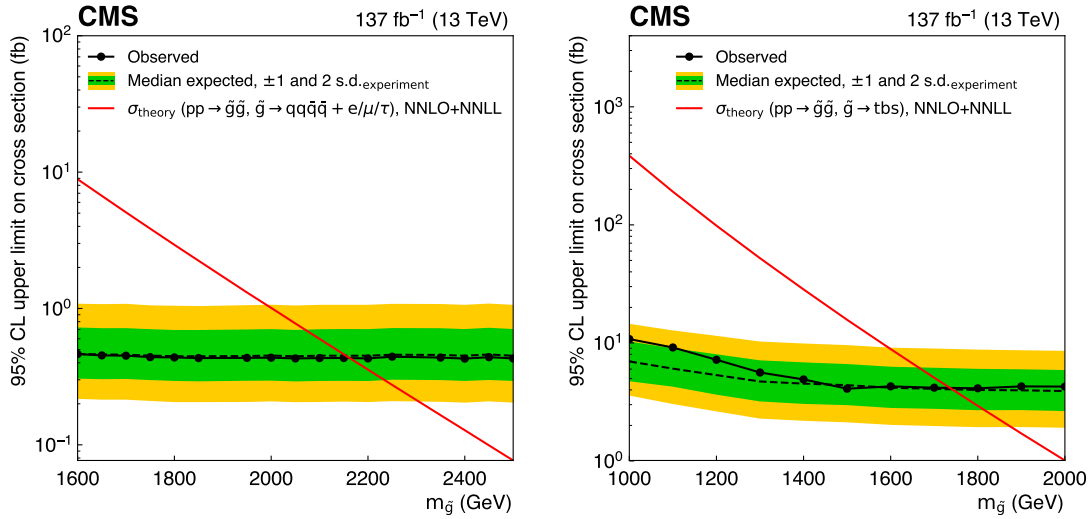


Figure 12: Upper limits at 95% CL on the cross section for RPV gluino pair production with each gluino decaying into four quarks and one lepton (T1qqqL, left), and each gluino decaying into a top, bottom, and strange quarks (T1tbs, right).

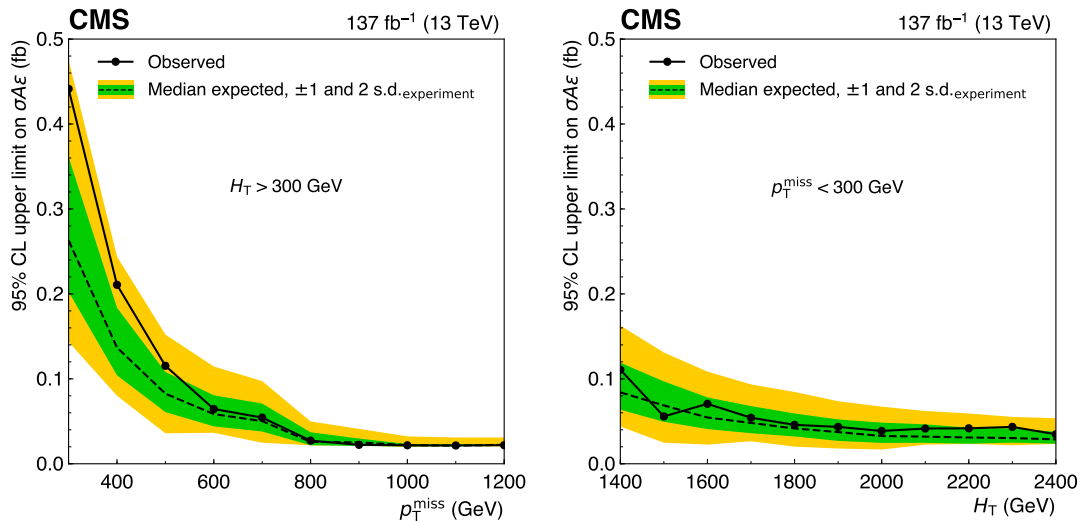


Figure 13: Upper limits at 95% CL on the product of cross section, detector acceptance, and selection efficiency, $\sigma A \epsilon$, for the production of an SS lepton pair with at least two jets, as a function of the minimum p_T^{miss} threshold, when $H_T > 300$ GeV (left), or the minimum H_T threshold, when $p_T^{\text{miss}} < 300$ GeV (right).

8 Summary

A sample of events with two same-sign or at least three charged leptons (electrons or muons) produced in association with several jets in proton-proton collisions at 13 TeV, corresponding to an integrated luminosity of 137 fb^{-1} , has been studied to search for manifestations of physics beyond the standard model. The data are found to be consistent with the standard model expectations. The results are interpreted as limits on cross sections at 95% confidence level for the production of new particles in simplified supersymmetric models, considering both R parity conserving and violating scenarios. Using calculations for these cross sections as functions of particle masses, the limits are translated into lower mass limits that are as large as 2.1 TeV for gluinos and 0.9 TeV for top and bottom squarks, depending on the details of the model. The results extend the gluino and squark mass observed and expected exclusions by up to 200 GeV, compared to the previous versions of this analysis. Finally, to facilitate further interpretations of the search, model-independent limits are provided as a function of the missing transverse momentum and the scalar sum of jet transverse momenta in an event, together with the background prediction and data yields in a set of simplified signal regions.

Acknowledgments

We congratulate our colleagues in the CERN accelerator departments for the excellent performance of the LHC and thank the technical and administrative staffs at CERN and at other CMS institutes for their contributions to the success of the CMS effort. In addition, we gratefully acknowledge the computing centers and personnel of the Worldwide LHC Computing Grid for delivering so effectively the computing infrastructure essential to our analyses. Finally, we acknowledge the enduring support for the construction and operation of the LHC and the CMS detector provided by the following funding agencies: BMBWF and FWF (Austria); FNRS and FWO (Belgium); CNPq, CAPES, FAPERJ, FAPERGS, and FAPESP (Brazil); MES (Bulgaria); CERN; CAS, MoST, and NSFC (China); COLCIENCIAS (Colombia); MSES and CSF (Croatia); RPF (Cyprus); SENESCYT (Ecuador); MoER, ERC IUT, PUT and ERDF (Estonia); Academy of Finland, MEC, and HIP (Finland); CEA and CNRS/IN2P3 (France); BMBF, DFG, and HGF (Germany); GSRT (Greece); NKFI (Hungary); DAE and DST (India); IPM (Iran); SFI (Ireland); INFN (Italy); MSIP and NRF (Republic of Korea); MES (Latvia); LAS (Lithuania); MOE and UM (Malaysia); BUAP, CINVESTAV, CONACYT, LNS, SEP, and UASLP-FAI (Mexico); MOS (Montenegro); MBIE (New Zealand); PAEC (Pakistan); MSHE and NSC (Poland); FCT (Portugal); JINR (Dubna); MON, RosAtom, RAS, RFBR, and NRC KI (Russia); MESTD (Serbia); SEIDI, CPAN, PCTI, and FEDER (Spain); MOSTR (Sri Lanka); Swiss Funding Agencies (Switzerland); MST (Taipei); ThEPCenter, IPST, STAR, and NSTDA (Thailand); TUBITAK and TAEK (Turkey); NASU (Ukraine); STFC (United Kingdom); DOE and NSF (USA).

Individuals have received support from the Marie-Curie program and the European Research Council and Horizon 2020 Grant, contract Nos. 675440, 752730, and 765710 (European Union); the Leventis Foundation; the A.P. Sloan Foundation; the Alexander von Humboldt Foundation; the Belgian Federal Science Policy Office; the Fonds pour la Formation à la Recherche dans l'Industrie et dans l'Agriculture (FRIA-Belgium); the Agentschap voor Innovatie door Wetenschap en Technologie (IWT-Belgium); the F.R.S.-FNRS and FWO (Belgium) under the "Excellence of Science – EOS" – be.h project n. 30820817; the Beijing Municipal Science & Technology Commission, No. Z191100007219010; the Ministry of Education, Youth and Sports (MEYS) of the Czech Republic; the Deutsche Forschungsgemeinschaft (DFG) under Germanys Excellence Strategy – EXC 2121 "Quantum Universe" – 390833306; the Lendület ("Momentum") Program and the János Bolyai Research Scholarship of the Hungarian Academy of Sci-

ences, the New National Excellence Program ÚNKP, the NKFIA research grants 123842, 123959, 124845, 124850, 125105, 128713, 128786, and 129058 (Hungary); the Council of Science and Industrial Research, India; the HOMING PLUS program of the Foundation for Polish Science, cofinanced from European Union, Regional Development Fund, the Mobility Plus program of the Ministry of Science and Higher Education, the National Science Center (Poland), contracts Harmonia 2014/14/M/ST2/00428, Opus 2014/13/B/ST2/02543, 2014/15/B/ST2/03998, and 2015/19/B/ST2/02861, Sonata-bis 2012/07/E/ST2/01406; the National Priorities Research Program by Qatar National Research Fund; the Ministry of Science and Education, grant no. 14.W03.31.0026 (Russia); the Programa Estatal de Fomento de la Investigación Científica y Técnica de Excelencia María de Maeztu, grant MDM-2015-0509 and the Programa Severo Ochoa del Principado de Asturias; the Thalís and Aristeia programs cofinanced by EU-ESF and the Greek NSRF; the Rachadapisek Sompot Fund for Postdoctoral Fellowship, Chulalongkorn University and the Chulalongkorn Academic into Its 2nd Century Project Advancement Project (Thailand); the Kavli Foundation; the Nvidia Corporation; the SuperMicro Corporation; the Welch Foundation, contract C-1845; and the Weston Havens Foundation (USA).

References

- [1] R. M. Barnett, J. F. Gunion, and H. E. Haber, "Discovering supersymmetry with like-sign dileptons", *Phys. Lett. B* **315** (1993) 349, doi:10.1016/0370-2693(93)91623-U, arXiv:hep-ph/9306204.
- [2] M. Guchait and D. P. Roy, "Like-sign dilepton signature for gluino production at CERN LHC including top quark and Higgs boson effects", *Phys. Rev. D* **52** (1995) 133, doi:10.1103/PhysRevD.52.133, arXiv:hep-ph/9412329.
- [3] Y. Bai and Z. Han, "Top-antitop and top-top resonances in the dilepton channel at the CERN LHC", *JHEP* **04** (2009) 056, doi:10.1088/1126-6708/2009/04/056, arXiv:0809.4487.
- [4] E. L. Berger et al., "Top quark forward-backward asymmetry and same-sign top quark pairs", *Phys. Rev. Lett.* **106** (2011) 201801, doi:10.1103/PhysRevLett.106.201801, arXiv:1101.5625.
- [5] T. Plehn and T. M. P. Tait, "Seeking sgluons", *J. Phys. G* **36** (2009) 075001, doi:10.1088/0954-3899/36/7/075001, arXiv:0810.3919.
- [6] S. Calvet, B. Fuks, P. Gris, and L. Valery, "Searching for sgluons in multitop events at a center-of-mass energy of 8 TeV", *JHEP* **04** (2013) 043, doi:10.1007/JHEP04(2013)043, arXiv:1212.3360.
- [7] K. J. F. Gaemers and F. Hoogeveen, "Higgs production and decay into heavy flavors with the gluon fusion mechanism", *Phys. Lett. B* **146** (1984) 347, doi:10.1016/0370-2693(84)91711-8.
- [8] G. C. Branco et al., "Theory and phenomenology of two-Higgs-doublet models", *Phys. Rept.* **516** (2012) 1, doi:10.1016/j.physrep.2012.02.002, arXiv:1106.0034.
- [9] F. M. L. Almeida, Jr. et al., "Same-sign dileptons as a signature for heavy Majorana neutrinos in hadron-hadron collisions", *Phys. Lett. B* **400** (1997) 331, doi:10.1016/S0370-2693(97)00143-3, arXiv:hep-ph/9703441.

-
- [10] R. Contino and G. Servant, “Discovering the top partners at the LHC using same-sign dilepton final states”, *JHEP* **06** (2008) 026, doi:10.1088/1126-6708/2008/06/026, arXiv:0801.1679.
- [11] P. Ramond, “Dual theory for free fermions”, *Phys. Rev. D* **3** (1971) 2415, doi:10.1103/PhysRevD.3.2415.
- [12] Y. A. Gol’fand and E. P. Likhtman, “Extension of the algebra of Poincaré group generators and violation of P invariance”, *JETP Lett.* **13** (1971) 323.
- [13] A. Neveu and J. H. Schwarz, “Factorizable dual model of pions”, *Nucl. Phys. B* **31** (1971) 86, doi:10.1016/0550-3213(71)90448-2.
- [14] D. V. Volkov and V. P. Akulov, “Possible universal neutrino interaction”, *JETP Lett.* **16** (1972) 438.
- [15] J. Wess and B. Zumino, “A Lagrangian model invariant under supergauge transformations”, *Phys. Lett. B* **49** (1974) 52, doi:10.1016/0370-2693(74)90578-4.
- [16] J. Wess and B. Zumino, “Supergauge transformations in four-dimensions”, *Nucl. Phys. B* **70** (1974) 39, doi:10.1016/0550-3213(74)90355-1.
- [17] P. Fayet, “Supergauge invariant extension of the Higgs mechanism and a model for the electron and its neutrino”, *Nucl. Phys. B* **90** (1975) 104, doi:10.1016/0550-3213(75)90636-7.
- [18] H. P. Nilles, “Supersymmetry, supergravity and particle physics”, *Phys. Rept.* **110** (1984) 1, doi:10.1016/0370-1573(84)90008-5.
- [19] S. P. Martin, “A supersymmetry primer”, in *Perspectives on Supersymmetry II*, G. L. Kane, ed., p. 1. World Scientific, 2010. Adv. Ser. Direct. High Energy Phys., vol. 21. doi:10.1142/9789814307505_0001.
- [20] G. R. Farrar and P. Fayet, “Phenomenology of the production, decay, and detection of new hadronic states associated with supersymmetry”, *Phys. Lett. B* **76** (1978) 575, doi:10.1016/0370-2693(78)90858-4.
- [21] E. Nikolidakis and C. Smith, “Minimal flavor violation, seesaw mechanism, and R -parity”, *Phys. Rev. D* **77** (2008) 015021, doi:10.1103/PhysRevD.77.015021, arXiv:0710.3129.
- [22] C. Csáki, Y. Grossman, and B. Heidenreich, “Minimal flavor violation supersymmetry: A natural theory for R -parity violation”, *Phys. Rev. D* **85** (2012) 095009, doi:10.1103/PhysRevD.85.095009, arXiv:1111.1239.
- [23] ATLAS Collaboration, “Search for supersymmetry in final states with two same-sign or three leptons and jets using 36 fb^{-1} of $\sqrt{s} = 13 \text{ TeV}$ pp collision data with the ATLAS detector”, *JHEP* **09** (2017) 084, doi:10.1007/JHEP09(2017)084, arXiv:1706.03731.
- [24] CMS Collaboration, “Search for physics beyond the standard model in events with two leptons of same sign, missing transverse momentum, and jets in proton-proton collisions at $\sqrt{s} = 13 \text{ TeV}$ ”, *Eur. Phys. J. C* **77** (2017) 578, doi:10.1140/epjc/s10052-017-5079-z, arXiv:1704.07323.

- [25] CMS Collaboration, “Search for supersymmetry in events with at least three electrons or muons, jets, and missing transverse momentum in proton-proton collisions at $\sqrt{s} = 13$ TeV”, *JHEP* **02** (2018) 067, doi:10.1007/JHEP02(2018)067, arXiv:1710.09154.
- [26] ATLAS Collaboration, “Search for squarks and gluinos in final states with same-sign leptons and jets using 139 fb^{-1} of data collected with the ATLAS detector”, *JHEP* **06** (2020) 046, doi:10.1007/JHEP06(2020)046, arXiv:1909.08457.
- [27] J. Alwall et al., “The automated computation of tree-level and next-to-leading order differential cross sections, and their matching to parton shower simulations”, *JHEP* **07** (2014) 079, doi:10.1007/JHEP07(2014)079, arXiv:1405.0301.
- [28] J. Alwall et al., “Comparative study of various algorithms for the merging of parton showers and matrix elements in hadronic collisions”, *Eur. Phys. J. C* **53** (2008) 473, doi:10.1140/epjc/s10052-007-0490-5, arXiv:0706.2569.
- [29] R. Frederix and S. Frixione, “Merging meets matching in MC@NLO”, *JHEP* **12** (2012) 061, doi:10.1007/JHEP12(2012)061, arXiv:1209.6215.
- [30] P. Nason, “A new method for combining NLO QCD with shower Monte Carlo algorithms”, *JHEP* **11** (2004) 040, doi:10.1088/1126-6708/2004/11/040, arXiv:hep-ph/0409146.
- [31] S. Frixione, P. Nason, and C. Oleari, “Matching NLO QCD computations with parton shower simulations: the POWHEG method”, *JHEP* **11** (2007) 070, doi:10.1088/1126-6708/2007/11/070, arXiv:0709.2092.
- [32] S. Alioli, P. Nason, C. Oleari, and E. Re, “A general framework for implementing NLO calculations in shower Monte Carlo programs: the POWHEG BOX”, *JHEP* **06** (2010) 043, doi:10.1007/JHEP06(2010)043, arXiv:1002.2581.
- [33] T. Melia, P. Nason, R. Rötsch, and G. Zanderighi, “ W^+W^- , WZ and ZZ production in the POWHEG BOX”, *JHEP* **11** (2011) 078, doi:10.1007/JHEP11(2011)078, arXiv:1107.5051.
- [34] P. Nason and G. Zanderighi, “ W^+W^- , WZ and ZZ production in the POWHEG BOX V2”, *Eur. Phys. J. C* **74** (2014) 2702, doi:10.1140/epjc/s10052-013-2702-5, arXiv:1311.1365.
- [35] NNPDF Collaboration, “Parton distributions for the LHC Run II”, *JHEP* **04** (2015) 040, doi:10.1007/JHEP04(2015)040, arXiv:1410.8849.
- [36] NNPDF Collaboration, “Parton distributions from high-precision collider data”, *Eur. Phys. J. C* **77** (2017) 663, doi:10.1140/epjc/s10052-017-5199-5, arXiv:1706.00428.
- [37] T. Sjöstrand et al., “An introduction to PYTHIA 8.2”, *Comput. Phys. Commun.* **191** (2015) 159, doi:10.1016/j.cpc.2015.01.024, arXiv:1410.3012.
- [38] P. Skands, S. Carrazza, and J. Rojo, “Tuning PYTHIA 8.1: the Monash 2013 tune”, *Eur. Phys. J. C* **74** (2014) 3024, doi:10.1140/epjc/s10052-014-3024-y, arXiv:1404.5630.

- [39] CMS Collaboration, “Event generator tunes obtained from underlying event and multiparton scattering measurements”, *Eur. Phys. J. C* **76** (2016) 155, doi:10.1140/epjc/s10052-016-3988-x, arXiv:1512.00815.
- [40] CMS Collaboration, “Extraction and validation of a new set of CMS PYTHIA8 tunes from underlying-event measurements”, *Eur. Phys. J. C* **80** (2020) 4, doi:10.1140/epjc/s10052-019-7499-4, arXiv:1903.12179.
- [41] GEANT4 Collaboration, “GEANT4 — a simulation toolkit”, *Nucl. Instrum. Meth. A* **506** (2003) 250, doi:10.1016/S0168-9002(03)01368-8.
- [42] S. Abdullin et al., “The fast simulation of the CMS detector at LHC”, *J. Phys. Conf. Ser.* **331** (2011) 032049, doi:10.1088/1742-6596/331/3/032049.
- [43] A. Giammanco, “The fast simulation of the CMS experiment”, *J. Phys. Conf. Ser.* **513** (2014) 022012, doi:10.1088/1742-6596/513/2/022012.
- [44] D. Alves et al., “Simplified models for LHC new physics searches”, *J. Phys. G* **39** (2012) 105005, doi:10.1088/0954-3899/39/10/105005, arXiv:1105.2838.
- [45] CMS Collaboration, “Interpretation of searches for supersymmetry with simplified models”, *Phys. Rev. D* **88** (2013) 052017, doi:10.1103/PhysRevD.88.052017, arXiv:1301.2175.
- [46] W. Beenakker et al., “NNLL-fast: predictions for coloured supersymmetric particle production at the LHC with threshold and Coulomb resummation”, *JHEP* **12** (2016) 133, doi:10.1007/JHEP12(2016)133, arXiv:1607.07741.
- [47] W. Beenakker, R. Höpker, M. Spira, and P. M. Zerwas, “Squark and gluino production at hadron colliders”, *Nucl. Phys. B* **492** (1997) 51, doi:10.1016/S0550-3213(97)80027-2, arXiv:hep-ph/9610490.
- [48] A. Kulesza and L. Motyka, “Threshold resummation for squark-antisquark and gluino-pair production at the LHC”, *Phys. Rev. Lett.* **102** (2009) 111802, doi:10.1103/PhysRevLett.102.111802, arXiv:0807.2405.
- [49] A. Kulesza and L. Motyka, “Soft gluon resummation for the production of gluino-gluino and squark-antisquark pairs at the LHC”, *Phys. Rev. D* **80** (2009) 095004, doi:10.1103/PhysRevD.80.095004, arXiv:0905.4749.
- [50] W. Beenakker et al., “Soft-gluon resummation for squark and gluino hadroproduction”, *JHEP* **12** (2009) 041, doi:10.1088/1126-6708/2009/12/041, arXiv:0909.4418.
- [51] W. Beenakker et al., “Squark and gluino hadroproduction”, *Int. J. Mod. Phys. A* **26** (2011) 2637, doi:10.1142/S0217751X11053560, arXiv:1105.1110.
- [52] W. Beenakker et al., “NNLL resummation for squark-antisquark pair production at the LHC”, *JHEP* **01** (2012) 076, doi:10.1007/JHEP01(2012)076, arXiv:1110.2446.
- [53] W. Beenakker et al., “Towards NNLL resummation: hard matching coefficients for squark and gluino hadroproduction”, *JHEP* **10** (2013) 120, doi:10.1007/JHEP10(2013)120, arXiv:1304.6354.
- [54] W. Beenakker et al., “NNLL resummation for squark and gluino production at the LHC”, *JHEP* **12** (2014) 023, doi:10.1007/JHEP12(2014)023, arXiv:1404.3134.

- [55] W. Beenakker et al., “Stop production at hadron colliders”, *Nucl. Phys. B* **515** (1998) 3, doi:10.1016/S0550-3213(98)00014-5, arXiv:hep-ph/9710451.
- [56] W. Beenakker et al., “Supersymmetric top and bottom squark production at hadron colliders”, *JHEP* **08** (2010) 098, doi:10.1007/JHEP08(2010)098, arXiv:1006.4771.
- [57] W. Beenakker et al., “NNLL resummation for stop pair-production at the LHC”, *JHEP* **05** (2016) 153, doi:10.1007/JHEP05(2016)153, arXiv:1601.02954.
- [58] C. Borschensky et al., “Squark and gluino production cross sections in pp collisions at $\sqrt{s} = 13, 14, 33$ and 100 TeV”, *Eur. Phys. J. C* **74** (2014) 3174, doi:10.1140/epjc/s10052-014-3174-y, arXiv:1407.5066.
- [59] CMS Collaboration, “The CMS experiment at the CERN LHC”, *JINST* **3** (2008) S08004, doi:10.1088/1748-0221/3/08/S08004.
- [60] CMS Collaboration, “The CMS trigger system”, *JINST* **12** (2017) P01020, doi:10.1088/1748-0221/12/01/P01020, arXiv:1609.02366.
- [61] M. Cacciari, G. P. Salam, and G. Soyez, “The anti- k_T jet clustering algorithm”, *JHEP* **04** (2008) 063, doi:10.1088/1126-6708/2008/04/063, arXiv:0802.1189.
- [62] M. Cacciari, G. P. Salam, and G. Soyez, “FastJet user manual”, *Eur. Phys. J. C* **72** (2012) 1896, doi:10.1140/epjc/s10052-012-1896-2, arXiv:1111.6097.
- [63] CMS Collaboration, “Particle-flow reconstruction and global event description with the CMS detector”, *JINST* **12** (2017) P10003, doi:10.1088/1748-0221/12/10/P10003, arXiv:1706.04965.
- [64] CMS Collaboration, “Performance of electron reconstruction and selection with the CMS detector in proton-proton collisions at $\sqrt{s} = 8$ TeV”, *JINST* **10** (2015) P06005, doi:10.1088/1748-0221/10/06/P06005, arXiv:1502.02701.
- [65] CMS Collaboration, “Performance of the CMS muon detector and muon reconstruction with proton-proton collisions at $\sqrt{s} = 13$ TeV”, *JINST* **13** (2018) P06015, doi:10.1088/1748-0221/13/06/P06015, arXiv:1804.04528.
- [66] M. Cacciari and G. P. Salam, “Pileup subtraction using jet areas”, *Phys. Lett. B* **659** (2008) 119, doi:10.1016/j.physletb.2007.09.077, arXiv:0707.1378.
- [67] CMS Collaboration, “Jet energy scale and resolution in the CMS experiment in pp collisions at 8 TeV”, *JINST* **12** (2016) P02014, doi:10.1088/1748-0221/12/02/P02014, arXiv:1607.03663.
- [68] CMS Collaboration, “Jet algorithms performance in 13 TeV data”, CMS Physics Analysis Summary CMS-PAS-JME-16-003, 2017.
- [69] CMS Collaboration, “Identification of heavy-flavour jets with the CMS detector in pp collisions at 13 TeV”, *JINST* **13** (2018) P05011, doi:10.1088/1748-0221/13/05/P05011, arXiv:1712.07158.
- [70] CMS Collaboration, “Performance of missing transverse momentum reconstruction in proton-proton collisions at $\sqrt{s} = 13$ TeV using the CMS detector”, *JINST* **14** (2019) P07004, doi:10.1088/1748-0221/14/07/P07004, arXiv:1903.06078.

- [71] CMS Collaboration, “Search for new physics in same-sign dilepton events in proton-proton collisions at $\sqrt{s} = 13$ TeV”, *Eur. Phys. J. C* **76** (2016) 439, doi:10.1140/epjc/s10052-016-4261-z, arXiv:1605.03171.
- [72] CMS Collaboration, “Performance of the reconstruction and identification of high-momentum muons in proton-proton collisions at $\sqrt{s} = 13$ TeV”, *JINST* **15** (2020) P02027, doi:10.1088/1748-0221/15/02/P02027, arXiv:1912.03516.
- [73] CMS Collaboration, “Performance of CMS muon reconstruction in pp collision events at $\sqrt{s} = 7$ TeV”, *JINST* **7** (2012) P10002, doi:10.1088/1748-0221/7/10/P10002, arXiv:1206.4071.
- [74] CMS Collaboration, “CMS luminosity measurements for the 2016 data-taking period”, CMS Physics Analysis Summary CMS-PAS-LUM-17-001, 2017.
- [75] CMS Collaboration, “CMS luminosity measurement for the 2017 data-taking period at $\sqrt{s} = 13$ TeV”, CMS Physics Analysis Summary CMS-PAS-LUM-17-004, 2018.
- [76] CMS Collaboration, “CMS luminosity measurement for the 2018 data-taking period at $\sqrt{s} = 13$ TeV”, CMS Physics Analysis Summary CMS-PAS-LUM-18-002, 2019.
- [77] CMS Collaboration, “Measurement of the inelastic proton-proton cross section at $\sqrt{s} = 13$ TeV”, *JHEP* **07** (2018) 161, doi:10.1007/JHEP07(2018)161, arXiv:1802.02613.
- [78] A. Kalogeropoulos and J. Alwall, “The SysCalc code: A tool to derive theoretical systematic uncertainties”, (2018). arXiv:1801.08401.
- [79] ATLAS Collaboration, “Measurement of the $t\bar{t}Z$ and $t\bar{t}W$ cross sections in proton-proton collisions at $\sqrt{s} = 13$ TeV with the ATLAS detector”, *Phys. Rev. D* **99** (2019) 072009, doi:10.1103/PhysRevD.99.072009, arXiv:1901.03584.
- [80] CMS Collaboration, “Measurement of the cross section for top quark pair production in association with a W or Z boson in proton-proton collisions at $\sqrt{s} = 13$ TeV”, *JHEP* **08** (2018) 011, doi:10.1007/JHEP08(2018)011, arXiv:1711.02547.
- [81] CMS Collaboration, “Measurements of $t\bar{t}$ cross sections in association with b jets and inclusive jets and their ratio using dilepton final states in pp collisions at $\sqrt{s} = 13$ TeV”, *Phys. Lett. B* **776** (2018) 355, doi:10.1016/j.physletb.2017.11.043, arXiv:1705.10141.
- [82] T. Junk, “Confidence level computation for combining searches with small statistics”, *Nucl. Instrum. Meth. A* **434** (1999) 435, doi:10.1016/S0168-9002(99)00498-2, arXiv:hep-ex/9902006.
- [83] A. L. Read, “Presentation of search results: the CL_s technique”, in *Durham IPPP Workshop: Advanced Statistical Techniques in Particle Physics*, p. 2693. *J. Phys. G* **28** (2002) 2693. doi:10.1088/0954-3899/28/10/313.
- [84] ATLAS and CMS Collaborations, “Procedure for the LHC Higgs boson search combination in summer 2011”, ATL-PHYS-PUB-2011-011, CMS NOTE-2011/005, 2011.
- [85] G. Cowan, K. Cranmer, E. Gross, and O. Vitells, “Asymptotic formulae for likelihood-based tests of new physics”, *Eur. Phys. J. C* **71** (2011) 1554, doi:10.1140/epjc/s10052-011-1554-0, arXiv:1007.1727. [Erratum: doi:10.1140/epjc/s10052-013-2501-z].

-
- [86] CMS Collaboration, “Search for supersymmetry in pp collisions at $\sqrt{s} = 13$ TeV with 137 fb^{-1} in final states with a single lepton using the sum of masses of large-radius jets”, *Phys. Rev. D* **101** (2020), no. 5, 052010, doi:10.1103/PhysRevD.101.052010, arXiv:1911.07558.
- [87] CMS Collaboration, “Search for supersymmetry in proton-proton collisions at 13 TeV in final states with jets and missing transverse momentum”, *JHEP* **10** (2019) 244, doi:10.1007/JHEP10(2019)244, arXiv:1908.04722.
- [88] CMS Collaboration, “Searches for physics beyond the standard model with the M_{T2} variable in hadronic final states with and without disappearing tracks in proton-proton collisions at $\sqrt{s} = 13$ TeV”, *Eur. Phys. J. C* **80** (2020), no. 1, 3, doi:10.1140/epjc/s10052-019-7493-x, arXiv:1909.03460.
- [89] CMS Collaboration, “Search for R -parity violating supersymmetry in pp collisions at $\sqrt{s} = 13$ TeV using b jets in a final state with a single lepton, many jets, and high sum of large-radius jet masses”, *Phys. Lett. B* **783** (2018) 114, doi:10.1016/j.physletb.2018.06.028, arXiv:1712.08920.

A Extended results

Tables 11–16, corresponding to Figures 5–6, show background predictions per process within each signal region.

Table 11: Event yields in HH regions. Yields shown as “-” have a contribution smaller than 0.01, or do not contribute to a particular region.

| SR | ttW | ttZ | ttH | W Z | WW | X+ γ | Rare | Charge misid. | Nonprompt lep. | SM expected | Data |
|-------|-----------|-----------|-----------|-----------|-----------|-------------|-----------|---------------|----------------|-------------|------|
| SR1 | 53±15 | 14.1±4.1 | 13.7±3.5 | 349±97 | 129±37 | 300±120 | 105±43 | 136±16 | 460±260 | 1560±300 | 1673 |
| SR2 | 28.5±8.1 | 7.7±2.2 | 7.7±2.0 | 124±34 | 161±46 | 86±40 | 38±16 | 34.6±3.9 | 94±60 | 582±93 | 653 |
| SR3 | 8.1±2.3 | 1.46±0.41 | 1.64±0.42 | 19.8±5.6 | 13.0±3.8 | 7.3±7.3 | 8.8±3.7 | 14.0±1.6 | 26±21 | 100±25 | 128 |
| SR4 | 6.2±1.8 | 2.34±0.67 | 3.45±0.86 | 4.0±1.1 | 4.4±1.3 | 0.50±0.23 | 4.3±1.8 | 2.01±0.22 | 12.4±7.7 | 39.5±8.5 | 54 |
| SR5 | 4.0±1.1 | 0.48±0.14 | 0.49±0.12 | 15.9±4.4 | 21.1±6.1 | 5.5±4.7 | 4.8±2.0 | 0.50±0.06 | 4.9±2.4 | 57.7±9.9 | 53 |
| SR6 | 1.64±0.49 | 0.49±0.14 | 0.57±0.15 | 6.7±2.0 | 5.2±1.6 | 8.6±5.3 | 2.6±1.0 | 0.61±0.07 | 6.0±3.3 | 32.5±7.1 | 24 |
| SR7 | 0.91±0.26 | 0.26±0.07 | 0.38±0.09 | 0.62±0.19 | 0.84±0.23 | 1.2±1.2 | 0.43±0.18 | 0.08±0.01 | 0.81±0.51 | 5.5±1.8 | 7 |
| SR8 | 1.67±0.48 | 0.27±0.09 | 0.24±0.06 | 3.10±0.89 | 6.9±2.0 | 2.6±2.6 | 1.83±0.81 | 4.15±0.48 | 2.1±2.0 | 22.9±5.1 | 33 |
| SR9 | 1.00±0.29 | 0.27±0.09 | 0.20±0.05 | 2.79±0.77 | 4.5±1.3 | 2.0±2.0 | 1.17±0.50 | 4.59±0.54 | 3.0±2.4 | 19.5±3.9 | 20 |
| SR10 | 1.45±0.42 | 0.26±0.07 | 0.27±0.07 | 0.99±0.27 | 2.71±0.82 | 0.02±0.02 | 1.66±0.68 | 0.66±0.08 | 1.61±0.84 | 9.6±1.9 | 11 |
| SR11 | 130±37 | 34.6±9.8 | 35.0±9.2 | 29.8±8.3 | 11.3±3.3 | 49±21 | 30±12 | 89±10 | 530±270 | 940±270 | 1115 |
| SR12 | 80±22 | 21.2±6.0 | 22.3±5.7 | 14.2±3.9 | 15.8±4.7 | 24±11 | 16.3±6.7 | 21.7±2.5 | 125±76 | 340±81 | 384 |
| SR13 | 12.8±3.6 | 1.96±0.56 | 1.97±0.51 | 1.54±0.44 | 0.77±0.29 | 1.43±0.90 | 1.35±0.54 | 3.91±0.44 | 10.6±8.3 | 36.3±9.5 | 40 |
| SR14 | 6.5±1.8 | 1.93±0.56 | 1.96±0.51 | 0.54±0.19 | 0.31±0.13 | 1.05±0.57 | 1.03±0.42 | 4.15±0.47 | 9.4±6.9 | 26.8±7.4 | 26 |
| SR15 | 13.9±3.9 | 4.0±1.2 | 6.4±1.6 | 0.44±0.15 | 0.67±0.20 | 0.67±0.32 | 3.5±1.4 | 1.16±0.13 | 12.1±7.0 | 42.7±8.6 | 68 |
| SR16 | 7.8±2.2 | 4.0±1.2 | 6.2±1.6 | 0.35±0.11 | 0.35±0.10 | 0.86±0.41 | 2.7±1.1 | 1.18±0.13 | 14.4±7.9 | 37.9±8.6 | 41 |
| SR17 | 9.3±2.7 | 1.21±0.35 | 1.38±0.35 | 1.86±0.53 | 1.96±0.57 | 3.3±3.3 | 1.74±0.70 | 0.89±0.10 | 4.9±3.1 | 26.5±6.2 | 29 |
| SR18 | 4.1±1.2 | 1.05±0.31 | 1.30±0.33 | 0.72±0.21 | 0.54±0.16 | 0.76±0.39 | 0.94±0.39 | 0.95±0.11 | 4.0±3.1 | 14.3±3.6 | 13 |
| SR19 | 2.76±0.78 | 0.87±0.25 | 1.24±0.32 | 0.14±0.04 | 0.14±0.04 | 1.6±1.5 | 0.73±0.31 | 0.20±0.02 | 2.9±1.5 | 10.6±2.5 | 12 |
| SR20 | 4.9±1.4 | 0.76±0.22 | 0.60±0.15 | 0.54±0.17 | 0.66±0.19 | 1.7±1.7 | 0.72±0.31 | 1.17±0.13 | 1.2±1.2 | 12.3±2.9 | 14 |
| SR21 | 2.66±0.74 | 0.68±0.20 | 0.59±0.15 | 0.27±0.13 | 0.62±0.18 | 0.53±0.30 | 0.59±0.25 | 1.27±0.14 | 1.9±1.9 | 9.2±2.7 | 17 |
| SR22 | 4.5±1.3 | 0.75±0.22 | 1.00±0.25 | 0.16±0.06 | 0.30±0.09 | 0.42±0.19 | 1.30±0.55 | 0.49±0.05 | 1.2±1.2 | 10.1±2.1 | 17 |
| SR23 | 77±22 | 20.5±5.9 | 22.2±6.0 | 1.62±0.51 | 0.59±0.17 | 22.4±9.3 | 8.8±3.7 | 56.9±6.5 | 61±31 | 272±43 | 354 |
| SR24 | 55±16 | 14.8±4.2 | 16.8±4.4 | 1.16±0.35 | 0.85±0.25 | 9.4±3.6 | 7.8±3.2 | 13.6±1.6 | 27±15 | 147±25 | 177 |
| SR25 | 7.5±2.2 | 1.05±0.30 | 1.19±0.32 | 0.09±0.03 | - | 0.60±0.35 | 0.79±0.33 | 2.18±0.25 | 1.9±1.7 | 15.3±2.9 | 12 |
| SR26 | 4.1±1.2 | 0.89±0.28 | 1.29±0.34 | 0.02±0.02 | 0.02±0.01 | 0.76±0.35 | 0.53±0.22 | 2.14±0.25 | 1.7±1.7 | 11.4±2.4 | 19 |
| SR27 | 12.2±3.6 | 3.7±1.1 | 6.0±1.6 | 0.15±0.06 | 0.05±0.03 | 1.01±0.49 | 3.9±1.6 | 0.96±0.11 | 5.4±2.8 | 33.4±5.4 | 49 |
| SR28 | 7.4±2.1 | 3.6±1.1 | 6.0±1.6 | 0.02±0.01 | 0.12±0.04 | 0.95±0.40 | 3.3±1.4 | 1.06±0.12 | 7.6±3.3 | 30.1±4.9 | 38 |
| SR29 | 5.4±1.5 | 0.61±0.18 | 0.79±0.21 | 0.16±0.06 | 0.04±0.03 | 0.16±0.09 | 0.65±0.27 | 0.39±0.04 | 2.2±1.5 | 10.4±2.2 | 9 |
| SR30 | 2.68±0.80 | 0.57±0.15 | 0.80±0.21 | 0.20±0.06 | 0.08±0.03 | 0.47±0.23 | 0.37±0.15 | 0.48±0.06 | 0.94±0.79 | 6.6±1.3 | 7 |
| SR31 | 2.74±0.84 | 0.56±0.17 | 1.16±0.30 | 0.06±0.02 | 0.07±0.03 | 0.15±0.06 | 1.10±0.46 | 0.18±0.02 | 0.92±0.92 | 6.9±1.5 | 6 |
| SR32 | 3.41±0.96 | 0.60±0.18 | 0.47±0.12 | - | 0.05±0.02 | 0.35±0.17 | 0.38±0.16 | 0.52±0.06 | 0.10±0.10 | 5.9±1.1 | 14 |
| SR33 | 2.09±0.60 | 0.59±0.18 | 0.58±0.15 | - | 0.01±0.01 | 0.24±0.12 | 0.31±0.13 | 0.55±0.06 | 1.7±1.3 | 6.1±1.6 | 7 |
| SR34 | 2.97±0.90 | 0.89±0.20 | 0.81±0.21 | 0.02±0.00 | 0.08±0.03 | 0.24±0.10 | 1.12±0.46 | 0.33±0.04 | 0.58±0.58 | 6.8±1.3 | 10 |
| SR35 | 3.25±0.95 | 0.83±0.26 | 1.19±0.33 | - | - | 0.27±0.22 | 0.57±0.25 | 0.95±0.11 | 1.75±0.98 | 8.8±1.5 | 16 |
| SR36 | 1.83±0.55 | 0.80±0.24 | 1.22±0.34 | - | - | 0.48±0.28 | 0.49±0.21 | 0.97±0.11 | 2.9±1.8 | 8.7±2.0 | 11 |
| SR37 | 3.3±1.0 | 0.98±0.30 | 1.11±0.31 | - | 0.02±0.01 | 0.40±0.17 | 1.03±0.42 | 0.55±0.06 | 2.0±1.3 | 9.4±1.9 | 7 |
| SR38 | 1.93±0.58 | 0.89±0.26 | 1.07±0.30 | 0.01±0.01 | - | 0.38±0.27 | 0.97±0.40 | 0.56±0.07 | 1.17±0.80 | 7.0±1.3 | 5 |
| SR39 | 2.16±0.65 | 0.65±0.21 | 1.16±0.33 | 0.02±0.01 | - | 0.22±0.09 | 3.4±1.4 | 0.20±0.02 | 1.7±1.1 | 9.6±2.1 | 9 |
| SR40 | 1.54±0.49 | 0.82±0.28 | 1.29±0.36 | - | - | 0.36±0.17 | 3.1±1.3 | 0.21±0.03 | 1.26±0.67 | 8.6±1.7 | 11 |
| SR41 | 0.46±0.14 | 0.14±0.04 | 0.16±0.05 | - | - | 0.07±0.04 | 0.13±0.05 | 0.14±0.02 | - | 1.10±0.32 | 2 |
| SR42 | 0.24±0.09 | 0.08±0.05 | 0.08±0.03 | - | - | 0.02±0.02 | 0.17±0.07 | 0.04±0.01 | - | 0.63±0.49 | 0 |
| SR43 | 0.21±0.09 | 0.04±0.04 | 0.07±0.02 | - | - | 0.12±0.12 | 0.14±0.06 | 0.04±0.01 | 0.04±0.04 | 0.67±0.60 | 1 |
| SR44 | 0.14±0.04 | 0.03±0.01 | 0.08±0.02 | - | - | 0.02±0.01 | 0.39±0.16 | 0.04±0.00 | 0.04±0.04 | 0.74±0.27 | 1 |
| SR45 | 0.16±0.08 | 0.04±0.04 | 0.07±0.03 | 0.03±0.03 | - | 0.04±0.04 | 0.36±0.15 | 0.01±0.01 | - | 0.71±0.53 | 1 |
| SR46 | 9.6±2.8 | 0.93±0.26 | 0.91±0.23 | 8.3±2.3 | 14.7±4.3 | 6.9±6.8 | 3.5±1.5 | 0.61±0.07 | 2.3±2.0 | 47.8±9.7 | 59 |
| SR47 | 3.5±1.0 | 0.84±0.28 | 0.92±0.23 | 3.04±0.84 | 2.92±0.88 | 1.9±1.9 | 1.51±0.62 | 0.66±0.07 | 2.0±1.4 | 17.3±3.8 | 24 |
| SR48 | 1.27±0.40 | 0.12±0.04 | 0.05±0.02 | 1.64±0.46 | 4.7±1.4 | 1.8±1.8 | 0.44±0.18 | 0.05±0.01 | 0.20±0.16 | 10.3±2.9 | 11 |
| SR49 | 0.37±0.11 | 0.13±0.04 | 0.08±0.02 | 0.62±0.23 | 0.41±0.13 | 0.02±0.01 | 0.34±0.17 | 0.04±0.00 | 0.03±0.03 | 2.06±0.49 | 3 |
| SR50 | 2.57±0.79 | 0.30±0.10 | 0.54±0.15 | 0.43±0.12 | 0.72±0.23 | 0.06±0.03 | 1.11±0.45 | 0.09±0.01 | 0.72±0.31 | 6.5±1.1 | 13 |
| SR51 | 1.16±0.38 | 0.35±0.14 | 0.57±0.15 | 0.20±0.07 | 0.15±0.06 | 0.02±0.01 | 0.79±0.34 | 0.08±0.01 | 0.40±0.38 | 3.72±0.79 | 4 |
| SR52 | 0.45±0.12 | 0.06±0.02 | 0.05±0.02 | 0.22±0.09 | 0.15±0.05 | 0.02±0.01 | 0.20±0.08 | - | 0.05±0.05 | 1.21±0.29 | 4 |
| SR53 | 0.20±0.09 | 0.05±0.04 | 0.06±0.03 | - | 0.03±0.03 | - | 0.08±0.04 | 0.01±0.01 | - | 0.44±0.44 | 2 |
| SR54 | 1.75±0.53 | 0.26±0.09 | 0.23±0.07 | 0.95±0.29 | 4.6±1.4 | 0.65±0.58 | 0.63±0.27 | 0.46±0.05 | 0.29±0.12 | 9.8±1.8 | 24 |
| SR55 | 0.99±0.28 | 0.15±0.05 | 0.12±0.04 | 0.78±0.23 | 4.0±1.1 | 0.03±0.03 | 0.58±0.24 | 0.35±0.04 | 0.33±0.33 | 7.3±1.4 | 4 |
| SR56 | 0.57±0.16 | 0.04±0.01 | 0.07±0.02 | 0.39±0.13 | 2.46±0.72 | 0.34±0.34 | 0.17±0.07 | 0.18±0.02 | 0.22±0.17 | 4.44±0.98 | 6 |
| SR57 | 2.04±0.59 | 0.48±0.13 | 0.53±0.16 | 0.29±0.10 | 0.47±0.15 | 0.04±0.02 | 0.71±0.29 | 0.22±0.03 | 0.89±0.73 | 5.7±1.1 | 6 |
| SR58 | 1.65±0.56 | 0.17±0.05 | 0.30±0.09 | 0.14±0.05 | 0.47±0.15 | - | 0.70±0.31 | 0.13±0.02 | 0.48±0.48 | 4.0±1.0 | 6 |
| SR59 | 0.99±0.35 | 0.06±0.02 | 0.16±0.06 | 0.15±0.06 | 0.37±0.11 | - | 0.27±0.12 | 0.13±0.01 | 0.11±0.11 | 2.24±0.53 | 2 |
| SR60 | 0.61±0.18 | 0.08±0.04 | 0.33±0.09 | - | 0.01±0.01 | 0.03±0.02 | 0.67±0.29 | 0.04±0.00 | 0.06±0.06 | 1.83±0.44 | 5 |
| SR61 | 0.65±0.21 | 0.12±0.04 | 0.20±0.06 | 0.08±0.05 | 0.09±0.03 | - | 0.50±0.20 | 0.03±0.00 | 0.19±0.14 | 1.88±0.40 | 5 |
| SR62 | 0.41±0.12 | 0.05±0.02 | 0.14±0.05 | 0.04±0.01 | 0.03±0.01 | 0.01±0.01 | 0.22±0.09 | 0.02±0.00 | 0.43±0.43 | 1.35±0.56 | 0 |
| Total | 610±180 | 158±40 | 180±44 | 600±160 | 420±120 | 540±250 | 280±150 | 409±43 | 1460±740 | 4660±880 | 5376 |

Table 12: Event yields in HL regions. Yields shown as “-” have a contribution smaller than 0.01, or do not contribute to a particular region.

| | t̄tW | t̄tZ | t̄tH | W Z | WW | X+̳ | Rare | Charge misid. | Nonprompt lep. | SM expected | Data |
|-------|-----------|-----------|-----------|-----------|-----------|-----------|-----------|---------------|----------------|-------------|------|
| SR1 | 17.5±4.9 | 6.2±1.8 | 6.8±1.8 | 168±47 | 49±14 | 145±67 | 51±21 | 33.6±3.8 | 910±290 | 1390±300 | 1593 |
| SR2 | 7.2±2.1 | 2.63±0.76 | 3.21±0.82 | 38±10 | 46±13 | 41±25 | 11.3±4.8 | 6.54±0.73 | 192±62 | 348±67 | 337 |
| SR3 | 0.97±0.28 | 0.20±0.07 | 0.34±0.09 | 5.0±1.4 | 2.24±0.68 | 0.04±0.04 | 1.88±0.79 | 0.24±0.03 | 16.0±5.3 | 26.9±8.8 | 39 |
| SR4 | 1.85±0.54 | 0.81±0.23 | 1.67±0.42 | 1.19±0.34 | 1.45±0.42 | 0.30±0.13 | 1.25±0.50 | 0.48±0.06 | 26.9±9.1 | 35.9±9.1 | 34 |
| SR5 | 1.15±0.33 | 0.20±0.06 | 0.23±0.06 | 5.5±1.5 | 7.8±2.3 | 4.2±3.7 | 1.12±0.46 | 0.10±0.01 | 9.4±3.0 | 29.8±6.0 | 34 |
| SR6 | 0.36±0.10 | 0.21±0.07 | 0.22±0.06 | 2.73±0.76 | 1.43±0.43 | 8.4±6.7 | 0.49±0.22 | 0.19±0.02 | 8.2±2.5 | 22.2±7.2 | 12 |
| SR7 | 0.22±0.07 | 0.10±0.05 | 0.19±0.05 | 0.29±0.10 | 0.25±0.09 | 0.07±0.04 | 0.32±0.14 | 0.02±0.00 | 3.2±1.4 | 4.7±1.4 | 6 |
| SR8 | 46±13 | 16.5±4.7 | 18.0±4.7 | 14.6±4.0 | 3.4±1.0 | 36±16 | 13.5±5.5 | 25.4±2.9 | 920±280 | 1100±280 | 1342 |
| SR9 | 22.0±6.2 | 8.2±2.3 | 9.9±2.5 | 4.4±1.2 | 4.1±1.2 | 8.8±3.8 | 4.6±1.9 | 4.53±0.51 | 232±70 | 299±71 | 330 |
| SR10 | 1.65±0.48 | 0.27±0.08 | 0.35±0.09 | 0.16±0.06 | 0.16±0.05 | 0.64±0.29 | 0.22±0.11 | 0.23±0.03 | 5.5±2.1 | 9.1±2.3 | 8 |
| SR11 | 0.81±0.25 | 0.23±0.08 | 0.41±0.11 | 0.12±0.05 | 0.05±0.02 | 0.17±0.09 | 0.21±0.09 | 0.20±0.02 | 4.2±1.6 | 6.4±1.6 | 9 |
| SR12 | 4.2±1.2 | 1.26±0.38 | 3.23±0.82 | 0.08±0.03 | 0.25±0.10 | 1.58±0.86 | 0.85±0.34 | 0.29±0.03 | 30.3±9.0 | 42.1±9.2 | 49 |
| SR13 | 1.95±0.58 | 1.37±0.41 | 3.18±0.81 | 0.10±0.06 | 0.06±0.02 | 1.14±0.44 | 0.92±0.38 | 0.32±0.04 | 24.0±8.2 | 33.0±8.4 | 39 |
| SR14 | 4.3±1.3 | 0.88±0.25 | 1.16±0.30 | 1.14±0.33 | 0.90±0.26 | 0.51±0.23 | 0.59±0.25 | 0.45±0.05 | 15.9±5.5 | 25.8±5.9 | 25 |
| SR15 | 0.62±0.23 | 0.10±0.10 | 0.30±0.09 | - | 0.04±0.04 | 0.03±0.03 | 0.15±0.08 | 0.03±0.01 | 1.6±1.6 | 2.8±2.0 | 7 |
| SR16 | 0.30±0.11 | 0.17±0.08 | 0.34±0.09 | 0.06±0.06 | 0.02±0.02 | - | 0.14±0.07 | 0.03±0.01 | 1.4±1.2 | 2.5±1.3 | 2 |
| SR17 | 28.9±8.2 | 10.3±3.0 | 11.7±3.1 | 0.68±0.21 | 0.09±0.04 | 15.6±6.7 | 3.9±1.6 | 17.9±2.1 | 133±39 | 222±42 | 260 |
| SR18 | 16.8±4.8 | 6.2±1.8 | 7.9±2.1 | 0.53±0.15 | 0.24±0.08 | 6.4±2.6 | 2.40±1.00 | 3.34±0.38 | 43±13 | 86±15 | 104 |
| SR19 | 0.72±0.24 | 0.12±0.04 | 0.28±0.07 | - | - | 0.04±0.04 | 0.05±0.03 | 0.13±0.01 | 0.87±0.69 | 2.22±0.90 | 4 |
| SR20 | 0.58±0.17 | 0.11±0.04 | 0.26±0.07 | 0.05±0.03 | 0.03±0.02 | 0.12±0.05 | 0.09±0.04 | 0.13±0.01 | 1.8±1.1 | 3.2±1.1 | 4 |
| SR21 | 4.4±1.3 | 1.69±0.47 | 3.13±0.82 | - | 0.11±0.03 | 2.5±1.9 | 1.23±0.50 | 0.25±0.03 | 6.5±2.2 | 19.8±3.8 | 28 |
| SR22 | 2.06±0.57 | 1.41±0.41 | 3.15±0.82 | - | - | 1.01±0.49 | 0.95±0.38 | 0.23±0.03 | 7.3±2.5 | 16.1±3.0 | 19 |
| SR23 | 1.96±0.56 | 0.21±0.08 | 0.42±0.11 | 0.05±0.02 | 0.09±0.04 | 0.21±0.09 | 0.16±0.07 | 0.12±0.01 | 1.5±1.0 | 4.7±1.3 | 1 |
| SR24 | 0.83±0.25 | 0.27±0.09 | 0.37±0.10 | 0.09±0.04 | 0.01±0.01 | 0.17±0.08 | 0.16±0.06 | 0.15±0.02 | 1.9±1.2 | 4.0±1.2 | 2 |
| SR25 | 1.11±0.34 | 0.26±0.08 | 0.57±0.15 | - | - | 0.21±0.09 | 0.31±0.13 | 0.05±0.01 | 1.52±0.98 | 4.0±1.1 | 5 |
| SR26 | 1.02±0.30 | 0.41±0.12 | 0.61±0.17 | - | 0.01±0.00 | 0.49±0.20 | 0.21±0.09 | 0.27±0.03 | 5.4±2.3 | 8.5±2.4 | 7 |
| SR27 | 0.53±0.15 | 0.47±0.14 | 0.60±0.17 | - | - | 0.53±0.22 | 0.17±0.08 | 0.28±0.03 | 5.8±2.5 | 8.4±2.5 | 7 |
| SR28 | 1.36±0.41 | 0.60±0.20 | 1.14±0.31 | - | - | 0.21±0.09 | 1.02±0.42 | 0.18±0.02 | 4.4±2.0 | 8.9±2.2 | 11 |
| SR29 | 0.92±0.28 | 0.43±0.14 | 1.12±0.31 | - | - | 0.34±0.14 | 0.98±0.41 | 0.22±0.03 | 6.9±3.0 | 10.9±3.1 | 11 |
| SR30 | 0.36±0.13 | 0.15±0.05 | 0.20±0.06 | - | - | 0.02±0.01 | 0.30±0.12 | 0.03±0.00 | 0.18±0.18 | 1.25±0.39 | 3 |
| SR31 | 0.41±0.12 | 0.05±0.02 | 0.17±0.04 | 0.15±0.05 | 0.12±0.05 | 0.05±0.02 | 0.08±0.04 | 0.09±0.01 | 0.81±0.29 | 1.92±0.37 | 4 |
| SR32 | 0.73±0.24 | 0.06±0.02 | 0.19±0.05 | 0.18±0.07 | 0.31±0.11 | 0.06±0.03 | 0.33±0.14 | 0.07±0.01 | 0.83±0.38 | 2.77±0.56 | 3 |
| SR33 | 2.51±0.71 | 0.32±0.08 | 0.33±0.09 | 2.66±0.76 | 5.0±1.4 | 0.16±0.16 | 1.62±0.69 | 0.12±0.01 | 6.4±1.9 | 19.1±4.1 | 23 |
| SR34 | 0.99±0.27 | 0.24±0.07 | 0.30±0.08 | 1.19±0.34 | 0.70±0.21 | 0.08±0.05 | 0.72±0.32 | 0.11±0.01 | 3.2±1.2 | 7.5±1.5 | 9 |
| SR35 | 0.30±0.09 | 0.03±0.01 | 0.03±0.01 | 0.55±0.17 | 0.95±0.30 | 0.01±0.01 | 0.15±0.08 | - | 0.09±0.09 | 2.12±0.49 | 5 |
| SR36 | 0.11±0.05 | 0.02±0.02 | - | 0.10±0.10 | 0.06±0.06 | - | 0.08±0.08 | - | 0.09±0.09 | 0.47±0.33 | 1 |
| SR37 | 0.71±0.21 | 0.13±0.04 | 0.20±0.05 | 0.18±0.06 | 0.34±0.10 | 0.01±0.01 | 0.19±0.09 | 0.02±0.00 | 0.96±0.65 | 2.75±0.77 | 4 |
| SR38 | 0.19±0.06 | 0.11±0.04 | 0.21±0.06 | 0.02±0.02 | 0.06±0.02 | 0.01±0.01 | 0.18±0.08 | 0.02±0.00 | 0.88±0.45 | 1.68±0.50 | 0 |
| SR39 | 0.21±0.08 | 0.02±0.02 | 0.03±0.01 | - | 0.07±0.06 | - | 0.04±0.02 | - | 0.59±0.59 | 0.97±0.97 | 0 |
| SR40 | 0.60±0.17 | 0.05±0.04 | 0.18±0.05 | 0.11±0.08 | 1.01±0.30 | - | 0.30±0.13 | 0.05±0.01 | 0.54±0.43 | 2.83±0.70 | 7 |
| SR41 | 0.24±0.12 | 0.12±0.07 | 0.18±0.06 | 0.05±0.05 | 0.17±0.12 | 2.1±2.1 | 0.11±0.06 | 0.04±0.01 | 0.79±0.54 | 3.8±3.8 | 0 |
| SR42 | 0.92±0.29 | 0.12±0.04 | 0.15±0.05 | 0.27±0.08 | 1.59±0.46 | 0.03±0.01 | 0.21±0.09 | 0.06±0.01 | 1.57±0.81 | 4.9±1.0 | 9 |
| SR43 | 0.24±0.07 | 0.11±0.04 | 0.21±0.07 | 0.16±0.05 | 0.32±0.10 | 0.51±0.51 | 0.19±0.08 | 0.09±0.01 | 0.53±0.20 | 2.36±0.72 | 5 |
| Total | 180±52 | 63±16 | 83±20 | 248±64 | 129±36 | 270±120 | 105±56 | 97±10 | 2640±590 | 3820±620 | 4402 |

Table 13: Event yields in LL regions. Yields shown as “-” have a contribution smaller than 0.01, or do not contribute to a particular region.

| | t̄tW | t̄tZ | t̄tH | W Z | WW | X+̳ | Rare | Charge misid. | Nonprompt lep. | SM expected | Data |
|-------|-----------|-----------|-----------|-----------|-----------|-----------|-----------|---------------|----------------|-------------|------|
| SR1 | 0.34±0.10 | 0.27±0.08 | 0.30±0.08 | 1.93±0.57 | 2.27±0.66 | 0.41±0.28 | 0.38±0.17 | 0.06±0.01 | 17.0±7.2 | 23.0±7.2 | 29 |
| SR2 | 0.10±0.04 | 0.05±0.03 | 0.07±0.02 | 0.93±0.31 | 0.86±0.25 | 0.03±0.01 | 0.37±0.16 | - | 2.6±1.5 | 5.0±1.6 | 6 |
| SR3 | 1.00±0.27 | 0.90±0.26 | 1.03±0.26 | 0.19±0.06 | 0.14±0.04 | 0.14±0.14 | 0.33±0.14 | 0.09±0.01 | 19.9±6.5 | 23.8±6.6 | 27 |
| SR4 | 0.47±0.14 | 0.11±0.03 | 0.28±0.07 | 0.05±0.02 | 0.08±0.02 | 0.09±0.04 | 0.19±0.08 | 0.01±0.00 | 3.4±1.5 | 4.7±1.5 | 7 |
| SR5 | 0.92±0.26 | 0.68±0.20 | 0.96±0.25 | 0.01±0.00 | 0.02±0.02 | 0.16±0.14 | 0.28±0.12 | 0.09±0.01 | 4.8±1.8 | 8.0±1.9 | 15 |
| SR6 | 0.33±0.13 | 0.14±0.07 | 0.21±0.06 | - | 0.04±0.04 | 0.03±0.03 | 0.05±0.02 | 0.02±0.01 | 1.2±1.1 | 2.0±1.1 | 0 |
| SR7 | 0.17±0.06 | 0.09±0.03 | 0.19±0.06 | - | - | 0.12±0.05 | 0.21±0.09 | 0.02±0.00 | 0.81±0.56 | 1.61±0.59 | 3 |
| SR8 | 0.02±0.02 | 0.01±0.01 | 0.01±0.01 | - | - | - | - | - | - | 0.06±0.06 | 0 |
| Total | 3.36±0.98 | 2.25±0.60 | 3.04±0.80 | 3.09±0.82 | 3.42±0.96 | 0.79±0.42 | 1.84±0.97 | 0.30±0.03 | 50±13 | 68±13 | 87 |

Table 14: Event yields in on-Z ML regions. Yields shown as “-” have a contribution smaller than 0.01, or do not contribute to a particular region.

| | $t\bar{t}W$ | $t\bar{t}Z$ | $t\bar{t}H$ | W Z | X+ γ | Rare | Nonprompt lep. | SM expected | Data |
|-------|-------------|-------------|-------------|-----------|-------------|-----------|----------------|-------------|------|
| SR1 | 1.12±0.30 | 46±13 | 1.67±0.43 | 620±170 | 11.9±5.7 | 105±42 | 54±18 | 840±170 | 985 |
| SR2 | 0.71±0.21 | 6.8±1.9 | 0.46±0.12 | 68±19 | 3.1±2.6 | 17.8±7.3 | 9.9±4.6 | 107±21 | 136 |
| SR3 | 0.18±0.05 | 8.5±2.4 | 0.23±0.06 | 95±26 | 0.02±0.01 | 11.7±4.8 | 3.2±1.8 | 119±27 | 146 |
| SR4 | 0.17±0.06 | 1.99±0.54 | 0.17±0.04 | 5.8±1.6 | 0.03±0.01 | 2.19±0.87 | 0.68±0.46 | 11.1±2.1 | 10 |
| SR5 | 0.13±0.04 | 7.7±2.2 | 0.25±0.06 | 83±23 | 2.3±1.2 | 11.0±4.5 | 4.5±2.1 | 109±24 | 126 |
| SR6 | 0.09±0.03 | 1.42±0.39 | 0.06±0.02 | 13.6±3.8 | 0.74±0.61 | 2.5±1.0 | 0.93±0.69 | 19.3±4.1 | 24 |
| SR7 | 0.10±0.03 | 2.55±0.73 | 0.09±0.02 | 35±10 | 0.09±0.04 | 3.7±1.6 | 0.89±0.53 | 42±10 | 47 |
| SR8 | 0.11±0.03 | 0.45±0.15 | 0.04±0.01 | 2.02±0.67 | - | 0.61±0.25 | 0.25±0.18 | 3.47±0.84 | 3 |
| SR9 | 5.6±1.6 | 140±39 | 6.1±1.6 | 52±14 | 5.3±2.4 | 72±29 | 46±17 | 327±54 | 419 |
| SR10 | 1.70±0.48 | 23.4±6.7 | 1.18±0.31 | 7.6±2.1 | 0.20±0.09 | 9.1±3.8 | 3.2±2.0 | 46.5±8.4 | 53 |
| SR11 | 0.61±0.17 | 25.9±7.5 | 0.98±0.25 | 11.0±3.0 | 0.27±0.16 | 9.5±3.9 | 3.1±1.3 | 51.3±9.1 | 62 |
| SR12 | 0.30±0.08 | 7.5±2.1 | 0.36±0.09 | 3.48±0.99 | 0.04±0.02 | 2.9±1.2 | 0.95±0.67 | 15.6±2.8 | 27 |
| SR13 | 4.8±1.4 | 89±25 | 4.5±1.2 | 3.7±1.0 | 2.17±0.90 | 22.4±9.0 | 4.9±1.9 | 131±27 | 162 |
| SR14 | 0.98±0.29 | 13.4±3.9 | 0.76±0.20 | 0.62±0.19 | 0.09±0.03 | 2.8±1.1 | 1.24±0.83 | 19.9±4.3 | 26 |
| SR15 | 0.54±0.16 | 20.3±5.8 | 0.91±0.24 | 0.96±0.29 | 0.13±0.06 | 3.7±1.5 | 0.42±0.31 | 26.9±6.1 | 35 |
| SR16 | 0.25±0.08 | 5.2±1.6 | 0.34±0.09 | 0.38±0.12 | 0.05±0.02 | 1.17±0.48 | 0.38±0.38 | 7.8±1.8 | 12 |
| SR17 | 0.12±0.04 | 9.5±2.8 | 0.56±0.16 | 0.24±0.07 | 0.04±0.02 | 2.22±0.90 | 1.25±0.98 | 14.0±3.1 | 19 |
| SR18 | 0.52±0.16 | 20.5±5.9 | 0.84±0.22 | 44±12 | 1.8±1.1 | 11.7±4.8 | 4.8±1.6 | 84±15 | 117 |
| SR19 | 0.20±0.06 | 3.8±1.1 | 0.24±0.06 | 8.2±2.3 | 0.83±0.61 | 3.3±1.3 | 1.66±0.84 | 18.2±3.3 | 26 |
| SR20 | 0.34±0.11 | 9.5±2.7 | 0.48±0.12 | 23.5±6.5 | 0.01±0.01 | 5.3±2.2 | 1.34±0.66 | 40.4±7.6 | 34 |
| SR21 | 0.36±0.10 | 1.75±0.51 | 0.17±0.05 | 1.52±0.48 | 0.01±0.01 | 0.89±0.36 | 0.23±0.10 | 4.92±0.88 | 7 |
| SR22 | 0.28±0.09 | 7.0±2.0 | 0.20±0.05 | 32.3±9.1 | - | 6.3±2.6 | 0.87±0.34 | 46.9±9.9 | 50 |
| SR23 | 0.34±0.10 | 1.68±0.48 | 0.12±0.03 | 2.02±0.59 | - | 1.16±0.46 | 0.50±0.50 | 5.8±1.2 | 10 |
| Total | 19.5±5.6 | 450±110 | 20.8±5.0 | 1110±280 | 29±12 | 310±160 | 145±41 | 2090±360 | 2536 |

Table 15: Event yields in off-Z ML regions. Yields shown as “-” have a contribution smaller than 0.01, or do not contribute to a particular region.

| | $t\bar{t}W$ | $t\bar{t}Z$ | $t\bar{t}H$ | W Z | X+ γ | Rare | Nonprompt lep. | SM expected | Data |
|-------|-------------|-------------|-------------|-----------|-------------|-----------|----------------|-------------|------|
| SR1 | 8.8±2.5 | 11.2±3.2 | 7.0±1.8 | 87±24 | 18.8±9.5 | 22.0±9.0 | 68±25 | 222±36 | 285 |
| SR2 | 0.15±0.07 | 0.15±0.08 | 0.10±0.03 | 1.23±0.50 | 0.02±0.02 | 0.43±0.22 | 0.61±0.61 | 2.7±1.7 | 2 |
| SR3 | 2.38±0.69 | 2.07±0.59 | 1.60±0.42 | 13.6±3.8 | 0.26±0.11 | 4.2±1.7 | 11.3±4.9 | 35.5±6.4 | 34 |
| SR4 | 0.18±0.06 | 0.14±0.04 | 0.08±0.02 | 0.24±0.11 | - | 0.22±0.12 | 0.13±0.13 | 0.99±0.31 | 2 |
| SR5 | 1.11±0.31 | 1.64±0.47 | 1.02±0.26 | 11.2±3.1 | 0.89±0.84 | 1.68±0.68 | 4.6±2.0 | 22.1±4.0 | 29 |
| SR6 | 0.91±0.25 | 0.64±0.19 | 0.59±0.15 | 4.7±1.4 | 0.05±0.02 | 1.05±0.44 | 1.76±0.80 | 9.7±1.7 | 8 |
| SR7 | 26.8±7.5 | 29.7±8.5 | 21.9±5.7 | 7.0±2.0 | 6.9±3.3 | 11.3±4.7 | 113±41 | 217±44 | 272 |
| SR8 | 7.9±2.3 | 5.0±1.5 | 4.6±1.2 | 1.14±0.36 | 0.87±0.37 | 2.43±0.99 | 15.7±5.6 | 37.7±6.8 | 56 |
| SR9 | 3.8±1.1 | 5.3±1.5 | 3.47±0.89 | 0.82±0.26 | 0.86±0.40 | 1.91±0.78 | 5.2±2.5 | 21.4±3.7 | 21 |
| SR10 | 2.69±0.78 | 1.78±0.52 | 1.76±0.45 | 0.35±0.12 | 0.27±0.11 | 1.07±0.45 | 2.9±1.4 | 10.9±1.9 | 18 |
| SR11 | 22.1±6.4 | 19.5±5.7 | 16.1±4.3 | 0.44±0.13 | 6.4±2.6 | 5.1±2.1 | 19.4±6.6 | 89±14 | 112 |
| SR12 | 5.0±1.5 | 2.99±0.86 | 2.93±0.79 | 0.09±0.03 | 0.64±0.27 | 1.28±0.53 | 2.67±0.94 | 15.6±2.4 | 20 |
| SR13 | 3.22±0.96 | 4.2±1.2 | 3.21±0.84 | 0.12±0.05 | 0.56±0.24 | 1.56±0.64 | 3.5±1.7 | 16.4±2.7 | 23 |
| SR14 | 1.53±0.45 | 1.31±0.38 | 1.23±0.32 | - | 0.16±0.07 | 0.77±0.32 | 0.36±0.36 | 5.36±0.95 | 7 |
| SR15 | 0.91±0.28 | 2.00±0.60 | 1.94±0.54 | 0.03±0.01 | 0.26±0.11 | 2.6±1.1 | 1.27±0.83 | 9.0±1.6 | 12 |
| SR16 | 4.6±1.4 | 4.6±1.3 | 3.30±0.87 | 5.4±1.5 | 1.9±1.1 | 3.4±1.4 | 5.3±1.7 | 28.4±3.9 | 46 |
| SR17 | 0.13±0.06 | 0.18±0.07 | 0.05±0.02 | 0.19±0.19 | - | 0.16±0.11 | - | 0.72±0.41 | 2 |
| SR18 | 3.7±1.1 | 2.24±0.67 | 2.42±0.66 | 3.8±1.1 | 0.15±0.07 | 3.1±1.3 | 2.4±1.1 | 17.8±2.8 | 25 |
| SR19 | 0.25±0.09 | 0.18±0.05 | 0.07±0.02 | 0.10±0.03 | - | 0.26±0.12 | 0.04±0.04 | 0.89±0.29 | 0 |
| SR20 | 3.4±1.0 | 1.71±0.50 | 1.59±0.42 | 4.2±1.2 | 0.12±0.05 | 3.1±1.3 | 3.6±2.0 | 17.7±3.3 | 31 |
| SR21 | 0.28±0.09 | 0.21±0.06 | 0.07±0.02 | 0.16±0.07 | - | 0.36±0.15 | 0.12±0.12 | 1.20±0.32 | 2 |
| Total | 100±29 | 97±24 | 75±19 | 141±36 | 38±18 | 68±36 | 262±73 | 780±100 | 1007 |

Table 16: Event yields in LM regions. Yields shown as “-” have a contribution smaller than 0.01, or do not contribute to a particular region.

| | ttW | ttZ | ttH | W Z | WW | X+ γ | Rare | Charge misid. | Nonprompt lep. | SM expected | Data |
|-------|-----------------|-----------------|-----------------|-----------------|-----------------|-----------------|-----------------|-----------------|-----------------|-----------------|------|
| SR1 | 7.7 \pm 2.1 | 2.86 \pm 0.84 | 2.22 \pm 0.57 | 56 \pm 15 | 53 \pm 15 | 38 \pm 19 | 12.5 \pm 5.3 | 13.4 \pm 1.5 | 51 \pm 36 | 235 \pm 47 | 309 |
| SR2 | 1.69 \pm 0.50 | 1.06 \pm 0.30 | 1.12 \pm 0.28 | 1.99 \pm 0.56 | 1.80 \pm 0.53 | 3.5 \pm 2.3 | 1.14 \pm 0.53 | 0.70 \pm 0.08 | 6.3 \pm 4.3 | 19.3 \pm 5.2 | 26 |
| SR3 | 23.0 \pm 6.4 | 8.6 \pm 2.5 | 7.1 \pm 1.9 | 5.9 \pm 1.7 | 5.5 \pm 1.6 | 14.8 \pm 7.7 | 6.1 \pm 2.6 | 6.97 \pm 0.79 | 64 \pm 37 | 142 \pm 39 | 156 |
| SR4 | 6.3 \pm 1.8 | 3.15 \pm 0.89 | 4.4 \pm 1.1 | 0.34 \pm 0.09 | 0.25 \pm 0.10 | 1.22 \pm 0.57 | 1.96 \pm 0.81 | 0.77 \pm 0.09 | 13.8 \pm 8.2 | 32.2 \pm 8.8 | 38 |
| SR5 | 17.6 \pm 5.0 | 6.1 \pm 1.7 | 5.6 \pm 1.5 | 0.48 \pm 0.14 | 0.37 \pm 0.12 | 4.2 \pm 2.1 | 2.6 \pm 1.1 | 4.71 \pm 0.54 | 11.4 \pm 5.8 | 53.0 \pm 9.1 | 69 |
| SR6 | 6.0 \pm 1.7 | 3.17 \pm 0.91 | 4.2 \pm 1.1 | 0.10 \pm 0.04 | 0.12 \pm 0.04 | 1.05 \pm 0.45 | 2.00 \pm 0.83 | 0.68 \pm 0.08 | 4.8 \pm 3.0 | 22.0 \pm 4.0 | 30 |
| SR7 | 2.37 \pm 0.71 | 1.19 \pm 0.36 | 1.42 \pm 0.40 | 0.08 \pm 0.03 | - | 0.61 \pm 0.36 | 2.08 \pm 0.86 | 0.53 \pm 0.06 | 1.8 \pm 1.4 | 10.1 \pm 2.0 | 21 |
| SR8 | 0.09 \pm 0.05 | 0.01 \pm 0.01 | 0.02 \pm 0.01 | 0.23 \pm 0.10 | 0.80 \pm 0.22 | - | 0.04 \pm 0.02 | 0.06 \pm 0.01 | 0.27 \pm 0.27 | 1.53 \pm 0.48 | 3 |
| SR9 | 0.36 \pm 0.11 | 0.17 \pm 0.06 | 0.11 \pm 0.03 | 0.12 \pm 0.04 | 0.11 \pm 0.04 | 0.17 \pm 0.10 | 0.19 \pm 0.08 | 0.03 \pm 0.00 | 0.32 \pm 0.30 | 1.58 \pm 0.41 | 0 |
| SR10 | 0.16 \pm 0.08 | 0.04 \pm 0.03 | 0.01 \pm 0.01 | 0.25 \pm 0.17 | 0.77 \pm 0.27 | 1.3 \pm 1.3 | 0.10 \pm 0.10 | 0.06 \pm 0.02 | 0.16 \pm 0.16 | 2.9 \pm 2.9 | 1 |
| SR11 | 0.44 \pm 0.18 | 0.02 \pm 0.02 | 0.08 \pm 0.03 | - | 0.13 \pm 0.08 | 0.01 \pm 0.01 | 0.16 \pm 0.07 | 0.05 \pm 0.02 | 0.41 \pm 0.41 | 1.31 \pm 0.93 | 4 |
| Total | 66 \pm 19 | 26.3 \pm 6.6 | 26.2 \pm 6.5 | 65 \pm 17 | 62 \pm 18 | 65 \pm 32 | 29 \pm 16 | 27.9 \pm 3.0 | 154 \pm 89 | 520 \pm 110 | 657 |

Table 17: Top five SRs for several representative models, ranked based on the largest values of $N_{\text{sig.}} / \sqrt{N_{\text{bkg.}} + N_{\text{sig.}}}$, where $N_{\text{sig.}}$ and $N_{\text{bkg.}}$ are the signal and total background yields in each SR, respectively.

| model | mass point | top SRs |
|---|--|---|
| T1tttt | $m_{\tilde{g}} = 1400, m_{\tilde{\chi}_1^0} = 400$ | off-Z ML21, HH53, HH52, HH51, HH50 |
| T1tttt | $m_{\tilde{g}} = 2000, m_{\tilde{\chi}_1^0} = 100$ | HH53, HH52, off-Z ML21, HL39, HH49 |
| T1tttt | $m_{\tilde{g}} = 1800, m_{\tilde{\chi}_1^0} = 100$ | HH53, off-Z ML21, HH52, HL39, HH51 |
| T1tttt | $m_{\tilde{g}} = 1800, m_{\tilde{\chi}_1^0} = 1000$ | off-Z ML21, HH53, HH52, HH51, HH50 |
| T1tttt | $m_{\tilde{g}} = 1800, m_{\tilde{\chi}_1^0} = 1550$ | HH53, HL39, off-Z ML21, HH49, HH52 |
| T6ttWW | $m_{\tilde{b}_1} = 1000, m_{\tilde{\chi}_1^\pm} = 600$ | off-Z ML21, HH53, HH51, HH50, HH52 |
| T6ttWW | $m_{\tilde{b}_1} = 900, m_{\tilde{\chi}_1^\pm} = 400$ | off-Z ML21, HH51, HH50, HH53, off-Z ML20 |
| T6ttWW | $m_{\tilde{b}_1} = 800, m_{\tilde{\chi}_1^\pm} = 400$ | off-Z ML21, HH51, HH50, HH34, off-Z ML20 |
| T5qqqqWZ | $m_{\tilde{g}} = 1400, m_{\tilde{\chi}_1^0} = 1$ | on-Z ML23, HH53, HH52, HH51, HH49 |
| T5qqqqWZ | $m_{\tilde{g}} = 900, m_{\tilde{\chi}_1^0} = 600$ | on-Z ML4, HH3, HH10, on-Z ML23, HH4 |
| T5qqqqWW | $m_{\tilde{g}} = 1400, m_{\tilde{\chi}_1^0} = 1$ | HH53, HH52, HH49, HH51, HH50 |
| T5qqqqWW | $m_{\tilde{g}} = 900, m_{\tilde{\chi}_1^0} = 600$ | HH3, HH10, HH4, HH7, HH50 |
| T5qqqqWZ ($m_{\tilde{\chi}_1^\pm} = m_{\tilde{\chi}_1^0} + 20 \text{ GeV}$) | $m_{\tilde{g}} = 1400, m_{\tilde{\chi}_1^0} = 1$ | HH59, HH53, HH52, HH62, HH51 |
| T5qqqqWZ ($m_{\tilde{\chi}_1^\pm} = m_{\tilde{\chi}_1^0} + 20 \text{ GeV}$) | $m_{\tilde{g}} = 900, m_{\tilde{\chi}_1^0} = 600$ | LL2, LL1, LL4, HL39, HL37 |
| T5qqqqWW ($m_{\tilde{\chi}_1^\pm} = m_{\tilde{\chi}_1^0} + 20 \text{ GeV}$) | $m_{\tilde{g}} = 1400, m_{\tilde{\chi}_1^0} = 1$ | HH59, HH53, HH52, HH51, HH62 |
| T5qqqqWW ($m_{\tilde{\chi}_1^\pm} = m_{\tilde{\chi}_1^0} + 20 \text{ GeV}$) | $m_{\tilde{g}} = 900, m_{\tilde{\chi}_1^0} = 600$ | LL2, LL4, HL39, LL1, HL37 |
| T6ttHZ ($\mathcal{B}(\tilde{t}_2 \rightarrow \tilde{t}_1 Z) = 1$) | $m_{\tilde{t}_2} = 850, m_{\tilde{t}_1} = 625$ | on-Z ML23, on-Z ML21, on-Z ML16, on-Z ML14, on-Z ML17 |
| T6ttHZ ($\mathcal{B}(\tilde{t}_2 \rightarrow \tilde{t}_1 Z) = 0.5$) | $m_{\tilde{t}_2} = 850, m_{\tilde{t}_1} = 625$ | on-Z ML17, on-Z ML23, on-Z ML21, on-Z ML14, on-Z ML16 |
| T6ttHZ ($\mathcal{B}(\tilde{t}_2 \rightarrow \tilde{t}_1 Z) = 0$) | $m_{\tilde{t}_2} = 850, m_{\tilde{t}_1} = 625$ | off-Z ML15, HH40, HH39, HH45, HH44 |
| T1qqqqL | $m_{\tilde{g}} = 1600$ | HH62, LM11, HH59, HH61, HH51 |
| T1qqqqL | $m_{\tilde{g}} = 2400$ | HH62, LM11, HH59, HH53, HH52 |
| T1tbs | $m_{\tilde{g}} = 1200$ | HH62, HH50, HH59, HH61, HH58 |
| T1tbs | $m_{\tilde{g}} = 1700$ | HH62, HH59, HH50, HH52, LM11 |

B Top five SRs for several representative models

Table 17 presents the top five SRs for several representative models, ranked based on the largest values of $N_{\text{sig.}} / \sqrt{N_{\text{bkg.}} + N_{\text{sig.}}}$, where $N_{\text{sig.}}$ and $N_{\text{bkg.}}$ are the signal and total background yields in each SR, respectively.

C The CMS Collaboration

Yerevan Physics Institute, Yerevan, Armenia

A.M. Sirunyan[†], A. Tumasyan

Institut für Hochenergiephysik, Wien, Austria

W. Adam, F. Ambrogi, T. Bergauer, M. Dragicevic, J. Erö, A. Escalante Del Valle, M. Flechl, R. Frühwirth¹, M. Jeitler¹, N. Krammer, I. Krätschmer, D. Liko, T. Madlener, I. Mikulec, N. Rad, J. Schieck¹, R. Schöfbeck, M. Spanring, W. Waltenberger, C.-E. Wulz¹, M. Zarucki

Institute for Nuclear Problems, Minsk, Belarus

V. Drugakov, V. Mossolov, J. Suarez Gonzalez

Universiteit Antwerpen, Antwerpen, Belgium

M.R. Darwish, E.A. De Wolf, D. Di Croce, X. Janssen, A. Lelek, M. Pieters, H. Rejeb Sfar, H. Van Haevermaet, P. Van Mechelen, S. Van Putte, N. Van Remortel

Vrije Universiteit Brussel, Brussel, Belgium

F. Blekman, E.S. Bols, S.S. Chhibra, J. D'Hondt, J. De Clercq, D. Lontkovskyi, S. Lowette, I. Marchesini, S. Moortgat, Q. Python, S. Tavernier, W. Van Doninck, P. Van Mulders

Université Libre de Bruxelles, Bruxelles, Belgium

D. Beghin, B. Bilin, B. Clerboux, G. De Lentdecker, H. Delannoy, B. Dorney, L. Favart, A. Grebenyuk, A.K. Kalsi, L. Moureaux, A. Popov, N. Postiau, E. Starling, L. Thomas, C. Vander Velde, P. Vanlaer, D. Vannerom

Ghent University, Ghent, Belgium

T. Cornelis, D. Dobur, I. Khvastunov², M. Niedziela, C. Roskas, K. Skovpen, M. Tytgat, W. Verbeke, B. Vermassen, M. Vit

Université Catholique de Louvain, Louvain-la-Neuve, Belgium

O. Bondu, G. Bruno, C. Caputo, P. David, C. Delaere, M. Delcourt, A. Giammanco, V. Lemaître, J. Prisciandaro, A. Saggio, M. Vidal Marono, P. Vischia, J. Zobec

Centro Brasileiro de Pesquisas Físicas, Rio de Janeiro, Brazil

G.A. Alves, G. Correia Silva, C. Hensel, A. Moraes

Universidade do Estado do Rio de Janeiro, Rio de Janeiro, Brazil

E. Belchior Batista Das Chagas, W. Carvalho, J. Chinellato³, E. Coelho, E.M. Da Costa, G.G. Da Silveira⁴, D. De Jesus Damiao, C. De Oliveira Martins, S. Fonseca De Souza, L.M. Huertas Guativa, H. Malbouisson, J. Martins⁵, D. Matos Figueiredo, M. Medina Jaime⁶, M. Melo De Almeida, C. Mora Herrera, L. Mundim, H. Nogima, W.L. Prado Da Silva, P. Rebello Teles, L.J. Sanchez Rosas, A. Santoro, A. Sznajder, M. Thiel, E.J. Tonelli Manganote³, F. Torres Da Silva De Araujo, A. Vilela Pereira

Universidade Estadual Paulista ^a, Universidade Federal do ABC ^b, São Paulo, Brazil

C.A. Bernardes^a, L. Calligaris^a, T.R. Fernandez Perez Tomei^a, E.M. Gregores^b, D.S. Lemos, P.G. Mercadante^b, S.F. Novaes^a, Sandra S. Padula^a

Institute for Nuclear Research and Nuclear Energy, Bulgarian Academy of Sciences, Sofia, Bulgaria

A. Aleksandrov, G. Antchev, R. Hadjiiska, P. Iaydjiev, M. Misheva, M. Rodozov, M. Shopova, G. Sultanov

University of Sofia, Sofia, Bulgaria

M. Bonchev, A. Dimitrov, T. Ivanov, L. Litov, B. Pavlov, P. Petkov, A. Petrov

Beihang University, Beijing, ChinaW. Fang⁷, X. Gao⁷, L. Yuan**Department of Physics, Tsinghua University, Beijing, China**

M. Ahmad, Z. Hu, Y. Wang

Institute of High Energy Physics, Beijing, ChinaG.M. Chen⁸, H.S. Chen⁸, M. Chen, C.H. Jiang, D. Leggat, H. Liao, Z. Liu, A. Spiezia, J. Tao, E. Yazgan, H. Zhang, S. Zhang⁸, J. Zhao**State Key Laboratory of Nuclear Physics and Technology, Peking University, Beijing, China**

A. Agapitos, Y. Ban, G. Chen, A. Levin, J. Li, L. Li, Q. Li, Y. Mao, S.J. Qian, D. Wang, Q. Wang

Zhejiang University, Hangzhou, China

M. Xiao

Universidad de Los Andes, Bogota, Colombia

C. Avila, A. Cabrera, C. Florez, C.F. González Hernández, M.A. Segura Delgado

Universidad de Antioquia, Medellin, Colombia

J. Mejia Guisao, J.D. Ruiz Alvarez, C.A. Salazar González, N. Vanegas Arbelaez

University of Split, Faculty of Electrical Engineering, Mechanical Engineering and Naval Architecture, Split, Croatia

D. Giljanović, N. Godinovic, D. Lelas, I. Puljak, T. Sculac

University of Split, Faculty of Science, Split, Croatia

Z. Antunovic, M. Kovac

Institute Rudjer Boskovic, Zagreb, CroatiaV. Brigljevic, D. Ferencek, K. Kadija, B. Mesic, M. Roguljic, A. Starodumov⁹, T. Susa**University of Cyprus, Nicosia, Cyprus**

M.W. Ather, A. Attikis, E. Erodotou, A. Ioannou, M. Kolosova, S. Konstantinou, G. Mavromanolakis, J. Mousa, C. Nicolaou, F. Ptochos, P.A. Razis, H. Rykaczewski, H. Saka, D. Tsiakkouri

Charles University, Prague, Czech RepublicM. Finger¹⁰, M. Finger Jr.¹⁰, A. Kveton, J. Tomsa**Escuela Politecnica Nacional, Quito, Ecuador**

E. Ayala

Universidad San Francisco de Quito, Quito, Ecuador

E. Carrera Jarrin

Academy of Scientific Research and Technology of the Arab Republic of Egypt, Egyptian Network of High Energy Physics, Cairo, EgyptH. Abdalla¹¹, S. Khalil¹²**National Institute of Chemical Physics and Biophysics, Tallinn, Estonia**

S. Bhowmik, A. Carvalho Antunes De Oliveira, R.K. Dewanjee, K. Ehataht, M. Kadastik, M. Raidal, C. Veelken

Department of Physics, University of Helsinki, Helsinki, Finland

P. Eerola, L. Forthomme, H. Kirschenmann, K. Osterberg, M. Voutilainen

Helsinki Institute of Physics, Helsinki, Finland

F. Garcia, J. Havukainen, J.K. Heikkilä, V. Karimäki, M.S. Kim, R. Kinnunen, T. Lampén, K. Lassila-Perini, S. Laurila, S. Lehti, T. Lindén, H. Siikonen, E. Tuominen, J. Tuominiemi

Lappeenranta University of Technology, Lappeenranta, Finland

P. Luukka, T. Tuuva

IRFU, CEA, Université Paris-Saclay, Gif-sur-Yvette, France

M. Besancon, F. Couderc, M. Dejardin, D. Denegri, B. Fabbro, J.L. Faure, F. Ferri, S. Ganjour, A. Givernaud, P. Gras, G. Hamel de Monchenault, P. Jarry, C. Leloup, B. Lenzi, E. Locci, J. Malcles, J. Rander, A. Rosowsky, M.Ö. Sahin, A. Savoy-Navarro¹³, M. Titov, G.B. Yu

Laboratoire Leprince-Ringuet, CNRS/IN2P3, Ecole Polytechnique, Institut Polytechnique de Paris

S. Ahuja, C. Amendola, F. Beaudette, P. Busson, C. Charlot, B. Diab, G. Falmagne, R. Granier de Cassagnac, I. Kucher, A. Lobanov, C. Martin Perez, M. Nguyen, C. Ochando, P. Paganini, J. Rembser, R. Salerno, J.B. Sauvan, Y. Sirois, A. Zabi, A. Zghiche

Université de Strasbourg, CNRS, IPHC UMR 7178, Strasbourg, France

J.-L. Agram¹⁴, J. Andrea, D. Bloch, G. Bourgatte, J.-M. Brom, E.C. Chabert, C. Collard, E. Conte¹⁴, J.-C. Fontaine¹⁴, D. Gelé, U. Goerlach, M. Jansová, A.-C. Le Bihan, N. Tonon, P. Van Hove

Centre de Calcul de l'Institut National de Physique Nucleaire et de Physique des Particules, CNRS/IN2P3, Villeurbanne, France

S. Gadrat

Université de Lyon, Université Claude Bernard Lyon 1, CNRS-IN2P3, Institut de Physique Nucléaire de Lyon, Villeurbanne, France

S. Beauceron, C. Bernet, G. Boudoul, C. Camen, A. Carle, N. Chanon, R. Chierici, D. Contardo, P. Depasse, H. El Mamouni, J. Fay, S. Gascon, M. Gouzevitch, B. Ille, Sa. Jain, I.B. Laktineh, H. Lattaud, A. Lesauvage, M. Lethuillier, L. Mirabito, S. Perries, V. Sordini, L. Torterotot, G. Touquet, M. Vander Donckt, S. Viret

Georgian Technical University, Tbilisi, Georgia

A. Khvedelidze¹⁰

Tbilisi State University, Tbilisi, Georgia

Z. Tsamalaidze¹⁰

RWTH Aachen University, I. Physikalisches Institut, Aachen, Germany

C. Autermann, L. Feld, K. Klein, M. Lipinski, D. Meuser, A. Pauls, M. Preuten, M.P. Rauch, J. Schulz, M. Teroerde

RWTH Aachen University, III. Physikalisches Institut A, Aachen, Germany

M. Erdmann, B. Fischer, S. Ghosh, T. Hebbeker, K. Hoepfner, H. Keller, L. Mastrolorenzo, M. Merschmeyer, A. Meyer, P. Millet, G. Mocellin, S. Mondal, S. Mukherjee, D. Noll, A. Novak, T. Pook, A. Pozdnyakov, T. Quast, M. Radziej, Y. Rath, H. Reithler, J. Roemer, A. Schmidt, S.C. Schuler, A. Sharma, S. Wiedenbeck, S. Zaleski

RWTH Aachen University, III. Physikalisches Institut B, Aachen, Germany

G. Flügge, W. Haj Ahmad¹⁵, O. Hlushchenko, T. Kress, T. Müller, A. Nowack, C. Pistone, O. Pooth, D. Roy, H. Sert, A. Stahl¹⁶

Deutsches Elektronen-Synchrotron, Hamburg, Germany

M. Aldaya Martin, P. Asmuss, I. Babounikau, H. Bakhshiansohi, K. Beernaert, O. Behnke, A. Bermúdez Martínez, A.A. Bin Anuar, K. Borrás¹⁷, V. Botta, A. Campbell, A. Cardini, P. Connor, S. Consuegra Rodríguez, C. Contreras-Campana, V. Danilov, A. De Wit, M.M. Defranchis, C. Diez Pardos, D. Domínguez Damiani, G. Eckerlin, D. Eckstein, T. Eichhorn, A. Elwood, E. Eren, E. Gallo¹⁸, A. Geiser, A. Grohsjean, M. Guthoff, M. Haranko, A. Harb, A. Jafari¹⁹, N.Z. Jomhari, H. Jung, A. Kasem¹⁷, M. Kasemann, H. Kaveh, J. Keaveney, C. Kleinwort, J. Knolle, D. Krücker, W. Lange, T. Lenz, J. Lidrych, K. Lipka, W. Lohmann²⁰, R. Mankel, I.-A. Melzer-Pellmann, A.B. Meyer, M. Meyer, M. Missiroli, J. Mnich, A. Mussgiller, V. Myronenko, D. Pérez Adán, S.K. Pflitsch, D. Pitzl, A. Raspereza, A. Saibel, M. Savitskyi, V. Scheurer, P. Schütze, C. Schwanenberger, R. Shevchenko, A. Singh, R.E. Sosa Ricardo, H. Tholen, O. Turkot, A. Vagnerini, M. Van De Klundert, R. Walsh, Y. Wen, K. Wichmann, C. Wissing, O. Zenaiev, R. Zlebcik

University of Hamburg, Hamburg, Germany

R. Aggleton, S. Bein, L. Benato, A. Benecke, T. Dreyer, A. Ebrahimi, F. Feindt, A. Fröhlich, C. Garbers, E. Garutti, D. Gonzalez, P. Gunnellini, J. Haller, A. Hinzmann, A. Karavdina, G. Kasieczka, R. Klanner, R. Kogler, N. Kovalchuk, S. Kurz, V. Kutzner, J. Lange, T. Lange, A. Malara, J. Multhaupt, C.E.N. Niemeyer, A. Reimers, O. Rieger, P. Schleper, S. Schumann, J. Schwandt, J. Sonneveld, H. Stadie, G. Steinbrück, B. Vormwald, I. Zoi

Karlsruher Institut fuer Technologie, Karlsruhe, Germany

M. Akbiyik, M. Baselga, S. Baur, T. Berger, E. Butz, R. Caspart, T. Chwalek, W. De Boer, A. Dierlamm, K. El Morabit, N. Faltermann, M. Giffels, A. Gottmann, M.A. Harrendorf, F. Hartmann¹⁶, C. Heidecker, U. Husemann, S. Kudella, S. Maier, S. Mitra, M.U. Mozer, D. Müller, Th. Müller, M. Musich, A. Nürnberg, G. Quast, K. Rabbertz, D. Schäfer, M. Schröder, I. Shvetsov, H.J. Simonis, R. Ulrich, M. Wassmer, M. Weber, C. Wöhrmann, R. Wolf, S. Wozniewski

Institute of Nuclear and Particle Physics (INPP), NCSR Demokritos, Aghia Paraskevi, Greece

G. Anagnostou, P. Asenov, G. Daskalakis, T. Geralis, A. Kyriakis, D. Loukas, G. Paspalaki

National and Kapodistrian University of Athens, Athens, Greece

M. Diamantopoulou, G. Karathanasis, P. Kontaxakis, A. Manousakis-katsikakis, A. Panagiotou, I. Papavergou, N. Saoulidou, A. Stakia, K. Theofilatos, K. Vellidis, E. Vourliotis

National Technical University of Athens, Athens, Greece

G. Bakas, K. Kousouris, I. Papakrivopoulos, G. Tsipolitis

University of Ioánnina, Ioánnina, Greece

I. Evangelou, C. Foudas, P. Giannelis, P. Katsoulis, P. Kokkas, S. Mallios, K. Manitará, N. Manthos, I. Papadopoulos, J. Strologas, F.A. Triantis, D. Tsitsionis

MTA-ELTE Lendület CMS Particle and Nuclear Physics Group, Eötvös Loránd University, Budapest, Hungary

M. Bartók²¹, R. Chudasama, M. Csanad, P. Major, K. Mandal, A. Mehta, G. Pasztor, O. Surányi, G.I. Veres

Wigner Research Centre for Physics, Budapest, Hungary

G. Bencze, C. Hajdu, D. Horvath²², F. Sikler, V. Veszpremi, G. Vesztergombi[†]

Institute of Nuclear Research ATOMKI, Debrecen, Hungary

N. Beni, S. Czellar, J. Karancsi²¹, J. Molnar, Z. Szillasi

Institute of Physics, University of Debrecen, Debrecen, Hungary

P. Raics, D. Teyssier, Z.L. Trocsanyi, B. Ujvari

Eszterhazy Karoly University, Karoly Robert Campus, Gyongyos, Hungary

T. Csorgo, W.J. Metzger, F. Nemes, T. Novak

Indian Institute of Science (IISc), Bangalore, India

S. Choudhury, J.R. Komaragiri, P.C. Tiwari

National Institute of Science Education and Research, HBNI, Bhubaneswar, IndiaS. Bahinipati²⁴, C. Kar, G. Kole, P. Mal, V.K. Muraleedharan Nair Bindhu, A. Nayak²⁵, D.K. Sahoo²⁴, S.K. Swain**Panjab University, Chandigarh, India**S. Bansal, S.B. Beri, V. Bhatnagar, S. Chauhan, N. Dhingra²⁶, R. Gupta, A. Kaur, M. Kaur, S. Kaur, P. Kumari, M. Lohan, M. Meena, K. Sandeep, S. Sharma, J.B. Singh, A.K. Viridi, G. Walia**University of Delhi, Delhi, India**

A. Bhardwaj, B.C. Choudhary, R.B. Garg, M. Gola, S. Keshri, Ashok Kumar, M. Naimuddin, P. Priyanka, K. Ranjan, Aashaq Shah, R. Sharma

Saha Institute of Nuclear Physics, HBNI, Kolkata, IndiaR. Bhardwaj²⁷, M. Bharti²⁷, R. Bhattacharya, S. Bhattacharya, U. Bhawandeep²⁷, D. Bhowmik, S. Dutta, S. Ghosh, B. Gomber²⁸, M. Maity²⁹, K. Mondal, S. Nandan, A. Purohit, P.K. Rout, G. Saha, S. Sarkar, T. Sarkar²⁹, M. Sharan, B. Singh²⁷, S. Thakur²⁷**Indian Institute of Technology Madras, Madras, India**

P.K. Behera, P. Kalbhor, A. Muhammad, P.R. Pujahari, A. Sharma, A.K. Sikdar

Bhabha Atomic Research Centre, Mumbai, India

D. Dutta, V. Jha, D.K. Mishra, P.K. Netrakanti, L.M. Pant, P. Shukla

Tata Institute of Fundamental Research-A, Mumbai, India

T. Aziz, M.A. Bhat, S. Dugad, G.B. Mohanty, N. Sur, RavindraKumar Verma

Tata Institute of Fundamental Research-B, Mumbai, India

S. Banerjee, S. Bhattacharya, S. Chatterjee, P. Das, M. Guchait, S. Karmakar, S. Kumar, G. Majumder, K. Mazumdar, N. Sahoo, S. Sawant

Indian Institute of Science Education and Research (IISER), Pune, India

S. Dube, B. Kansal, A. Kapoor, K. Kothekar, S. Pandey, A. Rane, A. Rastogi, S. Sharma

Institute for Research in Fundamental Sciences (IPM), Tehran, Iran

S. Chenarani, S.M. Etesami, M. Khakzad, M. Mohammadi Najafabadi, M. Naseri, F. Rezaei Hosseinabadi

University College Dublin, Dublin, Ireland

M. Felcini, M. Grunewald

INFN Sezione di Bari ^a, Università di Bari ^b, Politecnico di Bari ^c, Bari, ItalyM. Abbrescia^{a,b}, R. Aly^{a,b,30}, C. Calabria^{a,b}, A. Colaleo^a, D. Creanza^{a,c}, L. Cristella^{a,b}, N. De Filippis^{a,c}, M. De Palma^{a,b}, A. Di Florio^{a,b}, W. Elmetenawee^{a,b}, L. Fiore^a, A. Gelmi^{a,b}, G. Iaselli^{a,c}, M. Ince^{a,b}, S. Lezki^{a,b}, G. Maggi^{a,c}, M. Maggi^a, J.A. Merlin^a, G. Miniello^{a,b}, S. My^{a,b}, S. Nuzzo^{a,b}, A. Pompili^{a,b}, G. Pugliese^{a,c}, R. Radogna^a, A. Ranieri^a, G. Selvaggi^{a,b}, L. Silvestris^a, F.M. Simone^{a,b}, R. Venditti^a, P. Verwilligen^a

INFN Sezione di Bologna ^a, Università di Bologna ^b, Bologna, Italy

G. Abbiendi^a, C. Battilana^{a,b}, D. Bonacorsi^{a,b}, L. Borgonovi^{a,b}, S. Braibant-Giacomelli^{a,b}, R. Campanini^{a,b}, P. Capiluppi^{a,b}, A. Castro^{a,b}, F.R. Cavallo^a, C. Ciocca^a, G. Codispoti^{a,b}, M. Cuffiani^{a,b}, G.M. Dallavalle^a, F. Fabbri^a, A. Fanfani^{a,b}, E. Fontanesi^{a,b}, P. Giacomelli^a, C. Grandi^a, L. Guiducci^{a,b}, F. Iemmi^{a,b}, S. Lo Meo^{a,31}, S. Marcellini^a, G. Masetti^a, F.L. Navarria^{a,b}, A. Perrotta^a, F. Primavera^{a,b}, A.M. Rossi^{a,b}, T. Rovelli^{a,b}, G.P. Siroli^{a,b}, N. Tosi^a

INFN Sezione di Catania ^a, Università di Catania ^b, Catania, Italy

S. Albergo^{a,b,32}, S. Costa^{a,b}, A. Di Mattia^a, R. Potenza^{a,b}, A. Tricomi^{a,b,32}, C. Tuve^{a,b}

INFN Sezione di Firenze ^a, Università di Firenze ^b, Firenze, Italy

G. Barbagli^a, A. Cassese, R. Ceccarelli, V. Ciulli^{a,b}, C. Civinini^a, R. D'Alessandro^{a,b}, F. Fiori^{a,c}, E. Focardi^{a,b}, G. Latino^{a,b}, P. Lenzi^{a,b}, M. Meschini^a, S. Paoletti^a, G. Sguazzoni^a, L. Viliani^a

INFN Laboratori Nazionali di Frascati, Frascati, Italy

L. Benussi, S. Bianco, D. Piccolo

INFN Sezione di Genova ^a, Università di Genova ^b, Genova, Italy

M. Bozzo^{a,b}, F. Ferro^a, R. Mulargia^{a,b}, E. Robutti^a, S. Tosi^{a,b}

INFN Sezione di Milano-Bicocca ^a, Università di Milano-Bicocca ^b, Milano, Italy

A. Benaglia^a, A. Beschi^{a,b}, F. Brivio^{a,b}, V. Ciriolo^{a,b,16}, M.E. Dinardo^{a,b}, P. Dini^a, S. Gennai^a, A. Ghezzi^{a,b}, P. Govoni^{a,b}, L. Guzzi^{a,b}, M. Malberti^a, S. Malvezzi^a, D. Menasce^a, F. Monti^{a,b}, L. Moroni^a, M. Paganoni^{a,b}, D. Pedrini^a, S. Ragazzi^{a,b}, T. Tabarelli de Fatis^{a,b}, D. Valsecchi^{a,b}, D. Zuolo^{a,b}

INFN Sezione di Napoli ^a, Università di Napoli 'Federico II' ^b, Napoli, Italy, Università della Basilicata ^c, Potenza, Italy, Università G. Marconi ^d, Roma, Italy

S. Buontempo^a, N. Cavallo^{a,c}, A. De Iorio^{a,b}, A. Di Crescenzo^{a,b}, F. Fabozzi^{a,c}, F. Fienga^a, G. Galati^a, A.O.M. Iorio^{a,b}, L. Layer^{a,b}, L. Lista^{a,b}, S. Meola^{a,d,16}, P. Paolucci^{a,16}, B. Rossi^a, C. Sciacca^{a,b}, E. Voevodina^{a,b}

INFN Sezione di Padova ^a, Università di Padova ^b, Padova, Italy, Università di Trento ^c, Trento, Italy

P. Azzi^a, N. Bacchetta^a, D. Bisello^{a,b}, A. Boletti^{a,b}, A. Bragagnolo^{a,b}, R. Carlin^{a,b}, P. Checchia^a, P. De Castro Manzano^a, T. Dorigo^a, U. Dosselli^a, F. Gasparini^{a,b}, U. Gasparini^{a,b}, A. Gozzelino^a, S.Y. Hoh^{a,b}, M. Margoni^{a,b}, A.T. Meneguzzo^{a,b}, J. Pazzini^{a,b}, M. Presilla^b, P. Ronchese^{a,b}, R. Rossin^{a,b}, F. Simonetto^{a,b}, A. Tiko^a, M. Tosi^{a,b}, M. Zanetti^{a,b}, P. Zotto^{a,b}, G. Zumerle^{a,b}

INFN Sezione di Pavia ^a, Università di Pavia ^b, Pavia, Italy

A. Braghieri^a, D. Fiorina^{a,b}, P. Montagna^{a,b}, S.P. Ratti^{a,b}, V. Re^a, M. Ressegotti^{a,b}, C. Riccardi^{a,b}, P. Salvini^a, I. Vai^a, P. Vitulo^{a,b}

INFN Sezione di Perugia ^a, Università di Perugia ^b, Perugia, Italy

M. Biasini^{a,b}, G.M. Bilei^a, D. Ciangottini^{a,b}, L. Fanò^{a,b}, P. Lariccia^{a,b}, R. Leonardi^{a,b}, E. Manoni^a, G. Mantovani^{a,b}, V. Mariani^{a,b}, M. Menichelli^a, A. Rossi^{a,b}, A. Santocchia^{a,b}, D. Spiga^a

INFN Sezione di Pisa ^a, Università di Pisa ^b, Scuola Normale Superiore di Pisa ^c, Pisa, Italy

K. Androsov^a, P. Azzurri^a, G. Bagliesi^a, V. Bertacchi^{a,c}, L. Bianchini^a, T. Boccali^a, R. Castaldi^a, M.A. Ciocci^{a,b}, R. Dell'Orso^a, S. Donato^a, L. Giannini^{a,c}, A. Giassi^a, M.T. Grippo^a, F. Ligabue^{a,c}, E. Manca^{a,c}, G. Mandorli^{a,c}, A. Messineo^{a,b}, F. Palla^a, A. Rizzi^{a,b}, G. Rolandi³³, S. Roy Chowdhury, A. Scribano^a, P. Spagnolo^a, R. Tenchini^a, G. Tonelli^{a,b}, N. Turini, A. Venturi^a, P.G. Verdini^a

INFN Sezione di Roma ^a, Sapienza Università di Roma ^b, Rome, Italy

F. Cavallari^a, M. Cipriani^{a,b}, D. Del Re^{a,b}, E. Di Marco^a, M. Diemoz^a, E. Longo^{a,b}, P. Meridiani^a, G. Organtini^{a,b}, F. Pandolfi^a, R. Paramatti^{a,b}, C. Quaranta^{a,b}, S. Rahatlou^{a,b}, C. Rovelli^a, F. Santanastasio^{a,b}, L. Soffi^{a,b}

INFN Sezione di Torino ^a, Università di Torino ^b, Torino, Italy, Università del Piemonte Orientale ^c, Novara, Italy

N. Amapane^{a,b}, R. Arcidiacono^{a,c}, S. Argiro^{a,b}, M. Arneodo^{a,c}, N. Bartosik^a, R. Bellan^{a,b}, A. Bellora, C. Biino^a, A. Cappati^{a,b}, N. Cartiglia^a, S. Cometti^a, M. Costa^{a,b}, R. Covarelli^{a,b}, N. Demaria^a, B. Kiani^{a,b}, F. Legger, C. Mariotti^a, S. Maselli^a, E. Migliore^{a,b}, V. Monaco^{a,b}, E. Monteil^{a,b}, M. Monteno^a, M.M. Obertino^{a,b}, G. Ortona^{a,b}, L. Pacher^{a,b}, N. Pastrone^a, M. Pelliccioni^a, G.L. Pinna Angioni^{a,b}, A. Romero^{a,b}, M. Ruspa^{a,c}, R. Salvatico^{a,b}, V. Sola^a, A. Solano^{a,b}, D. Soldi^{a,b}, A. Staiano^a, D. Trocino^{a,b}

INFN Sezione di Trieste ^a, Università di Trieste ^b, Trieste, Italy

S. Belforte^a, V. Candelise^{a,b}, M. Casarsa^a, F. Cossutti^a, A. Da Rold^{a,b}, G. Della Ricca^{a,b}, F. Vazzoler^{a,b}, A. Zanetti^a

Kyungpook National University, Daegu, Korea

B. Kim, D.H. Kim, G.N. Kim, J. Lee, S.W. Lee, C.S. Moon, Y.D. Oh, S.I. Pak, S. Sekmen, D.C. Son, Y.C. Yang

Chonnam National University, Institute for Universe and Elementary Particles, Kwangju, Korea

H. Kim, D.H. Moon, G. Oh

Hanyang University, Seoul, Korea

B. Francois, T.J. Kim, J. Park

Korea University, Seoul, Korea

S. Cho, S. Choi, Y. Go, S. Ha, B. Hong, K. Lee, K.S. Lee, J. Lim, J. Park, S.K. Park, Y. Roh, J. Yoo

Kyung Hee University, Department of Physics

J. Goh

Sejong University, Seoul, Korea

H.S. Kim

Seoul National University, Seoul, Korea

J. Almond, J.H. Bhyun, J. Choi, S. Jeon, J. Kim, J.S. Kim, H. Lee, K. Lee, S. Lee, K. Nam, M. Oh, S.B. Oh, B.C. Radburn-Smith, U.K. Yang, H.D. Yoo, I. Yoon

University of Seoul, Seoul, Korea

D. Jeon, J.H. Kim, J.S.H. Lee, I.C. Park, I.J. Watson

Sungkyunkwan University, Suwon, Korea

Y. Choi, C. Hwang, Y. Jeong, J. Lee, Y. Lee, I. Yu

Riga Technical University, Riga, Latvia

V. Veckalns³⁴

Vilnius University, Vilnius, Lithuania

V. Dudenas, A. Juodagalvis, A. Rinkevicius, G. Tamulaitis, J. Vaitkus

National Centre for Particle Physics, Universiti Malaya, Kuala Lumpur, Malaysia

Z.A. Ibrahim, F. Mohamad Idris³⁵, W.A.T. Wan Abdullah, M.N. Yusli, Z. Zolkapli

Universidad de Sonora (UNISON), Hermosillo, Mexico

J.F. Benitez, A. Castaneda Hernandez, J.A. Murillo Quijada, L. Valencia Palomo

Centro de Investigacion y de Estudios Avanzados del IPN, Mexico City, Mexico

H. Castilla-Valdez, E. De La Cruz-Burelo, I. Heredia-De La Cruz³⁶, R. Lopez-Fernandez, A. Sanchez-Hernandez

Universidad Iberoamericana, Mexico City, Mexico

S. Carrillo Moreno, C. Oropeza Barrera, M. Ramirez-Garcia, F. Vazquez Valencia

Benemerita Universidad Autonoma de Puebla, Puebla, Mexico

J. Eysermans, I. Pedraza, H.A. Salazar Ibarguen, C. Uribe Estrada

Universidad Autónoma de San Luis Potosí, San Luis Potosí, Mexico

A. Morelos Pineda

University of Montenegro, Podgorica, Montenegro

J. Mijuskovic², N. Raicevic

University of Auckland, Auckland, New Zealand

D. Krofcheck

University of Canterbury, Christchurch, New Zealand

S. Bheesette, P.H. Butler, P. Lujan

National Centre for Physics, Quaid-I-Azam University, Islamabad, Pakistan

A. Ahmad, M. Ahmad, M.I.M. Awan, Q. Hassan, H.R. Hoorani, W.A. Khan, M.A. Shah, M. Shoaib, M. Waqas

AGH University of Science and Technology Faculty of Computer Science, Electronics and Telecommunications, Krakow, Poland

V. Avati, L. Grzanka, M. Malawski

National Centre for Nuclear Research, Swierk, Poland

H. Bialkowska, M. Bluj, B. Boimska, M. Górski, M. Kazana, M. Szeleper, P. Zalewski

Institute of Experimental Physics, Faculty of Physics, University of Warsaw, Warsaw, Poland

K. Bunkowski, A. Byszuk³⁷, K. Doroba, A. Kalinowski, M. Konecki, J. Krolikowski, M. Olszewski, M. Walczak

Laboratório de Instrumentação e Física Experimental de Partículas, Lisboa, Portugal

M. Araujo, P. Bargassa, D. Bastos, A. Di Francesco, P. Faccioli, B. Galinhas, M. Gallinaro, J. Hollar, N. Leonardo, T. Niknejad, J. Seixas, K. Shchelina, G. Strong, O. Toldaiev, J. Varela

Joint Institute for Nuclear Research, Dubna, Russia

S. Afanasiev, P. Bunin, M. Gavrilenko, I. Golutvin, I. Gorbunov, A. Kamenev, V. Karjavine, A. Lanev, A. Malakhov, V. Matveev^{38,39}, P. Moisenz, V. Palichik, V. Perelygin, M. Savina, S. Shmatov, S. Shulha, N. Skatchkov, V. Smirnov, N. Voytishin, A. Zarubin

Petersburg Nuclear Physics Institute, Gatchina (St. Petersburg), Russia

L. Chtchipounov, V. Golovtcov, Y. Ivanov, V. Kim⁴⁰, E. Kuznetsova⁴¹, P. Levchenko, V. Murzin, V. Oreshkin, I. Smirnov, D. Sosnov, V. Sulimov, L. Uvarov, A. Vorobyev

Institute for Nuclear Research, Moscow, Russia

Yu. Andreev, A. Dermenev, S. Gninenko, N. Golubev, A. Karneyeu, M. Kirsanov, N. Krasnikov, A. Pashenkov, D. Tlisov, A. Toropin

Institute for Theoretical and Experimental Physics named by A.I. Alikhanov of NRC 'Kurchatov Institute', Moscow, Russia

V. Epshteyn, V. Gavrilov, N. Lychkovskaya, A. Nikitenko⁴², V. Popov, I. Pozdnyakov, G. Safronov, A. Spiridonov, A. Stepenov, M. Toms, E. Vlasov, A. Zhokin

Moscow Institute of Physics and Technology, Moscow, Russia

T. Aushev

National Research Nuclear University 'Moscow Engineering Physics Institute' (MEPhI), Moscow, Russia

R. Chistov⁴³, M. Danilov⁴³, P. Parygin, S. Polikarpov⁴³, E. Tarkovskii

P.N. Lebedev Physical Institute, Moscow, Russia

V. Andreev, M. Azarkin, I. Dremin, M. Kirakosyan, A. Terkulov

Skobeltsyn Institute of Nuclear Physics, Lomonosov Moscow State University, Moscow, Russia

A. Belyaev, E. Boos, M. Dubinin⁴⁴, L. Dudko, A. Ershov, A. Gribushin, V. Klyukhin, O. Kodolova, I. Lokhtin, S. Obraztsov, S. Petrushanko, V. Savrin, A. Snigirev

Novosibirsk State University (NSU), Novosibirsk, Russia

A. Barnyakov⁴⁵, V. Blinov⁴⁵, T. Dimova⁴⁵, L. Kardapoltsev⁴⁵, Y. Skovpen⁴⁵

Institute for High Energy Physics of National Research Centre 'Kurchatov Institute', Protvino, Russia

I. Azhgirey, I. Bayshev, S. Bitioukov, V. Kachanov, D. Konstantinov, P. Mandrik, V. Petrov, R. Ryutin, S. Slabospitskii, A. Sobol, S. Troshin, N. Tyurin, A. Uzunian, A. Volkov

National Research Tomsk Polytechnic University, Tomsk, Russia

A. Babaev, A. Iuzhakov, V. Okhotnikov

Tomsk State University, Tomsk, Russia

V. Borchsh, V. Ivanchenko, E. Tcherniaev

University of Belgrade: Faculty of Physics and VINCA Institute of Nuclear Sciences

P. Adzic⁴⁶, P. Cirkovic, M. Dordevic, P. Milenovic, J. Milosevic, M. Stojanovic

Centro de Investigaciones Energéticas Medioambientales y Tecnológicas (CIEMAT), Madrid, Spain

M. Aguilar-Benitez, J. Alcaraz Maestre, A. Álvarez Fernández, I. Bachiller, M. Barrio Luna, Cristina F. Bedoya, J.A. Brochero Cifuentes, C.A. Carrillo Montoya, M. Cepeda, M. Cerrada, N. Colino, B. De La Cruz, A. Delgado Peris, J.P. Fernández Ramos, J. Flix, M.C. Fouz, O. Gonzalez Lopez, S. Goy Lopez, J.M. Hernandez, M.I. Josa, D. Moran, Á. Navarro Tobar, A. Pérez-Calero Yzquierdo, J. Puerta Pelayo, I. Redondo, L. Romero, S. Sánchez Navas, M.S. Soares, A. Triossi, C. Willmott

Universidad Autónoma de Madrid, Madrid, Spain

C. Albajar, J.F. de Trocóniz, R. Reyes-Almanza

Universidad de Oviedo, Instituto Universitario de Ciencias y Tecnologías Espaciales de Asturias (ICTEA), Oviedo, Spain

B. Alvarez Gonzalez, J. Cuevas, C. Erice, J. Fernandez Menendez, S. Folgueras, I. Gonzalez Caballero, J.R. González Fernández, E. Palencia Cortezon, V. Rodríguez Bouza, S. Sanchez Cruz

Instituto de Física de Cantabria (IFCA), CSIC-Universidad de Cantabria, Santander, Spain

I.J. Cabrillo, A. Calderon, B. Chazin Quero, J. Duarte Campderros, M. Fernandez,

P.J. Fernández Manteca, A. García Alonso, G. Gomez, C. Martinez Rivero, P. Martinez Ruiz del Arbol, F. Matorras, J. Piedra Gomez, C. Prieels, T. Rodrigo, A. Ruiz-Jimeno, L. Russo⁴⁷, L. Scodellaro, I. Vila, J.M. Vizan Garcia

University of Colombo, Colombo, Sri Lanka

D.U.J. Sonnadara

University of Ruhuna, Department of Physics, Matara, Sri Lanka

W.G.D. Dharmaratna, N. Wickramage

CERN, European Organization for Nuclear Research, Geneva, Switzerland

D. Abbaneo, B. Akgun, E. Auffray, G. Auzinger, J. Baechler, P. Baillon, A.H. Ball, D. Barney, J. Bendavid, M. Bianco, A. Bocci, P. Bortignon, E. Bossini, E. Brondolin, T. Camporesi, A. Caratelli, G. Cerminara, E. Chapon, G. Cucciati, D. d'Enterria, A. Dabrowski, N. Daci, V. Daponte, A. David, O. Davignon, A. De Roeck, M. Deile, R. Di Maria, M. Dobson, M. Dünser, N. Dupont, A. Elliott-Peisert, N. Emriskova, F. Fallavollita⁴⁸, D. Fasanella, S. Fiorendi, G. Franzoni, J. Fulcher, W. Funk, S. Giani, D. Gigi, K. Gill, F. Glege, L. Gouskos, M. Gruchala, M. Guilbaud, D. Gulhan, J. Hegeman, C. Heidegger, Y. Iiyama, V. Innocente, T. James, P. Janot, O. Karacheban²⁰, J. Kaspar, J. Kieseler, M. Krammer¹, N. Kratochwil, C. Lange, P. Lecoq, C. Lourenço, L. Malgeri, M. Mannelli, A. Massironi, F. Meijers, S. Mersi, E. Meschi, F. Moortgat, M. Mulders, J. Ngadiuba, J. Niedziela, S. Nourbakhsh, S. Orfanelli, L. Orsini, F. Pantaleo¹⁶, L. Pape, E. Perez, M. Peruzzi, A. Petrilli, G. Petrucciani, A. Pfeiffer, M. Pierini, F.M. Pitters, D. Rabady, A. Racz, M. Rieger, M. Rovere, H. Sakulin, J. Salfeld-Nebgen, S. Scarfi, C. Schäfer, C. Schwick, M. Selvaggi, A. Sharma, P. Silva, W. Snoeys, P. Sphicas⁴⁹, J. Steggemann, S. Summers, V.R. Tavolaro, D. Treille, A. Tsirou, G.P. Van Onsem, A. Vartak, M. Verzetti, W.D. Zeuner

Paul Scherrer Institut, Villigen, Switzerland

L. Caminada⁵⁰, K. Deiters, W. Erdmann, R. Horisberger, Q. Ingram, H.C. Kaestli, D. Kotlinski, U. Langenegger, T. Rohe

ETH Zurich - Institute for Particle Physics and Astrophysics (IPA), Zurich, Switzerland

M. Backhaus, P. Berger, N. Chernyavskaya, G. Dissertori, M. Dittmar, M. Donegà, C. Dorfer, T.A. Gómez Espinosa, C. Grab, D. Hits, W. Luster, R.A. Manzoni, M.T. Meinhard, F. Micheli, P. Musella, F. Nessi-Tedaldi, F. Pauss, G. Perrin, L. Perrozzi, S. Pigazzini, M.G. Ratti, M. Reichmann, C. Reissel, T. Reitenspiess, B. Ristic, D. Ruini, D.A. Sanz Becerra, M. Schönenberger, L. Shchutska, M.L. Vesterbacka Olsson, R. Wallny, D.H. Zhu

Universität Zürich, Zurich, Switzerland

T.K. Aarrestad, C. Amsler⁵¹, C. Botta, D. Brzhechko, M.F. Canelli, A. De Cosa, R. Del Burgo, B. Kilminster, S. Leontsinis, V.M. Mikuni, I. Neutelings, G. Rauco, P. Robmann, K. Schweiger, C. Seitz, Y. Takahashi, S. Wertz, A. Zucchetta

National Central University, Chung-Li, Taiwan

C.M. Kuo, W. Lin, A. Roy, S.S. Yu

National Taiwan University (NTU), Taipei, Taiwan

P. Chang, Y. Chao, K.F. Chen, P.H. Chen, W.-S. Hou, Y.y. Li, R.-S. Lu, E. Paganis, A. Psallidas, A. Steen

Chulalongkorn University, Faculty of Science, Department of Physics, Bangkok, Thailand

B. Asavapibhop, C. Asawatangtrakuldee, N. Srimanobhas, N. Suwonjandee

Çukurova University, Physics Department, Science and Art Faculty, Adana, Turkey

A. Bat, F. Boran, A. Celik⁵², S. Damarseckin⁵³, Z.S. Demiroglu, F. Dolek, C. Dozen⁵⁴, I. Dumanoglu, G. Gokbulut, EmineGurpinar Guler⁵⁵, Y. Guler, I. Hos⁵⁶, C. Isik, E.E. Kangal⁵⁷, O. Kara, A. Kayis Topaksu, U. Kiminsu, G. Onengut, K. Ozdemir⁵⁸, S. Ozturk⁵⁹, A.E. Simsek, U.G. Tok, S. Turkcapar, I.S. Zorbakir, C. Zorbilmez

Middle East Technical University, Physics Department, Ankara, Turkey

B. Isildak⁶⁰, G. Karapinar⁶¹, M. Yalvac

Bogazici University, Istanbul, Turkey

I.O. Atakisi, E. Gülmez, M. Kaya⁶², O. Kaya⁶³, Ö. Özçelik, S. Tekten, E.A. Yetkin⁶⁴

Istanbul Technical University, Istanbul, Turkey

A. Cakir, K. Cankocak⁶⁵, Y. Komurcu, S. Sen⁶⁶

Istanbul University, Istanbul, Turkey

S. Cerci⁶⁷, B. Kaynak, S. Ozkorucuklu, D. Sunar Cerci⁶⁷

Institute for Scintillation Materials of National Academy of Science of Ukraine, Kharkov, Ukraine

B. Grynyov

National Scientific Center, Kharkov Institute of Physics and Technology, Kharkov, Ukraine

L. Levchuk

University of Bristol, Bristol, United Kingdom

E. Bhal, S. Bologna, J.J. Brooke, D. Burns⁶⁸, E. Clement, D. Cussans, H. Flacher, J. Goldstein, G.P. Heath, H.F. Heath, L. Kreczko, B. Krikler, S. Paramesvaran, T. Sakuma, S. Seif El Nasr-Storey, V.J. Smith, J. Taylor, A. Titterton

Rutherford Appleton Laboratory, Didcot, United Kingdom

K.W. Bell, A. Belyaev⁶⁹, C. Brew, R.M. Brown, D.J.A. Cockerill, J.A. Coughlan, K. Harder, S. Harper, J. Linacre, K. Manolopoulos, D.M. Newbold, E. Olaiya, D. Petyt, T. Reis, T. Schuh, C.H. Shepherd-Themistocleous, A. Thea, I.R. Tomalin, T. Williams

Imperial College, London, United Kingdom

R. Bainbridge, P. Bloch, J. Borg, S. Breeze, O. Buchmuller, A. Bundock, GurpreetSingh CHAHAL⁷⁰, D. Colling, P. Dauncey, G. Davies, M. Della Negra, P. Everaerts, G. Hall, G. Iles, M. Komm, L. Lyons, A.-M. Magnan, S. Malik, A. Martelli, V. Milosevic, A. Morton, J. Nash⁷¹, V. Palladino, M. Pesaresi, D.M. Raymond, A. Richards, A. Rose, E. Scott, C. Seez, A. Shtipliyski, M. Stoye, T. Strebler, A. Tapper, K. Uchida, T. Virdee¹⁶, N. Wardle, D. Winterbottom, A.G. Zecchinelli, S.C. Zenz

Brunel University, Uxbridge, United Kingdom

J.E. Cole, P.R. Hobson, A. Khan, P. Kyberd, C.K. Mackay, I.D. Reid, L. Teodorescu, S. Zahid

Baylor University, Waco, USA

A. Brinkerhoff, K. Call, B. Caraway, J. Dittmann, K. Hatakeyama, C. Madrid, B. McMaster, N. Pastika, C. Smith

Catholic University of America, Washington, DC, USA

R. Bartek, A. Dominguez, R. Uniyal, A.M. Vargas Hernandez

The University of Alabama, Tuscaloosa, USA

A. Buccilli, S.I. Cooper, S.V. Gleyzer, C. Henderson, P. Rumerio, C. West

Boston University, Boston, USA

A. Albert, D. Arcaro, Z. Demiragli, D. Gastler, C. Richardson, J. Rohlf, D. Sperka, D. Spitzbart, I. Suarez, L. Sulak, D. Zou

Brown University, Providence, USA

G. Benelli, B. Burkle, X. Coubez¹⁷, D. Cutts, Y.t. Duh, M. Hadley, U. Heintz, J.M. Hogan⁷², K.H.M. Kwok, E. Laird, G. Landsberg, K.T. Lau, J. Lee, M. Narain, S. Sagir⁷³, R. Syarif, E. Usai, W.Y. Wong, D. Yu, W. Zhang

University of California, Davis, Davis, USA

R. Band, C. Brainerd, R. Breedon, M. Calderon De La Barca Sanchez, M. Chertok, J. Conway, R. Conway, P.T. Cox, R. Erbacher, C. Flores, G. Funk, F. Jensen, W. Ko[†], O. Kukral, R. Lander, M. Mulhearn, D. Pellett, J. Pilot, M. Shi, D. Taylor, K. Tos, M. Tripathi, Z. Wang, F. Zhang

University of California, Los Angeles, USA

M. Bachtis, C. Bravo, R. Cousins, A. Dasgupta, A. Florent, J. Hauser, M. Ignatenko, N. Mccoll, W.A. Nash, S. Regnard, D. Saltzberg, C. Schnaible, B. Stone, V. Valuev

University of California, Riverside, Riverside, USA

K. Burt, Y. Chen, R. Clare, J.W. Gary, S.M.A. Ghiasi Shirazi, G. Hanson, G. Karapostoli, O.R. Long, M. Olmedo Negrete, M.I. Paneva, W. Si, L. Wang, S. Wimpenny, B.R. Yates, Y. Zhang

University of California, San Diego, La Jolla, USA

J.G. Branson, P. Chang, S. Cittolin, S. Cooperstein, N. Deelen, M. Derdzinski, J. Duarte, R. Gerosa, D. Gilbert, B. Hashemi, D. Klein, V. Krutelyov, J. Letts, M. Masciovecchio, S. May, S. Padhi, M. Pieri, V. Sharma, M. Tadel, F. Würthwein, A. Yagil, G. Zevi Della Porta

University of California, Santa Barbara - Department of Physics, Santa Barbara, USA

N. Amin, R. Bhandari, C. Campagnari, M. Citron, V. Dutta, M. Franco Sevilla, J. Incandela, J. Ling, B. Marsh, H. Mei, A. Ovcharova, H. Qu, J. Richman, U. Sarica, D. Stuart, S. Wang

California Institute of Technology, Pasadena, USA

D. Anderson, A. Bornheim, O. Cerri, I. Dutta, J.M. Lawhorn, N. Lu, J. Mao, H.B. Newman, T.Q. Nguyen, J. Pata, M. Spiropulu, J.R. Vlimant, S. Xie, Z. Zhang, R.Y. Zhu

Carnegie Mellon University, Pittsburgh, USA

M.B. Andrews, T. Ferguson, T. Mudholkar, M. Paulini, M. Sun, I. Vorobiev, M. Weinberg

University of Colorado Boulder, Boulder, USA

J.P. Cumalat, W.T. Ford, E. MacDonald, T. Mulholland, R. Patel, A. Perloff, K. Stenson, K.A. Ulmer, S.R. Wagner

Cornell University, Ithaca, USA

J. Alexander, Y. Cheng, J. Chu, A. Datta, A. Frankenthal, K. Mcdermott, J.R. Patterson, D. Quach, A. Ryd, S.M. Tan, Z. Tao, J. Thom, P. Wittich, M. Zientek

Fermi National Accelerator Laboratory, Batavia, USA

S. Abdullin, M. Albrow, M. Alyari, G. Apollinari, A. Apresyan, A. Apyan, S. Banerjee, L.A.T. Bauerdick, A. Beretvas, D. Berry, J. Berryhill, P.C. Bhat, K. Burkett, J.N. Butler, A. Canepa, G.B. Cerati, H.W.K. Cheung, F. Chlebana, M. Cremonesi, V.D. Elvira, J. Freeman, Z. Gecse, E. Gottschalk, L. Gray, D. Green, S. Grünendahl, O. Gutsche, J. Hanlon, R.M. Harris, S. Hasegawa, R. Heller, J. Hirschauer, B. Jayatilaka, S. Jindariani, M. Johnson, U. Joshi, T. Klijnsma, B. Klima, M.J. Kortelainen, B. Kreis, S. Lammel, J. Lewis, D. Lincoln, R. Lipton, M. Liu, T. Liu, J. Lykken, K. Maeshima, J.M. Marraffino, D. Mason, P. McBride, P. Merkel, S. Mrenna, S. Nahn, V. O'Dell, V. Papadimitriou, K. Pedro, C. Pena, F. Ravera,

A. Reinsvold Hall, L. Ristori, B. Schneider, E. Sexton-Kennedy, N. Smith, A. Soha, W.J. Spalding, L. Spiegel, S. Stoynev, J. Strait, L. Taylor, S. Tkaczyk, N.V. Tran, L. Uplegger, E.W. Vaandering, C. Vernieri, R. Vidal, M. Wang, H.A. Weber, A. Woodard

University of Florida, Gainesville, USA

D. Acosta, P. Avery, D. Bourilkov, L. Cadamuro, V. Cherepanov, F. Errico, R.D. Field, D. Guerrero, B.M. Joshi, M. Kim, J. Konigsberg, A. Korytov, K.H. Lo, K. Matchev, N. Menendez, G. Mitselmakher, D. Rosenzweig, K. Shi, J. Wang, S. Wang, X. Zuo

Florida International University, Miami, USA

Y.R. Joshi

Florida State University, Tallahassee, USA

T. Adams, A. Askew, S. Hagopian, V. Hagopian, K.F. Johnson, R. Khurana, T. Kolberg, G. Martinez, T. Perry, H. Prosper, C. Schiber, R. Yohay, J. Zhang

Florida Institute of Technology, Melbourne, USA

M.M. Baarmand, M. Hohlmann, D. Noonan, M. Rahmani, M. Saunders, F. Yumiceva

University of Illinois at Chicago (UIC), Chicago, USA

M.R. Adams, L. Apanasevich, R.R. Betts, R. Cavanaugh, X. Chen, S. Dittmer, O. Evdokimov, C.E. Gerber, D.A. Hangal, D.J. Hofman, V. Kumar, C. Mills, T. Roy, M.B. Tonjes, N. Varelas, J. Viinikainen, H. Wang, X. Wang, Z. Wu

The University of Iowa, Iowa City, USA

M. Alhousseini, B. Bilki⁵⁵, K. Dilsiz⁷⁴, S. Durgut, R.P. Gandrajula, M. Haytmyradov, V. Khristenko, O.K. Köseyan, J.-P. Merlo, A. Mestvirishvili⁷⁵, A. Moeller, J. Nachtman, H. Ogul⁷⁶, Y. Onel, F. Ozok⁷⁷, A. Penzo, C. Snyder, E. Tiras, J. Wetzel

Johns Hopkins University, Baltimore, USA

B. Blumenfeld, A. Cocoros, N. Eminizer, A.V. Gritsan, W.T. Hung, S. Kyriacou, P. Maksimovic, J. Roskes, M. Swartz, T.Á. Vámi

The University of Kansas, Lawrence, USA

C. Baldenegro Barrera, P. Baringer, A. Bean, S. Boren, A. Bylinkin, T. Isidori, S. Khalil, J. King, G. Krintiras, A. Kropivnitskaya, C. Lindsey, D. Majumder, W. Mcbrayer, N. Minafra, M. Murray, C. Rogan, C. Royon, S. Sanders, E. Schmitz, J.D. Tapia Takaki, Q. Wang, J. Williams, G. Wilson

Kansas State University, Manhattan, USA

S. Duric, A. Ivanov, K. Kaadze, D. Kim, Y. Maravin, D.R. Mendis, T. Mitchell, A. Modak, A. Mohammadi

Lawrence Livermore National Laboratory, Livermore, USA

F. Rebassoo, D. Wright

University of Maryland, College Park, USA

A. Baden, O. Baron, A. Belloni, S.C. Eno, Y. Feng, N.J. Hadley, S. Jabeen, G.Y. Jeng, R.G. Kellogg, A.C. Mignerey, S. Nabili, F. Ricci-Tam, M. Seidel, Y.H. Shin, A. Skuja, S.C. Tonwar, K. Wong

Massachusetts Institute of Technology, Cambridge, USA

D. Abercrombie, B. Allen, R. Bi, S. Brandt, W. Busza, I.A. Cali, M. D'Alfonso, G. Gomez Ceballos, M. Goncharov, P. Harris, D. Hsu, M. Hu, M. Klute, D. Kovalskyi, Y.-J. Lee, P.D. Luckey, B. Maier, A.C. Marini, C. McGinn, C. Mironov, S. Narayanan, X. Niu, C. Paus, D. Rankin, C. Roland, G. Roland, Z. Shi, G.S.F. Stephens, K. Sumorok, K. Tatar, D. Velicanu, J. Wang, T.W. Wang, B. Wyslouch

University of Minnesota, Minneapolis, USA

R.M. Chatterjee, A. Evans, S. Guts[†], P. Hansen, J. Hiltbrand, Sh. Jain, Y. Kubota, Z. Lesko, J. Mans, M. Revering, R. Rusack, R. Saradhy, N. Schroeder, N. Strobbe, M.A. Wadud

University of Mississippi, Oxford, USA

J.G. Acosta, S. Oliveros

University of Nebraska-Lincoln, Lincoln, USA

K. Bloom, S. Chauhan, D.R. Claes, C. Fangmeier, L. Finco, F. Golf, R. Kamalieddin, I. Kravchenko, J.E. Siado, G.R. Snow[†], B. Stieger, W. Tabb

State University of New York at Buffalo, Buffalo, USA

G. Agarwal, C. Harrington, I. Iashvili, A. Kharchilava, C. McLean, D. Nguyen, A. Parker, J. Pekkanen, S. Rappoccio, B. Roozbahani

Northeastern University, Boston, USA

G. Alverson, E. Barberis, C. Freer, Y. Haddad, A. Hortiangtham, G. Madigan, B. Marzocchi, D.M. Morse, T. Orimoto, L. Skinnari, A. Tishelman-Charny, T. Wamorkar, B. Wang, A. Wisecarver, D. Wood

Northwestern University, Evanston, USA

S. Bhattacharya, J. Bueghly, G. Fedi, A. Gilbert, T. Gunter, K.A. Hahn, N. Odell, M.H. Schmitt, K. Sung, M. Velasco

University of Notre Dame, Notre Dame, USA

R. Bucci, N. Dev, R. Goldouzian, M. Hildreth, K. Hurtado Anampa, C. Jessop, D.J. Karmgard, K. Lannon, W. Li, N. Loukas, N. Marinelli, I. Mcalister, F. Meng, Y. Musienko³⁸, R. Ruchti, P. Siddireddy, G. Smith, S. Taroni, M. Wayne, A. Wightman, M. Wolf

The Ohio State University, Columbus, USA

J. Alimena, B. Bylsma, L.S. Durkin, B. Francis, C. Hill, W. Ji, A. Lefeld, T.Y. Ling, B.L. Winer

Princeton University, Princeton, USA

G. Dezoort, P. Elmer, J. Hardenbrook, N. Haubrich, S. Higginbotham, A. Kalogeropoulos, S. Kwan, D. Lange, M.T. Lucchini, J. Luo, D. Marlow, K. Mei, I. Ojalvo, J. Olsen, C. Palmer, P. Piroué, D. Stickland, C. Tully

University of Puerto Rico, Mayaguez, USA

S. Malik, S. Norberg

Purdue University, West Lafayette, USA

A. Barker, V.E. Barnes, R. Chawla, S. Das, L. Gutay, M. Jones, A.W. Jung, B. Mahakud, D.H. Miller, G. Negro, N. Neumeister, C.C. Peng, S. Piperov, H. Qiu, J.F. Schulte, N. Trevisani, F. Wang, R. Xiao, W. Xie

Purdue University Northwest, Hammond, USA

T. Cheng, J. Dolen, N. Parashar

Rice University, Houston, USA

A. Baty, U. Behrens, S. Dildick, K.M. Ecklund, S. Freed, F.J.M. Geurts, M. Kilpatrick, Arun Kumar, W. Li, B.P. Padley, R. Redjimi, J. Roberts, J. Rorie, W. Shi, A.G. Stahl Leiton, Z. Tu, A. Zhang

University of Rochester, Rochester, USA

A. Bodek, P. de Barbaro, R. Demina, J.L. Dulemba, C. Fallon, T. Ferbel, M. Galanti, A. Garcia-Bellido, O. Hindrichs, A. Khukhunaishvili, E. Ranken, R. Taus

Rutgers, The State University of New Jersey, Piscataway, USA

B. Chiarito, J.P. Chou, A. Gandrakota, Y. Gershtein, E. Halkiadakis, A. Hart, M. Heindl, E. Hughes, S. Kaplan, I. Laflotte, A. Lath, R. Montalvo, K. Nash, M. Osherson, S. Salur, S. Schnetzer, S. Somalwar, R. Stone, S. Thomas

University of Tennessee, Knoxville, USA

H. Acharya, A.G. Delannoy, S. Spanier

Texas A&M University, College Station, USA

O. Bouhali⁷⁸, M. Dalchenko, M. De Mattia, A. Delgado, R. Eusebi, J. Gilmore, T. Huang, T. Kamon⁷⁹, H. Kim, S. Luo, S. Malhotra, D. Marley, R. Mueller, D. Overton, L. Perniè, D. Rathjens, A. Safonov

Texas Tech University, Lubbock, USA

N. Akchurin, J. Damgov, F. De Guio, V. Hegde, S. Kunori, K. Lamichhane, S.W. Lee, T. Mengke, S. Muthumuni, T. Peltola, S. Undleeb, I. Volobouev, Z. Wang, A. Whitbeck

Vanderbilt University, Nashville, USA

S. Greene, A. Gurrola, R. Janjam, W. Johns, C. Maguire, A. Melo, H. Ni, K. Padeken, F. Romeo, P. Sheldon, S. Tuo, J. Velkovska, M. Verweij

University of Virginia, Charlottesville, USA

M.W. Arenton, P. Barria, B. Cox, G. Cummings, J. Hakala, R. Hirosky, M. Joyce, A. Ledovskoy, C. Neu, B. Tannenwald, Y. Wang, E. Wolfe, F. Xia

Wayne State University, Detroit, USA

R. Harr, P.E. Karchin, N. Poudyal, J. Sturdy, P. Thapa

University of Wisconsin - Madison, Madison, WI, USA

K. Black, T. Bose, J. Buchanan, C. Caillol, D. Carlsmith, S. Dasu, I. De Bruyn, L. Dodd, C. Galloni, H. He, M. Herndon, A. Hervé, U. Hussain, A. Lanaro, A. Loeliger, K. Long, R. Loveless, J. Madhusudanan Sreekala, A. Mallampalli, D. Pinna, T. Ruggles, A. Savin, V. Sharma, W.H. Smith, D. Teague, S. Trembath-reichert

†: Deceased

1: Also at Vienna University of Technology, Vienna, Austria

2: Also at IRFU, CEA, Université Paris-Saclay, Gif-sur-Yvette, France

3: Also at Universidade Estadual de Campinas, Campinas, Brazil

4: Also at Federal University of Rio Grande do Sul, Porto Alegre, Brazil

5: Also at UFMS, Nova Andradina, Brazil

6: Also at Universidade Federal de Pelotas, Pelotas, Brazil

7: Also at Université Libre de Bruxelles, Bruxelles, Belgium

8: Also at University of Chinese Academy of Sciences, Beijing, China

9: Also at Institute for Theoretical and Experimental Physics named by A.I. Alikhanov of NRC 'Kurchatov Institute', Moscow, Russia

10: Also at Joint Institute for Nuclear Research, Dubna, Russia

11: Also at Cairo University, Cairo, Egypt

12: Also at Zewail City of Science and Technology, Zewail, Egypt

13: Also at Purdue University, West Lafayette, USA

14: Also at Université de Haute Alsace, Mulhouse, France

15: Also at Erzincan Binali Yildirim University, Erzincan, Turkey

16: Also at CERN, European Organization for Nuclear Research, Geneva, Switzerland

17: Also at RWTH Aachen University, III. Physikalisches Institut A, Aachen, Germany

- 18: Also at University of Hamburg, Hamburg, Germany
- 19: Also at Isfahan University of Technology, Isfahan, Iran
- 20: Also at Brandenburg University of Technology, Cottbus, Germany
- 21: Also at Institute of Physics, University of Debrecen, Debrecen, Hungary, Debrecen, Hungary
- 22: Also at Institute of Nuclear Research ATOMKI, Debrecen, Hungary
- 23: Also at MTA-ELTE Lendület CMS Particle and Nuclear Physics Group, Eötvös Loránd University, Budapest, Hungary, Budapest, Hungary
- 24: Also at IIT Bhubaneswar, Bhubaneswar, India, Bhubaneswar, India
- 25: Also at Institute of Physics, Bhubaneswar, India
- 26: Also at G.H.G. Khalsa College, Punjab, India
- 27: Also at Shoolini University, Solan, India
- 28: Also at University of Hyderabad, Hyderabad, India
- 29: Also at University of Visva-Bharati, Santiniketan, India
- 30: Now at INFN Sezione di Bari ^a, Università di Bari ^b, Politecnico di Bari ^c, Bari, Italy
- 31: Also at Italian National Agency for New Technologies, Energy and Sustainable Economic Development, Bologna, Italy
- 32: Also at Centro Siciliano di Fisica Nucleare e di Struttura Della Materia, Catania, Italy
- 33: Also at Scuola Normale e Sezione dell'INFN, Pisa, Italy
- 34: Also at Riga Technical University, Riga, Latvia, Riga, Latvia
- 35: Also at Malaysian Nuclear Agency, MOSTI, Kajang, Malaysia
- 36: Also at Consejo Nacional de Ciencia y Tecnología, Mexico City, Mexico
- 37: Also at Warsaw University of Technology, Institute of Electronic Systems, Warsaw, Poland
- 38: Also at Institute for Nuclear Research, Moscow, Russia
- 39: Now at National Research Nuclear University 'Moscow Engineering Physics Institute' (MEPhI), Moscow, Russia
- 40: Also at St. Petersburg State Polytechnical University, St. Petersburg, Russia
- 41: Also at University of Florida, Gainesville, USA
- 42: Also at Imperial College, London, United Kingdom
- 43: Also at P.N. Lebedev Physical Institute, Moscow, Russia
- 44: Also at California Institute of Technology, Pasadena, USA
- 45: Also at Budker Institute of Nuclear Physics, Novosibirsk, Russia
- 46: Also at Faculty of Physics, University of Belgrade, Belgrade, Serbia
- 47: Also at Università degli Studi di Siena, Siena, Italy
- 48: Also at INFN Sezione di Pavia ^a, Università di Pavia ^b, Pavia, Italy, Pavia, Italy
- 49: Also at National and Kapodistrian University of Athens, Athens, Greece
- 50: Also at Universität Zürich, Zurich, Switzerland
- 51: Also at Stefan Meyer Institute for Subatomic Physics, Vienna, Austria, Vienna, Austria
- 52: Also at Burdur Mehmet Akif Ersoy University, BURDUR, Turkey
- 53: Also at Şırnak University, Şırnak, Turkey
- 54: Also at Department of Physics, Tsinghua University, Beijing, China, Beijing, China
- 55: Also at Beykent University, Istanbul, Turkey, Istanbul, Turkey
- 56: Also at Istanbul Aydin University, Application and Research Center for Advanced Studies (App. & Res. Cent. for Advanced Studies), Istanbul, Turkey
- 57: Also at Mersin University, Mersin, Turkey
- 58: Also at Piri Reis University, Istanbul, Turkey
- 59: Also at Gaziosmanpasa University, Tokat, Turkey
- 60: Also at Ozyegin University, Istanbul, Turkey
- 61: Also at Izmir Institute of Technology, Izmir, Turkey

- 62: Also at Marmara University, Istanbul, Turkey
- 63: Also at Kafkas University, Kars, Turkey
- 64: Also at Istanbul Bilgi University, Istanbul, Turkey
- 65: Also at Near East University, Research Center of Experimental Health Science, Nicosia, Turkey
- 66: Also at Hacettepe University, Ankara, Turkey
- 67: Also at Adiyaman University, Adiyaman, Turkey
- 68: Also at Vrije Universiteit Brussel, Brussel, Belgium
- 69: Also at School of Physics and Astronomy, University of Southampton, Southampton, United Kingdom
- 70: Also at IPPP Durham University, Durham, United Kingdom
- 71: Also at Monash University, Faculty of Science, Clayton, Australia
- 72: Also at Bethel University, St. Paul, Minneapolis, USA, St. Paul, USA
- 73: Also at Karamanoğlu Mehmetbey University, Karaman, Turkey
- 74: Also at Bingol University, Bingol, Turkey
- 75: Also at Georgian Technical University, Tbilisi, Georgia
- 76: Also at Sinop University, Sinop, Turkey
- 77: Also at Mimar Sinan University, Istanbul, Istanbul, Turkey
- 78: Also at Texas A&M University at Qatar, Doha, Qatar
- 79: Also at Kyungpook National University, Daegu, Korea, Daegu, Korea